Relations between visual conditions, head motion and motion sickness in vehicle passengers

By

Yunyi Li

in partial fulfilment of the requirements for the degree of

Master of Science

in Mechanical Engineering

at the Delft University of Technology,

to be defended publicly on Friday August 31, 2018 at 12:00 AM.

Student Number: 4613996

Supervisor:	Dr. ir. Riender Happee	COR, 3ME, TU Delft
Thesis committee:	Ir. Tugrul Irmak	COR, 3ME, TU Delft
	Dr.ir. Arend Shwab	BMECHE, 3ME, TU Delft

TUDelft

Contents

* jointly written with Kenny Lie

* jointly written with Kenny Lie

* jointly written with Kenny Lie

Summary

Motion sickness is a phenomenon observed in a wide range of modern transports, triggering symptoms such as dizziness, nausea and vomiting. 95% of the normal population has suffered from motion sickness and 5% of them was very severe (Oosterveld, 1995). Among various types of motion sickness, carsickness is the most common one in our daily life, especially when the car motion is irritative involving large horizontal accelerations. This thesis investigates the motion sickness as well as head and body motions in car passengers when different visual conditions were provided. The results could help the motion sickness being understood more in depth and practically improve motion comfort for travelers.

The sensory conflict theory regards the contradictory spatial senses perceived by vestibular and visual system as the cause of motion sickness and has been widely accepted. Meanwhile, an ecological theory was also proposed, indicating that motion sickness could result from the postural instability when humans are lack of body control strategies. It has been observed that compared with internal vision, normal external vision could help car passengers effectively reduce MSI. According to the sensory conflict theory, this benefit could attribute to the visual cues in earth-fixed frame and anticipatory information provided by the external and forward vision, which are helpful in reducing visual-vestibular conflict of passengers when they are exposed to aggressive car motion. However, the passengers body control strategies as well as postural stability might be influenced by visual condition regarding the ecological theory, and it has not been investigated in previous studies.

An experiment was performed to investigate the relations between visual condition, body movement and MSI in car passengers. Two visual conditions have been realized in a car – natural external vision with eyes on road and internal vision with both forward and peripheral outside vision blocked. Every participant experienced both conditions for 30 minutes at most, when the car was performing slalom driving with a lateral acceleration up to 0.4g of 0.17 Hz. The participant's motion sickness ratings as well as head and body movements were recorded, which were then compared within participants between the two visual conditions.

Vision was found to significantly affect the motion sickness ratings by participants ($p = 0.025$), and the latter was almost double higher in internal visual condition compared with normal vision. Nevertheless, no significant difference was found in head and body motion amplitude under 1 Hz either between the two visual conditions or between sensitive and non-sensitive participants. Participants' head and body movements were not found changing in time as well. Although slight difference was observed in seat-to-head acceleration coherence between the two visual conditions, no significant difference was proved by statistical tests.

No evidence was found in this thesis that visual condition in a car would influence passengers' body motion or postural stability, although the former was found drastically affecting carsickness incidence. It is contradictory with the hypotheses of the ecological theory, but provides evidence

for sensory integration process in motion sickness. Future studies are needed to validate this result with larger sample size, a wider range of motion amplitude, frequency and directions and more controlled conditions, like stabilizing the passengers' head and body or measuring sitting body sway in a stable environment.

List of Abbreviations and Acronyms

MISC	Misery Scale
MSAQ	Motion Sickness Assessment Questionnaire
MSDV	Motion Sickness Dose Value
MSI	Motion Sickness Incidence
MSSQ	Motion Sickness Susceptibility Questionnaire

1. Introduction

1.1 Motion Sickness

An aphorism has been written by the Greek physician Hippocrates in 400 B.C.E – *"sailing on the sea shows that motion disorders the body"* (Bertolini & Straumann, 2016). Since modern transportation is rapidly developing, motion environments are becoming increasingly unfamiliar to humans. This has caused a drastic increase in the reports of motion sickness. An affliction which had once been isolated only to the seas. For example, the traditional cars increase our reach over land and drastically save travel time. However, they may also cause sickness in some individuals, reducing their overall utility. The same phenomena of motion sickness apply to autonomous vehicles, aircraft, spacecraft, ships and boats. Furthermore, motion sickness is not only induced by imposed motions like the various modes of transport highlighted above, but also evoked by viewing realistic moving scenes such as ubiquitous simulator sickness caused by virtual reality and even cinema sickness when watching 3D movies. Of the normal population, only 5% hardly gets motion sickness while 95% suffers from motion sickness from moderately to severely (Oosterveld, 1995). Study of motion sickness is essential and could help save time and improve comfort for travelers. Besides, preventing motion sickness could improve safety for lower-level automated vehicles if supervision of the driver is required.

Motion sickness is a biologically natural response observed in a wide range of species including humans (Treisman, 1977) whenever they are exposed to unnatural body motion. This triggers a variety of physical, physiological and even psychological symptoms. The most typical symptoms are known as drowsiness, stomach sickness, headache, dizziness, cold sweating, salivation, apathy and more severe ones like nausea, pallor, retching and vomiting (Bos, Mackinnon & Patterson, 2005). The development, the recovery, as well as the type of symptoms triggered all vary significantly between individuals. As a large number of studies suggest, this depends on gender, age, previous experience etc. Specifically, female compared with male, teenagers compared with adults and people who are less frequently travelling are more susceptible to provocative stimulus. Some people more easily suffer from head symptoms like headache and dizziness whilst others tend to experience gut discomfort like nausea and vomit (Lackner, 2014, Turner & Griffin, 1999a). Although motion sickness is pervasive in our daily lives, the mechanism of how motion sickness is induced is still vague.

1.2 The Sensory Conflict Theory

Various theories have been raised to explain the cause of motion sickness (Reason, 1978; Riccio & Stoffregen, 1991; Treisman, 1977), among which the most widely accepted one is the sensory conflict theory. Supporters of the sensory conflict theory consider motion sickness as the product of mismatch between human spatial senses (e.g., vestibular system perceiving head motion; proprioceptive system perceiving body motion and visual system perceiving motion of environment). With voluntary motion in a natural environment, our spatial senses are always in agreement with each other. If our expectation is always consistent with the motion perception by our spatial senses, we will perfectly adapt to the motion environment. (Reason, 1978).

However, with modern modes of transport, passive body motion produces incongruence between the spatial senses. For instance, car passengers could be exposed to low-frequency horizontal accelerations when the car is either braking or steering, while their views inside the car is comparably still instead. Contradictory sensed spatial information, especially by the vestibular and visual system, results in uncertainty in motion estimation for the passengers, which, according to the sensory conflict theory, induces motion sickness symptoms. Nevertheless, it is found that motion sickness symptoms will not keep increasing under exposure to regular passive movements. Instead, continuous interaction with such nauseous stimulus will finally result in the alleviation or even disappearance of symptoms. This process is referred to as habituation. It implies that motion sickness cannot simply be attributed to the temporary motion conflict perceived by visual and vestibular system, but our self-expectation of body motion should also be considered that will be eventually habituated with long-time exposure (Reason, 1978).

To explain the mechanism of adaptation, Reason (1978) proposed the neural mismatch model (Fig.1.1) with the neural store retaining the previous information of both motor commands and sensory inputs. The mismatch signal processed in CNS was supposed to be generated by the comparator when the current sensory inputs mismatched the previous experienced efference and retrieved reafferent sensory signal stored in the neutral store. Oman (1982) furthermore emphasized the importance of ‘expectation’, who postulated an internal model that is an internal signal processing path in our CNS predicting the expected body state, parallel to the primary path which deals with the actual state (Fig.1.2). Apart from calculating the estimated body state, the internal model can simultaneously predict the expected sensory input, and the latter is compared with the actual input producing the conflict. The conflict is hence exploited to trigger motion sickness symptoms as well as adapt the internal model to minimize the discrepancy. The sensory conflict theory with internal model has been accepted by most researchers and regarded as relatively significant way to predict the incidence of motion sickness symptoms during exposure to nauseogenic stimulus. For example, Bos and Bles (1998) derived a subjective vertical conflict model on basis of the internal model and experimental data from McCauley et al. (1976), having successfully derived the parameters for the model and predicted MSI (MSI) for passive vertical motion.

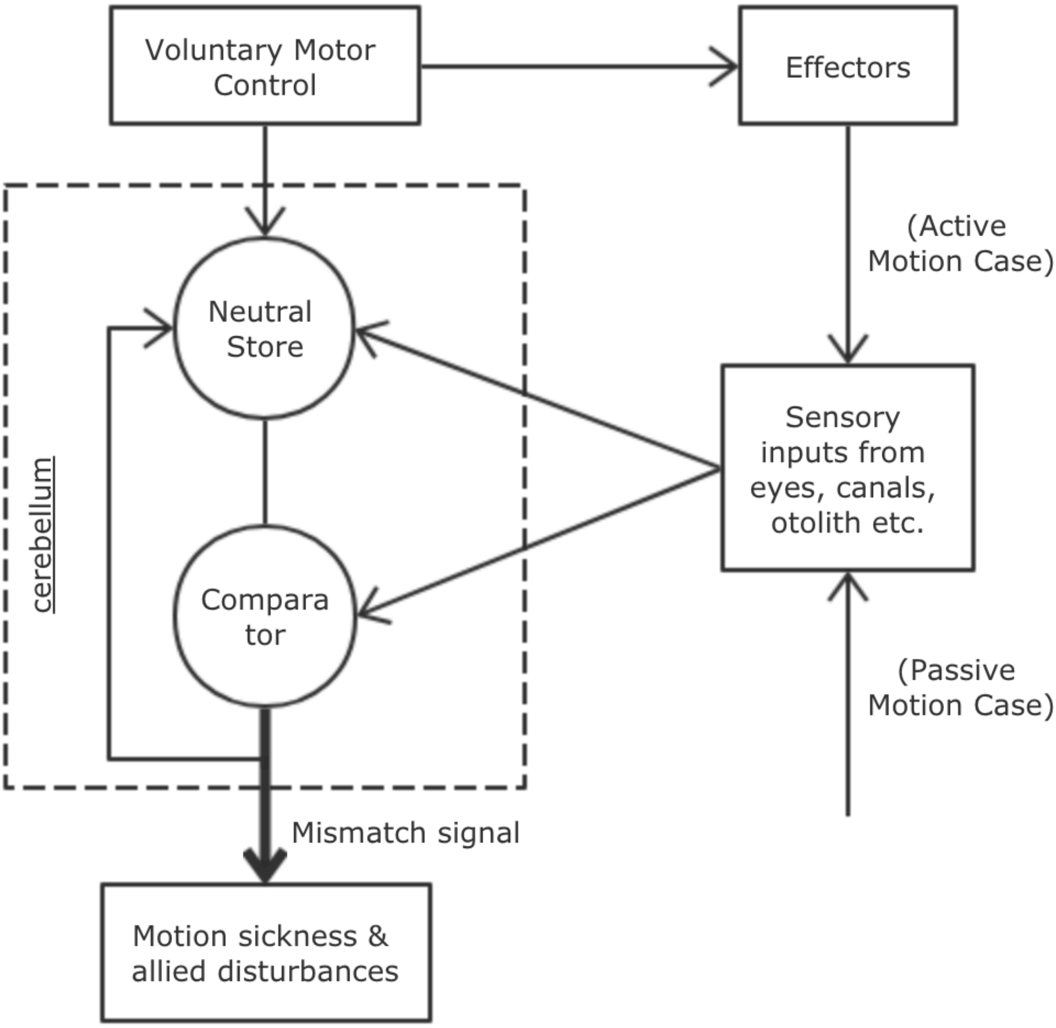

Fig.1.1 The basic structural components of the neural mismatch model (Reason, 1978)

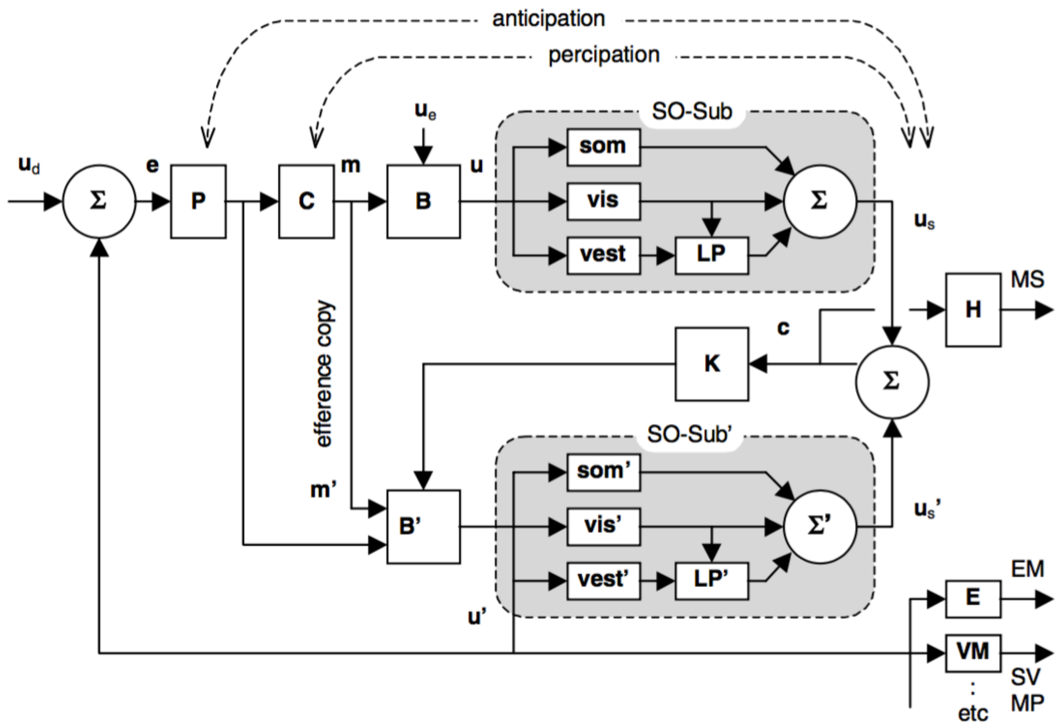

Fig.1.2 Global overview of the spatial orientation and motion sickness model

(Bos, Bles & Groen, 2008)

P = preparatory phase, C = motor commands generating controller, B = body, vis = visual system, som = somatosensory system, vest = vestibular system, LP = low-pass filter, H = transfer function for motion sickness, E = eye movement system, V/M = verbal/manual system to finally give the SV and motion perception (MP), K = internal feedback (or Kalman) gain. Within the internal model, all functions have been indicated with a prime. The model's inputs are the desired body state (ud) and the external disturbances (ue). The outputs are motion sickness (MS), eye movements (EM), the subjective vertical (SV), and motion perception variables (MP).

As early as the 19th century, Irwin (1881) found that individuals with malfunctioning inner ear apparatus were immune to any kind of motion sickness, even in the case of visually induced motion sickness where no physical motion was imposed, while the blind could also experience motion sickness. Such apparatus, namely vestibular system, consists of the non-auditory components of the labyrinth embedded in the temporal bone on each side of the head. That was then considered as the predominant organ in eliciting motion sickness. The vestibular system includes the otoliths (utricle and saccule) sensitive to horizontal and vertical linear accelerations, and the semi-circular canals which are sensitive to dynamic rotations of head in the three axes (Webb, 2000, citing Howard, 1986). Reason (1978) pointed out that the sensory mismatch can emerge either between the vision and vestibular system, or even within the vestibular system. The latter happens when rotation of head perceived by the semi-circular canals is not accompanied by a corresponding angular change in the direction of gravity vector recognized by the otoliths. Stott (1986) further indicated that the conflicts may also occur within the otoliths. This would occur whenever the constant acceleration perceived by the otoliths was inconsistent with the known magnitude of gravity (having an intensity of 1g and defining ‘downwards’). Such examples of otolith conflict may arise in space leading to the space sickness. In most situations, the three kinds of sensory conflicts co-exist, for example, when travelling on road, passengers are exposed to low-frequency translational oscillations, which may cause body and head tilting and orientation changing. These translational motions can be misidentified by the otolith membranes of the vestibular system, inconsistent with information from the visual system or from the semi-circular canals of the vestibular system.

1.3 The Ecological Theory

The ecological theory hypothesizes that motion sickness is caused by instability in postural control (Riccio & Stoffregen, 1991), moving the focus from perception to the perception and control of orientation and action. Typically, motion sickness is associated with situations where the “existing patterns of movement are no longer efficient and new patterns of movement must be learned” (Stoffregen et al., 2010). In unfamiliar or nauseogenic situations, body movements are inappropriately controlled while new movement control strategies must be learned, which lead to body postural instabilities temporarily, accompanied with motion sickness. Riccio and Stoffregen (1991) pointed out nine characteristics that might imply the occurrence of postural instability:

- The body sway may increase in horizontal directions;
- The pattern between acceleration and position may change with increasing accelerations over small angles;
- The coherence between the disturbances and the movements and center of mass may reduce at low frequencies.
- The amplitude distribution of body motion might become skew or asymmetric, and the kurtosis of distribution might become flat.
- Prolonged postural instability may result in physiological tremor – increased power spectral densities in higher frequencies, caused by the effortful attempt in postural control.
- Spreading instability may reduce the degree of coordination thus increase the degrees of freedom in the movements of body segments.
- The boundaries of patterns of coordination may become less stable and more variable.
- The postural instability might be specified by how the adaptive control system responds to perturbations, which might be no longer efficient.

In support of this theory, Owen, Leadbetter and Yardley (1998) related the susceptibility of motion sickness to the deficiency in perceptual-motor capabilities, finding that the healthy subjects who were more susceptible to motion sickness were more deficient in postural control and showed larger standing body sway especially when there were visual and somatosensory disturbances (with eyes closed, VR display and calf muscle vibration). They assumed that the individual differences in susceptibility of motion sickness were directly caused by the differences in perceptual-motor control, instead of the differences in sensitivity in discrepant perceptual information or adaptability to novel environments as revealed by sensory conflict theory. This assumption was also supported by Smart, Pagulayan & Stoffregen (1998), who observed motion sickness symptoms in 21% of healthy subjects during the study (effects of visual fixation on spontaneous postural sway) without any apparent imposed motion and sensory rearrangement, and therefore attributed this sickness to postural sway. As for visually induced motion sickness, Stoffregen et al. (2010) complementarily found that the incidence of sickness decreased with increasing stance width, associated with less postural sway when the subjects were standing and exposed to imposed visual motions. Stoffregen, Chen & Koslucher (2014) recently found the relationship between postural control and motion sickness in playing video games – subjects who were able to tilt the display by hands and easier to stabilize their visual gaze showed smaller head and body motions as well as lower sickness than subjects who had to spontaneously move their heads and bodies to stabilize visual gaze in a sitting position. However, there are also ones arguing that the postural instability could be elicited by motion sickness symptoms such as dizziness and nausea after the motion sickness has been induced (Lackner, 2014), which does not arise before the motion sickness as explained by the ecological theory. Moreover, the main criticism of the ecological theory is that motion sickness has been still observed in the conditions where no active postural stabilization is needed, such as supine postures, although the MSI of subjects lying on a stretcher showed only half of that of subjects in the sitting position (Vogel, Kohlhaas & von Baumgarten, 1982). Nevertheless, Vogel, Kohlhaas & von Baumgarten (1982) also stated that postural instability should be an essential dependent factor in inducing motion sickness, which should be combined with the sensory conflict and some other factors like the eye movements (see section 3.2) in researching the cause of motion sickness. In other words, motion sickness is the result of several correlated factors that is impossible to be explained by a single mechanism or theory.

1.4 Previous Studies on Car Sickness

According to the sensory conflict theory, visual-vestibular mismatch becomes the most to blame regarding carsickness, which implies that perceived head motion and vision are the two essential factors influencing MSI during driving. In order to verify the validity of the sensory conflict theory, a large number of studies on carsickness have been carried out in the previous decades. This was done by probing the relationship between motion, vision and MSI.

Vehicle Motion

Nauseogenic motion in land transports (e.g., cars, trains, buses and coaches) vary considerably from that in non-land transports (e.g., vessels and airplanes). The dominant motion in vessels or airplanes is low-frequency vertical and pitch motion. However, such vertical motion in land transports is mainly of high frequency and low amplitude, thus outside the nauseogenic range. It occurs due to tyre-road contact and suspension dynamics. The occurrence of carsickness, conversely, is mainly attributed to low-frequency longitudinal and lateral accelerations, as well as and yaw rotations. It is highly dependent on the driving style of the driver (Lawther & Griffin, 1986, Turner & Griffin, 1999b, Griffin & Newman, 2004).

The MSI is highly dependent on the frequency of motion. No matter what the direction of the dominant oscillation is, either vertical or horizontal, motion sickness is always found to peak at a frequency of approximately 0.2 Hz. Donohew and Griffin (2004) investigated six frequencies (0.0315, 0.05, 0.08, 0.125, 0.16, 0.20Hz) during a sinusoidal lateral oscillation exposure with a peak velocity of 1.0 ms-1. They found that both subjects' illness ratings and symptoms significantly increased with increasing frequency of lateral oscillation under 0.2 Hz (Mann-Whitney U-test: $p < 0.05$ between 0.08 and 0.16 Hz, 0.125 and 0.2 Hz; $p < 0.01$ between 0.0315 and 0.16 Hz, 0.0315 and 0.2 Hz, 0.05 and 0.16 Hz, 0.05 and 0.2 Hz, 0.08 and 0.2 Hz), but no differences between 0.16 Hz and 0.2 Hz ($p = 0.779$). By combining the experimental data from Griffin and Mills (2002) who investigated the lateral motion with frequencies above 0.2 Hz, Donohew and Griffin (2004) then developed the acceleration frequency weightings for lateral oscillation (Fig.1.3) which can be also applied to longitudinal oscillations.

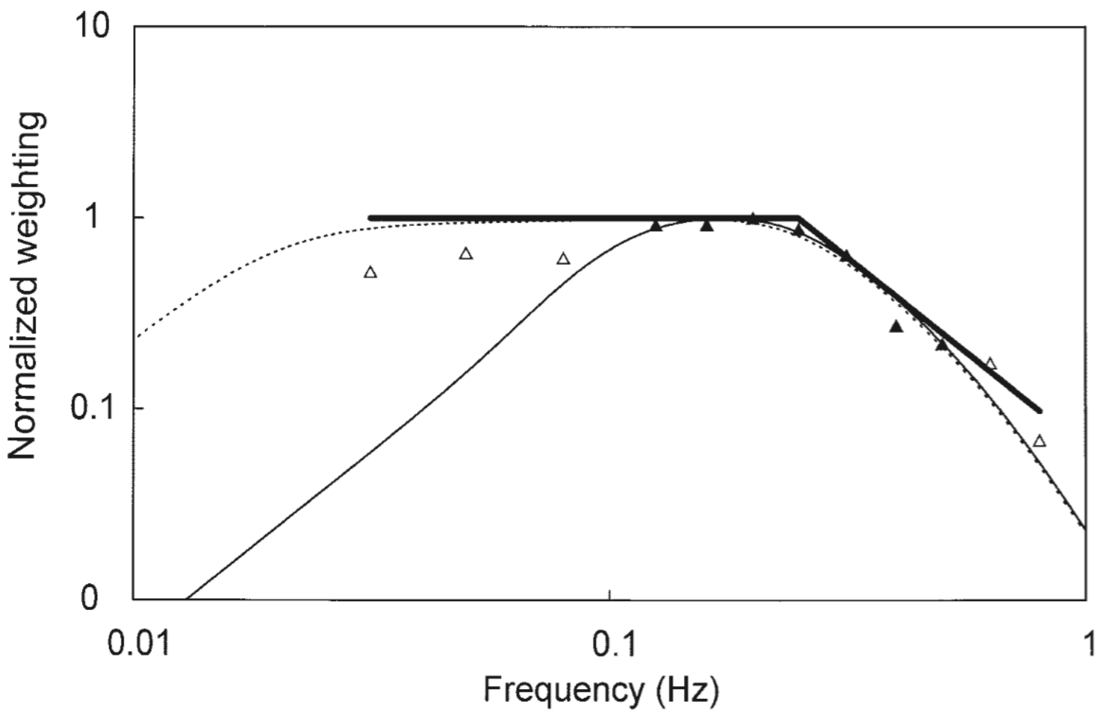

Fig.1.3 Normalized frequency weightings for lateral acceleration compared with weighting W_f for vertical oscillation defined in BS 6841 (Donohew and Griffin, 2004)
Asymptotic weighting solid thick line; realizable weighting (product of transfer functions of two component filters – a band-limiting filter and an acceleration weighting) dotted line; normalized mild nausea incidence: black triangles points at which values differ from static condition, open triangles points at which values are not different from static condition; W_f *for vertical acceleration solid thin line.*

The frequency weightings, recommended in International Standard (ISO 2631-1, 1997), are for evaluation of the effects of vibration on the incidence of motion sickness, which are multiplied with the original acceleration (Eq.1.1) to increase the correlation between the acceleration and the motion sickness ratings.

$$a_w = [\sum_i (W_i a_i)^2]^{\frac{1}{2}} \qquad (1.1)$$

In addition to the dependency of frequency, MSI has been found to be linearly increasing with the magnitude of acceleration for all 3 translations directions (Lawther & Griffin (1987)). McCauley et al. (1976) developed a model in three-dimension (Fig.1.4), showing the relationship between MSI and frequency and acceleration amplitude single sine motion.

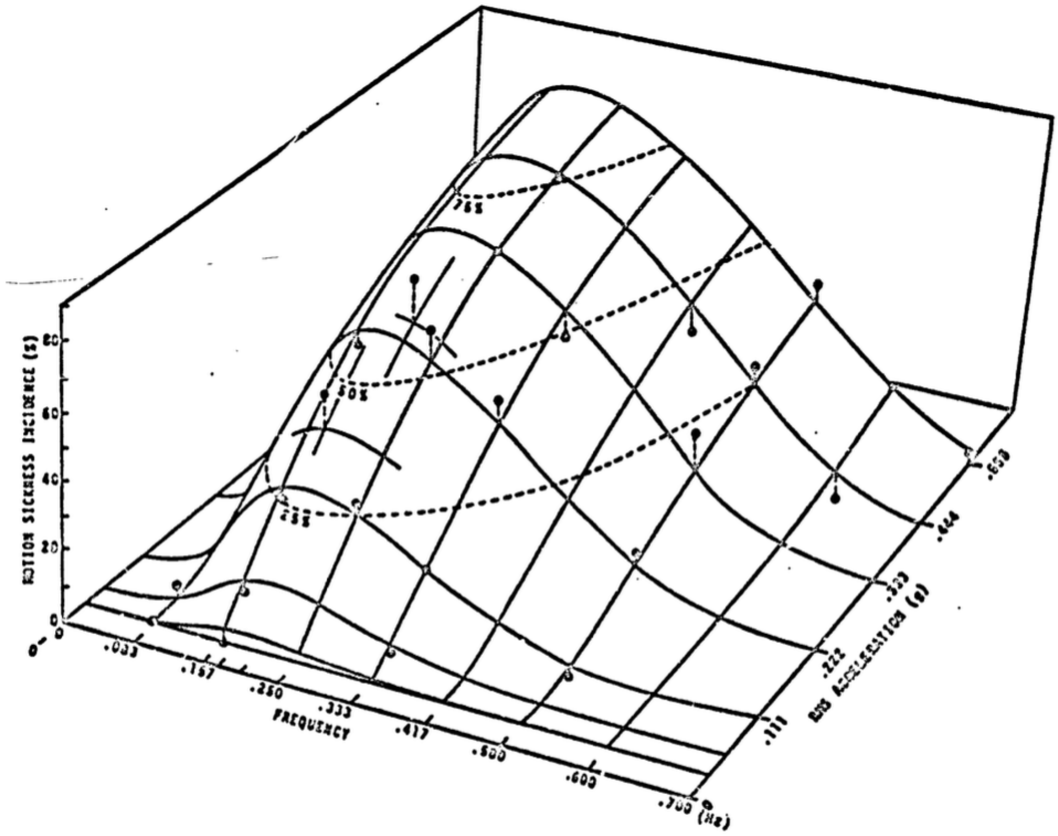

Fig.1.4 Three-dimensional representation of McCauley's model of MSI as a function of wave frequency and acceleration for 2-hour exposures to vertical sinusoidal motion (McCauley *et al.*, 1976)

Compared with motion amplitude, exposure duration is less influential in the severity of motion sickness symptoms, although longer exposure (before adaptation occurs) will provoke motion sickness. Combining the effect of motion magnitude, frequency and duration, the MSDV can be derived (Eq.1.2) that is used to predict MSI.

$$MSDV = \left[\int_{t=0}^{t=T} a_w^2(t)dt\right]^{\frac{1}{2}} \tag{1.2}$$

Though passengers in vehicles are in sitting posture and facing forward in most situations, thus within the application range of these studies. There are however also cases where the passenger is exposed to vehicle motion in other postures. For instance, supine posture in an ambulance, standing posture in a bus etc. In fact, studies have found that the orientation of body axes with respect to the direction of motion has a major effect on MSI. This, they hypothesize, is due to the perception of gravity. Specifically, the supine posture in a car, compared to upright seated posture, was found to be more effective in eliminating nauseogenicity. In this case, the principle direction of motion is through the frontal place, rather than the transverse (Golding et al, 1995). Golding hypothesized that motion through longitudinal head-body axis per se was more provocative than that of naso-occipital head-body axis. Besides, the supine posture might improve the postural stability and controllability which is also regarded as a cause of motion sickness (Riccio & Stoffregen, 1991).

Head and Body Motion

Most of the previous studies and analyses about the effect of motion on motion sickness were based on the assumption that the motion perceived by human vestibular system is identical to the seat or vehicle motion, which, unfortunately, is not always valid. During either laboratory or field motion sickness experiments, the passive motions were always imposed on the participants through oscillating seats or floors, where the stimulus was transferred from the pelvis or feet to head – the location of both visual and vestibular system. In the car, for example, passengers head motion is actually the one to blame in triggering visual-vestibular conflict, so that body-to-head transmissibility in all the moving directions becomes essential in analyzing the actual visual-vestibular conflict and motion sickness induction.

With sitting posture in the vehicle, the transmissibility for vibration in longitudinal, vertical and pitch directions peaks at around 2 Hz, while the backrest may increase the transmissibility in higher frequencies around 6 to 8 Hz. The transmissibility in lateral direction peaks at around 2 Hz as well, however, this is less affected by the backrest (Paddan & Griffin, 1988). Neither translational nor rotational motion shows a transmissibility gain more than 1 below 1 Hz (the gain peaks were at approximately 2 and 5 respectively) which is the frequency range that motion sickness occurs. Voluntary head motion is observed to affect MSI which can also partly explain the discrepancy between MSI among drivers and passengers. Wada and Yoshida (2016) investigated the difference between subjects actively tilting heads in centripetal and centrifugal direction while exposed to lateral oscillations, and they found that the carsickness of passengers significantly reduced (Wilcoxon signed-rank test: $p = 0.017$ in EYES-ON-ROAD condition) if they tilted their heads against the centrifugal direction. The active head tilting imitates the driver's posture – the head and trunk of a bus driver was observed to incline toward the right due to the hands behavior when he turns the wheel to the right (Rolnick & Lubow, 1991), and this benefit was irrelevant to whether the visual information was provided. Specifically, passengers with heads centripetally tilting, compared with those with heads balanced or centrifugally tilting when exposed to the same steering behavior, tend to turn in a smaller radius with smaller both motion magnitude and velocity, who are supposed to sense milder lateral motions and have lower visual-vestibular conflict in the opinion of the sensory conflict theory. While as the ecological theory suggests, the movements of passengers' body might relate to their postural control strategies. The passengers with visual information, as well as the driver, can have anticipatory clues that help adapting motion control strategies in advance, so that the postural stability might be improved.

Vision

Apart from motion, the visual condition of passengers is also closely related to carsickness incidence. As previous studies suggested, visual perception can be either beneficial or detrimental to motion sickness experienced in vehicles. Appropriate visual information, such as good forward view can help passengers estimate their body motion and reduce visual-vestibular conflict. Inappropriate visual information may cause redundant motion perception and aggravate motion sickness symptoms. An example of this may be watching video footage inside a car.

Griffin and Newman (2004) systematically investigated the effects of five different visual fields (normal external view, blindfolded condition, no external view, no forward view, narrow forward view) in eliciting motion sickness for car passengers sitting at the middle of rear seats. Results showed that carsickness was significantly higher (Mann- Whitney U test: $p < 0.02$) during a 30-min ride when the forward external view was absent (Fig.1.5). The conditions of internal view, side external view and no view were found to be equally provocative instead ($p > 0.3$). By comparing the normal forward view and narrow forward view, they also found that the benefit of forward view was not influenced by the view size as long as the central forward visual field was available.

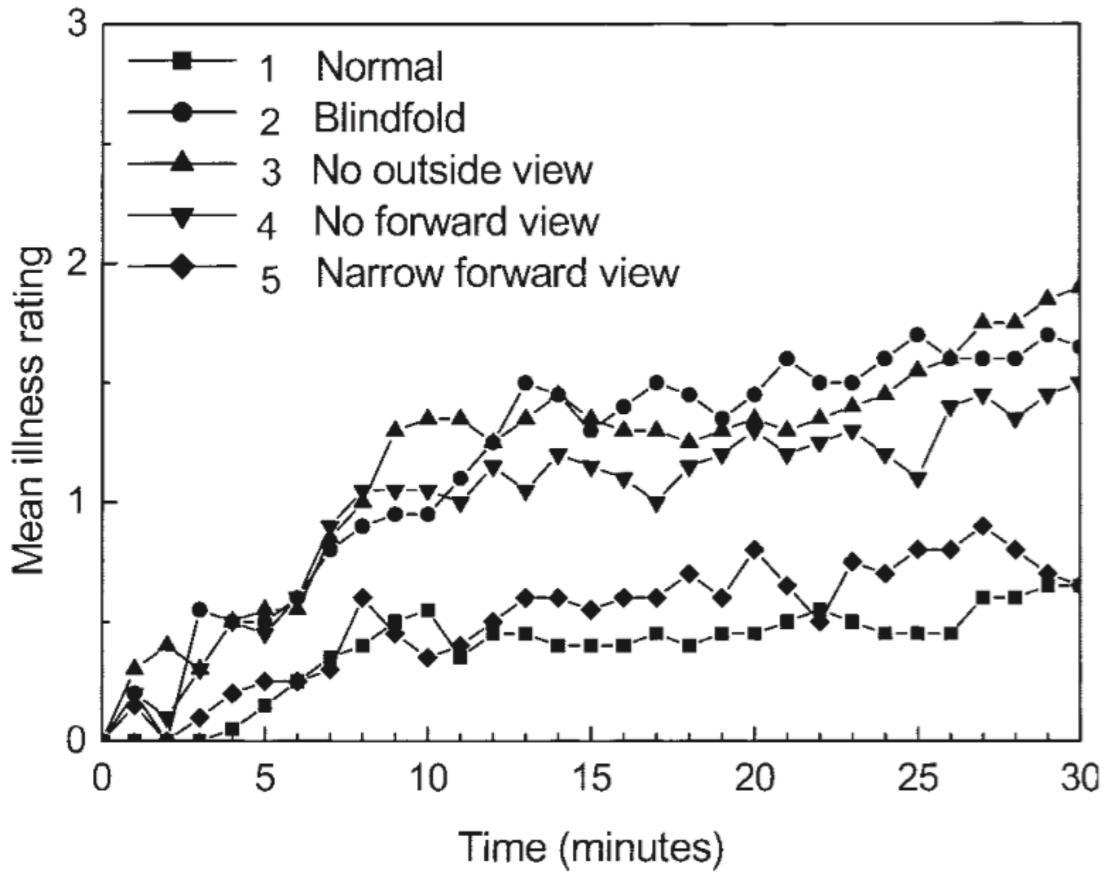

Fig.1.5 Mean illness ratings on a scale from 0-6 over 30 min with five viewing conditions as car passenger (Griffin & Newman, 2004)

Compared with internal vision or no vision, external vision in cars could provide visual information in earth-fixed frame that is a reference for passengers to estimate their head motion, so that the visual-vestibular conflict will be minimized. Furthermore, passengers can view the road which is followed with a forward external vision, which provides anticipatory information about the vehicle motion, such as when to brake and when to steer. With the anticipation, the internal model of passengers' central nervous system could adapt and be updated, for which the conflict between current senses and expectation will further reduce.

However, people are increasingly willing to regard the vehicle as a living space rather than simple transportation especially for autonomous vehicles. One of the aims of developing autonomous vehicles is to provide private space and free-time during driving, so that passengers are not required to monitor the road anymore, on the contrary, they are able to participate in internal-vision activities such as watching laptops or reading books. Such internal-vision activities were found to increase the risk of motion sickness (Griffin & Newman, 2004). Visual-vestibular conflict should be the chief culprit in inducing carsickness with internal visual tasks, when the passengers are looking at objects relatively stable to their bodies which are telling them that they are in still posture while their bodies are actually oscillating with the vehicle. Symptoms could be even worse if the passengers are watching moving images (e.g., watching movies) in the vehicle especially when the display is relatively large – visually induced motion sickness could be involved. The sensory conflict theory appears to implicate that vection (the illusion of self-motion when viewing a moving scene) is a cause of visually induced motion sickness (Webb, 2000), where passengers may experience an illusion of additional body motion resulting from watching the images moving on the display, and the conflict thus further increases between the illusionary motion and the actual body motion.

Interestingly, not only could the visual field influence MSI but it could affect passengers' head and body motion and stability. Although no previous study has investigated the effect of visual conditions on passengers' head stability in vehicles, correlations possibly exist. For example, the vestibular feedback in head-neck stabilization is assumed to increase with presence of visual information (Happee et al, 2017) that minimizes head translations and rotations in earth-fixed frame regardless of body motion caused by vibrating vehicle seats, in other words, head-in-space stabilization is possibly improved by the integration of external vision and vestibular senses. On the contrary, with internal vision due to activities like reading or viewing electronic devices, passengers may attempt to stabilize their gaze and heads relative to the books or screen which could result in larger head movements in space. Larger head movement or less head stability, naturally, increases vestibular stimulus as well as visual-vestibular conflict.

Turner and Griffin (1999a) first related the superiority of forward view to levels of vehicle motion during a survey of 3256 coach passengers, where illness ratings were found being influenced by different visibility significantly only when the acceleration-resulted motion sickness does value was above 12 ms-1.5 (for MSDV lower than 12 ms-1.5, $p = 0.36$; for MSDV from 12 ms-1.5 to 14 ms-1.5, from 14 ms-1.5 to 16 ms-1.5 and higher than 16 ms-1.5, $p < 0.001$). Turner's study provided a new research orientation, whose analysis however was only based on the accelerating-amplitude data measured by the accelerometers on the vehicle that was not consistent with the actual head motion of passengers as explained before. Additionally, subjects in Turner's survey were involved in natural activities without limitation on visibility during journey, who were only asked about their visions most of time treated as visibility of the whole journey. Therefore, the relationship between the effect of visibility and passengers' motion scenario still needs to be investigated by a more scientific method.

1.5 Present study

Although the sensory conflict theory is widely accepted relating the motion sickness to contradictory sensory perception between vestibular-perceived body motion and vision, several studies showed that people may adapt their body motion voluntarily depending on their visual information (Smart, Pagulayan & Stoffregen, 1998, Owen, Leadbetter and Yardley, 1998), as the ecological theory indicated. However, the voluntary body motion in nauseogenic motion environments has not been investigated in motion sickness studies. And whether this voluntary movement will affect the motion sickness level is still unknown.

As for the effect of vision in carsickness, experimental validations are still deficient, especially field tests. The field test is more uncontrollable with respect to variables; however, it is more natural and can better mimic real-life situations. Though the drawback of the field test is that it is hard to realize a motion in single direction or at specific frequency for analysis, unlike the simulator environment, the experiment in a real car could provide the actual body-car interface as well as a visual scene in earth-fixed coordinate system with no concern about the resolution or real-time performance of such scenes. The actual body-car interface, as the ecological theory mentioned, could imply the participants adapting different postural control strategies compared with the interaction with a car simulator, and affect the occurrence of motion sickness symptoms by affecting their postural stabilities. The actual visual scenes, as the sensory conflict theory indicates, plays an important role in visual perception and sensory integration which results in motion sickness as well. No matter which motion sickness theory is accepted, the motion sickness field test is more advantageous as long as the motion scenario can be controlled.

In this thesis, a motion sickness field experiment of a manually driven car has been executed. Two visual conditions were designed to investigate the relationship between the provided vision in cars, participants head and body motion and their degree of motion sickness. The two visual conditions are: 1. EYES-ON-ROAD – natural external vision for passengers; 2. EYES-OFF-ROAD – totally internal vision with blocks in the car. Lateral accelerations with frequency around 0.2 Hz was designed as motion scenario. This was realized by continuous S-shape slaloms on a straight road. The frequency chosen was shown in previous studies to be the most aggravating to motion sickness. The car velocity (25 km/h), slalom amplitude (3.5 m) and the experiment duration (30 mins) were designed with respect to an appropriate MSDV that is supposed to induce medium nausea in the population. The car was expected to manually realize the designed lateral acceleration with the driver instructed by a metronome. Except from the visual condition, the other possible variables – driver, car motion scenario, participants position (at the middle of rear seat) and instructed straight-sitting posture as well as the temperature and pressure inside the car, were kept the same between the two conditions. During the trials, the head and body motion of participants was measured by the Xsens MVN capture system, and the car motion was measured by the Xsens MTi-G IMU system. Participants were also wearing electrocardiography (ECG) and galvanic skin response (GSR) for physiological measurements which are reported in another thesis (Kenny Lie). Motion sickness level for the participants was measured by the Misery Scale (MISC) subjectively reported by the participants and recorded every minute during the trials.

The motion sickness assessment questionnaire (MSAQ) was filled out by the participants after each trial and indicates their severity of specific motion sickness symptoms. 23 participants joined the experiment and 18 of them finished both visual conditions in two sessions. Results were compared within these participants.

This study tries to validate the positive effect of external visual condition on carsickness as previous studies have suggested. The relations between this effect and passengers' head and body motion was further explored and examined in both time and frequency domain. Passengers' head and body motion may reveal their body control strategies and postural instabilities under different visual perception, thus provide positive or negative evidence for both the sensory conflict theory and the ecological theory. This thesis involves 4 hypotheses:

H1) External vision is beneficial in alleviating motion sickness symptoms compared with internal vision, in line with previous studies.

H2) Passengers' head and body motion are influenced by their visual fields.

H3) According to the ecological theory (Riccio & Stoffregen, 1991), the participants' postural stability could be reflected in their head and body motion, could be an indicator of motion sickness susceptibility (more head and body motion in sensitive participants).

H4) The participants' postural stability could change in time, with increased MSDV or the accumulated motion sickness symptoms.

The 4 hypotheses are all based on the sensory conflict theory and the ecological theory, and the principle of how vision affects carsickness is investigated.

2. Methods

2.1 Apparatus

Road and Vehicle*

For this experiment, TU Delft and the municipality agreed on closing Heertjeslaan in both directions from intersection with Huismansingel to intersection Molengraaffsingel for 14 work days. Companies in direct surrounding were notified in advance for the road closure. As required by the authorities, at both ends of the road, fences and cones were placed. Also, the assistants had to be near the closure to warn and provide information to road users that wanted to pass, as well as guarantee safety for both experimenters and road users. The total length of the road is approximately 240 meters and 10 meters wide (Fig.2.1a).

The vehicle that is used to do the experiments with, is the TU Delft's driverless Toyota Prius (Fig.2.1b). It is being equipped with TU Delft's technology to enable self-driving capabilities and provides a platform for researchers to work with. At first, automated driving was planned and routes were pre-programmed to keep the driving path conditions consistent, but during the testing period, the automation was temporarily disabled for an upgrade, therefore the Prius had to be manually driven. In and on the vehicle, different equipment was pre-mounted for the existing systems (e.g. in the trunk, in the center console, stereo-camera behind the front windshield etc), but did not hinder the participants nor the experiment in any way (vision, airflow, noise etc.). The equipment also did not change throughout the course of the experiment.

Participants were requested to sit in the center position of the back seat and wear seatbelt. During pilot tests, it was noticed that some of the participants slid off with their buttocks from the center seat towards either side, due to the relative slippery surface and the shape of the seat. This was solved by placing a friction mat on the backseat area. Since temperature might affect motion sickness, the air conditioner was turned on and set to 18 degrees Celsius with the blower on max on all trials to control for temperature(ref). The weather and road conditions were similar during all the trials.

(a)

(b)

Fig.2.1 TU Delft’s driverless Toyota Prius being manually driven on the experiment road – (a) road; (b) vehicle

Xsens MVN Motion Capture System

The Xsens MVN link system was used to measure the orientation and motion of participants' head as well as upper body during each session. Specifically, the MVN system is a fully ambulatory system for human full-body inertial kinematic measurement, which consists of miniature body-worn inertial sensors (MTx), containing 3D linear accelerometers, 3D rate gyroscopes, 3D magnetometers and a barometer, and wireless communication solutions. By integrating the gyroscope and accelerometer signals, the orientation and position of each body segment can be estimated continuously based on a biomechanical model of human body. Meanwhile, drift errors resulting from the presence of sensor noise, signal offset and orientation errors are corrected during the integration. The sensor fusion scheme is shown in Fig.2.2.

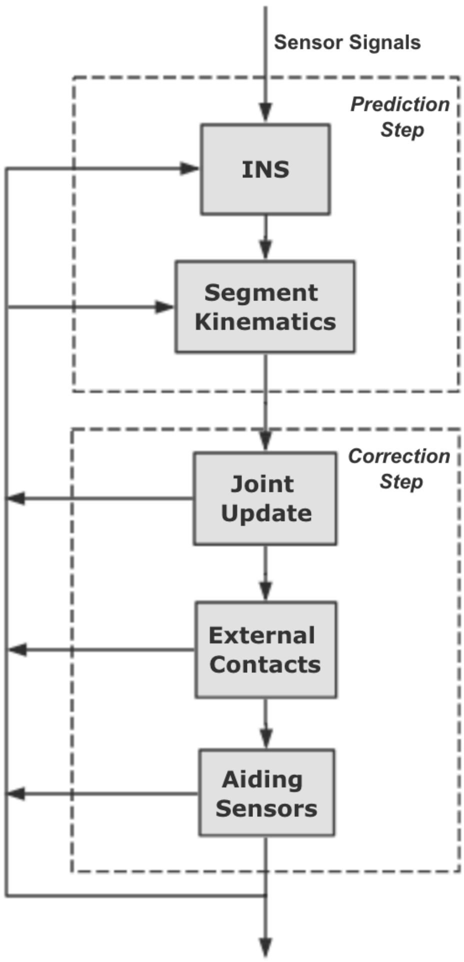

Fig.2.2 MVN sensor fusion scheme (Roetenberg, Luinge & Slycke, 2013)

In the prediction step, the signals of sensors are processed by the inertial navigation system (INS) and segment kinematics followed to generate the signals of body segments. Orientations of sensors are calculated from integrating the angular velocities measured by rate gyroscopes with respect to the initial angle information in global frame. With the linear accelerometers, combined linear accelerations and gravity components can be measured, where velocities and positions are calculated from. The segment kinematics, based on a biomechanical model, assume that the sensors are attached to the subject's body segments and that the body segments are rigidly linked by joints. For each segment, position of joint origin and length of segment are known through pre-setting the subjects' body dimension, when the position of any point on the segment can be calculated providing orientation. However, with the rigid-body assumption, effects of skin and soft tissue artifacts have been ignored which actually influence the accuracy of sensors – a correction step was added to bring uncertainty in and avoid cumulative errors.

For correcting the sensor noise and errors during the integration step, the correction step continuously updates the parameters for the prediction and integration based on, for example, joint relations (correcting position of segments), magnetic sensors (correcting rotation errors about the vertical), contact constraint (updating kinematics), other aiding sensors such as GPS, etc. The MVN system has been validated in standing subjects in a stationary environment (Faber et al., 2016, Damgrave & Lutters, 2009), Wedmark and Janson (2018) also succeeded to validate the pelvic orientation angles captured by the MVN system with subjects sitting in a driving vehicle with the full body suit. However, it was inconvenient and unnecessary to use the full body suit in this experiment, where only the upper body trackers were used. We are not aware of validation for both acceleration and orientation provided by the MVN system upper-body mode with participants seated in a moving vehicle. Thus, we used the 'multi-level scenario' in the MVN Analyze sofeware which does not require the strict single-level interaction between participants and ground when collecting position and orientation data, and is better for sitting posture. Furthermore, we stored both the raw measurements and the 3D motion derived through sensor fusion, and checked the sensor fusion results. The processed acceleration of different body positions corresponds with the sensor acceleration in global frames.

The Xsens MVN link system contains 17 MTx trackers positioned on head, sternum, pelvis, hands, shoulders, upper arms, forearms, upper legs, lower legs and feet (Fig.2.3a). For the experiment in this thesis, passengers were required to sit in the car without leg movement, so only the upper body (namely head, sternum, pelvis, shoulders, upper- and for-arms) trackers were involved, connected at specified positions fixed by the MVN shirt as well as straps (Fig.2.3b). Connecting point and orientation of the sensor on each segment was further confirmed through calibrating procedure, done as soon as the participant was suit up during each session. A N-pose calibration was used in this experiment – the participant was required to start with a standing posture with arms beside body neutrally, then perform a walking movement for around 10 seconds. After the calibration step, the sensor-segment alignment and dimension of segment were re-estimated combining the information of participant body dimension.

(a)

(b)

Fig.2.3 Xsens MVN link system consisted of sensor modules – (a) complete suit (Roetenberg, Luinge & Slycke, 2013); (b) only upper body sensors were used in this experiment

Graphical and statistical output can be instantly generated and recorded through the MVN Studio (Fig.2.4) at a sampling rate of 120 Hz, where a MVNX. file can be exported and imported to Matlab for data analysis. The MVNX. file includes the output of sensor fusion scheme such as position, velocity, acceleration, orientation, angular velocity and angular acceleration of each body segment as well as real timestamps read from computer at each sample. The dynamic accuracy of MTx trackers is 1deg RMS with gyroscope range ± 2000deg/s, and the accelerometer range is 16g. The original data is in global frame (earth-fixed reference coordinate system), defined as a right handed Cartesian coordinate system with positive (Fig.2.5):

- X pointing to the local magnetic North.
- Y according to right-handed coordinate system (West).
- Z pointing up.

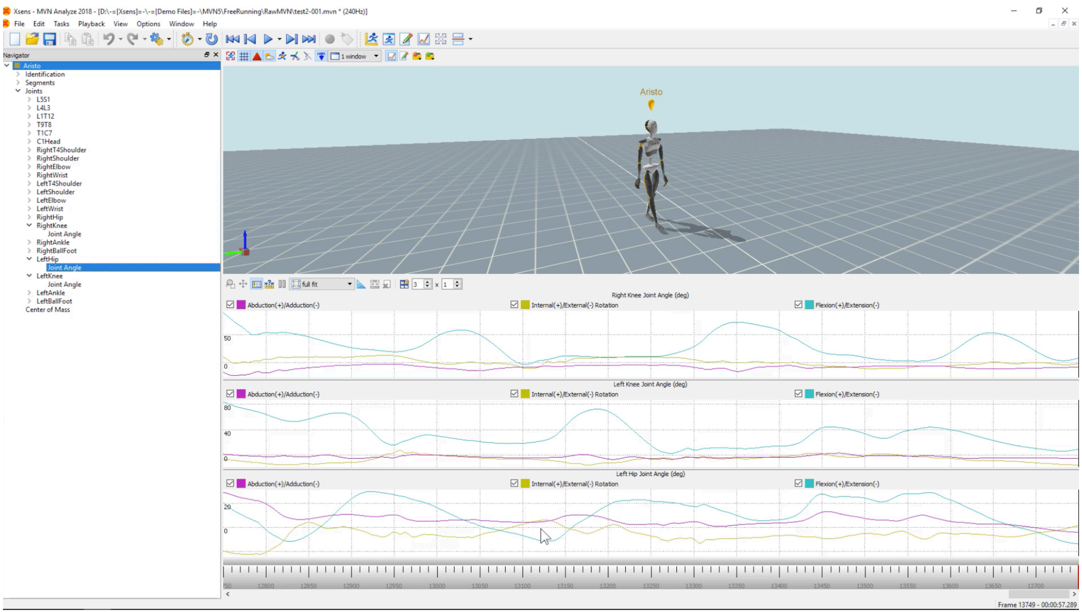

Fig.2.4 MVN Studio Interface (from tutorials Xsens, https://tutorial.xsens.com/)

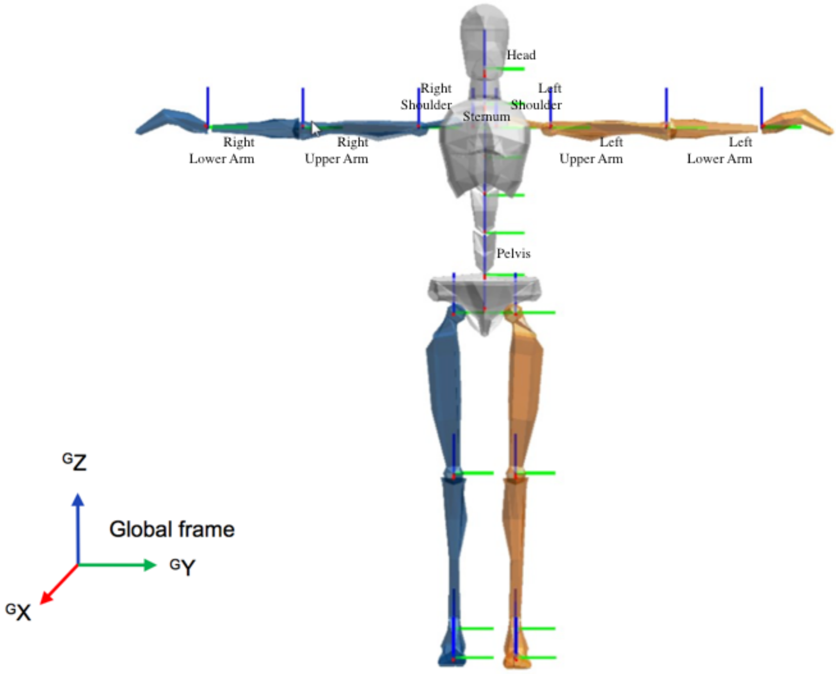

Fig.2.5 Segment coordinate system is aligned with global coordinated system when the subject is standing in T-pose (the location of trackers used in this experiment has been labelled) (MVN User Manual, 2017)

Xsens MTi-G

In order to measure the actual vehicle motion during the journey, the Xsens MTi-G (Fig.2.6), which is an integrated GPS and micro-electro-mechanical system (MEMS) inertial measurement unit (IMU) with a Navigation and Attitude and Heading Reference System (AHRS) processor, was positioned under the participant's seat (MTi-G User Manual and Technical Documentation, 2010). The MTi-G includes MEMS inertial sensors, a GPS receiver, a 3D magnetometer and a static pressure sensor, providing GPS enhanced 3D orientation estimates (drifted in this experiment), calibrated 3D acceleration in local frame and 3D rate of turn. The update rate of the MTi-G is around 90 Hz in this experiment, the signal of which was later resampled to realize a common frequency as the MVN system before data analysis. Real timestamps were recorded together with samples corresponding to the computer clock, and the timestamps of the MVN system as well, so that the two signals could be synchronized.

Fig.2.6 the Xsens MTi-G hardware (MTi-G User Manual and Technical Documentation, 2010)

2.2 Experiment Conditions*

Motion

To investigate motion sickness, it was necessary to induce provocative motion to the participants with the car. It has been shown in previous studies (O'Hanlon and McCauley, 1973, Donohew and Griffin, 2004) and in the ISO norms (ISO 2631-1, 1997), that in either longitudinal, lateral or vertical direction, motion sickness is caused mostly by accelerations around 0.16-0.20 Hz frequencies. Compared with the longitudinal accelerations, the vehicle lateral acceleration could result in more symmetric passenger's motion which is more synchronized with the car motion, due to the backrest. Besides, the lateral motion can provide more visual cues as well as anticipatory information if the passengers are looking at the forward road, where more effects of vision could be expected. Therefore, different road scenarios have been considered with frequencies ranging from 0.16 Hz to 0.2 Hz for lateral accelerations. The choice of the paths and velocities of the sickening drive was mostly determined and limited by the physical properties of the designated road, frequency range.

Knowing that motion sickness in vehicles usually develops in 20 to 30 minutes onwards and that the aim of this research is to investigate motion sickness caused by lateral acceleration in a realistic setting. The lateral acceleration has been selected in a relatively high range in order to make most of the participants reach slight nausea but not too sick in 20-30 minutes. The relatively-highly aggressive motion could acquire a larger range of MISC reaching the maximum of 7 which is easier for observing the growth in time and comparing between conditions. While the drawback of a high-acceleration motion that some of the participants could stop the session before 30 minutes and the different lengths of trials cause some troubles in time-domain data analysis. Furthermore, the lateral acceleration should fall within 0.1G and 0.4G to mimic similar conditions in urban driving and for safety reasons in case of the maximum 0.4G. Similarly, this holds true for the velocities from 15 to 30 km/h that has been considered. Another point that has to be taken into account is the drivability of the chosen path, as it has to be driven manually. The constraints of motion scenario are shown in Table 2.1.

Table 2.1 Design test criteria

Road width, max amplitude	8 m, 3.5 m
Road length	240 m
Frequency	0.16 – 0.2 Hz
Velocity	15 – 30 km/h
Peak lateral acceleration	0.1G – 0.4 G

Due to the constraints of the road and the focus on lateral acceleration of this research, a slalom path has been opted for. With this, the longitudinal, lateral acceleration, velocity and therefore its frequency, can be controlled for. Then matlab scripts were used to generate different sinusoidal paths with the aforementioned design constraints and its MSDV for comparison. The turning radius of the Toyota Prius is 5.5 meters, so for the experiment drive, it was necessary to make a 3-point u-turn upon reaching the end of the road. Considering drivability and optimum road usage, a slalom path with the following properties (Table 2.2) has been chosen:

Table 2.2 Motion scenario with slalom path

Amplitude	3.5 m
Road length	220 m
Frequency	0.175 Hz
Velocity	25 km/h
Lateral acceleration	0.4 G

The reference slalom (single section without u-turn) is depicted in Fig.2.7. To drive the intended slalom with the specific frequency, the driver set up a metronome with 21 bpm as reference to drive the slalom (0.175*60*2 = 21 for a signal per turn). The path length has been shortened to incorporate the 3 point u-turns and to handle a safety margin at the ends of the road. Throughout all the trials, the driver also was required to keep the velocity of vehicle as constant as possible and to take the 3 point u-turns as consistent as possible. A realized motion is shown in Fig.2.8.

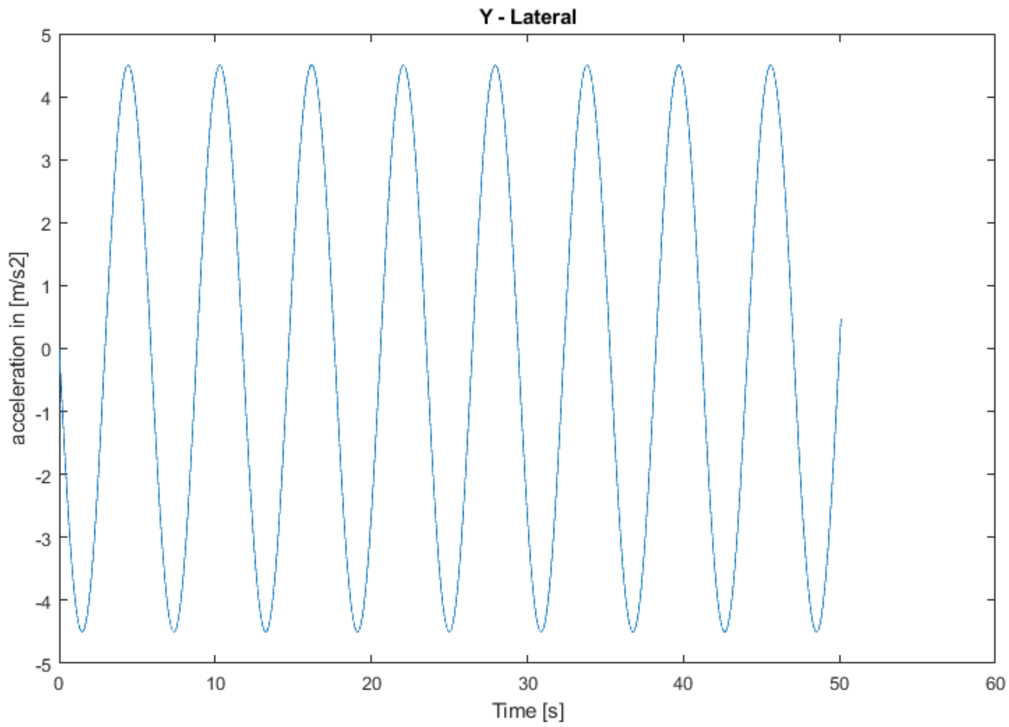

(a)

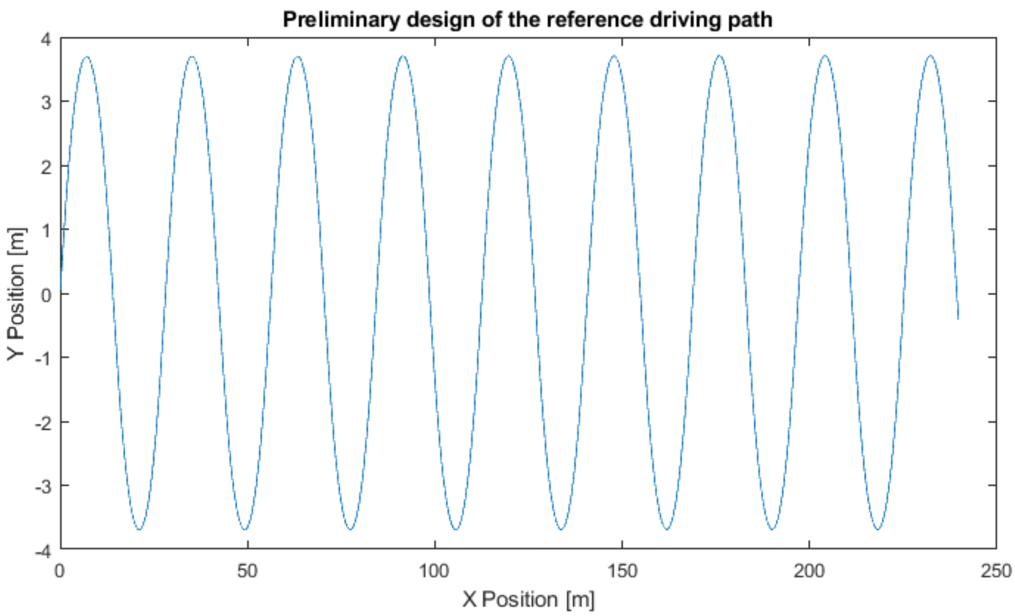

(b)

Fig.2.7 Designed vehicle movement for one slalom – (a) lateral acceleration; (b) path

Fig.2.8 Vehicle movement during experiment

Vision

All the participants finished two sessions with two different visual conditions in this experiment. The two conditions were tested on different days, and the order of the two conditions were balanced by Latin Square (half of participants did EYES-ON-ROAD condition first and the remaining half reversed). In both visual conditions, the participants were always seated in the middle of rear seat which ensured clear and broad road vision when there was no blockage between the passenger and the windscreen, and the participants were also asked to maintain the same straight-up sitting posture and facing forward with no active head or body pitching, rolling or yawing, while ensuring legs planted adequately wide for stability. A friction mat was positioned on the rear seat to prevent body slide of passengers during the car turning. To ensure the presence of external vision and internal vision, closing eyes is not allowed during all sessions.

- **EYES-ON-ROAD condition.** During the sessions with EYES-ON-ROAD condition, the participants were asked to always forward view the external environment of the vehicle without any blockage in the car, provided considerable both foreground view and peripheral view with road information.
- **EYES-OFF-ROAD condition.** During the sessions with EYES-OFF-ROAD condition, the participants were asked to view forward as well but with cardboards both in front of the rear seats and on the side windows, so that neither foreground view nor peripheral view was provided to the rear-seat passengers compared with EYES-ON-ROAD condition. The blocking cardboards are pure white without any mark or pattern that could provide visual cues for passengers.

Fig.2.9 Eyes-off-condition in the vehicle

Previous studies suggested that passengers with eyes on road tend to suffer from less motion sickness symptoms than those with eyes off road due to earth-fixed visual cues and anticipatory information provided by forward vision which are helpful for the passengers to estimate their body motion (Turner & Griffin, 1999, Griffin & Newman, 2004). In this experiment, cardboards in the EYES-OFF-ROAD condition positioned in front of the participants was to block all the outside visual cues and anticipation which was fully provided in the EYES-ON-ROAD condition.

In natural life, situations with EYES-OFF-ROAD riding are always accompanied by visual and mental tasks, such as reading and watching electronic displays. Such visual tasks were initially considered to add in this experiment for EYES-OFF-ROAD condition to mimic natural driving as well as guarantee no external vision achieved by the participants, however, additional visual or mental tasks will introduce additional and uncontrollable variables between the two visual conditions. For example, additional visually-induced motion sickness could be involved by visual tasks like reading or watching stable images; mental tasks could affect passengers' motion sickness per se (Bos, Mackinnon & Patterson, 2005). Therefore, a task must be added to both visual conditions to neutralize the effect induced by itself, which will on the contrary influence the completeness of external vision for EYES-ON-ROAD condition. Simply blocking view is more scientific and controllable for creating EYES-OFF-ROAD condition, where literally effect of visual cues and anticipatory information of external vision can be investigated.

2.3 Motion sickness measures*

MISC

During the sessions, the severity of motion sickness symptoms was repeatedly measured by the 11-point MISC (MISC, Table 2.3, Bos, Mackinnon & Patterson, 2005). Specifically, for each 30-min session, the participants were required to rate their temporary illness using the MISC before the sessions, every minute during the sessions and after the sessions respectively, being asked by an assistant sitting at the front seat. Any participant indicating an MISC of 7 or up during the sessions would automatically stop driving immediately and the rest of ratings would be considered as the largest point he/she ever rated.

The subjective illness rating has been widely used in motion sickness researches, providing the most intuitive information about the incidence of motion sickness symptoms, which was more natural and convenient compared with physiological measurements such as measuring the skin conductance of subjects, and more sensitive and detailed compared to observational methods such as recording the percentage of subjects who vomited, which was not considered since vomit would cause unnecessary excessive suffering and would also reduce the turnout rate for the preceding sessions in our within-participant experiment. The illness rating form was able to measure the mild sickness symptoms that subjects were aware of rather than reaching emesis. In comparison with the traditional 7-point illness rating scale (Griffin & Howarth, 2000), the 11-point MISC used in this experiment exploited more various symptoms for the participants as a reference, avoiding individual differences in the occurrence of symptoms, for example, discomfort in either head or stomach was considered as the same degree of sickness. Once the participants were familiar with this scaling form before the sessions, they only took a few seconds to rate during the journeys.

The 11-point MISC has been validated in the experiment by Bos, Mackinnon and Patterson (2005), who studied the motion sickness symptoms in a ship simulator among 24 participants and found the maximum MISC values observed per participant per trial correlating linearly with the predicted MISC by his/her symptom checklist as well as MSSQ result.

MSAQ

To investigate the specific sickness related symptoms appearing among participants an additional symptom checklist was applied after the stimulus exposure. The MSAQ (Table 2.4) was explored and validated by Gianaros, Muth et al. (2001), involving motion sickness related symptoms in four dimensions – gastrointestinal (1, 5, 11, 15), central (2, 6, 9, 13, 14), peripheral (4, 8, 12), and sopite-related (3, 7, 10, 16). This multidimensional assessment was used after each trial for the participants to rate the severity of symptom in each dimension that has appeared during the travel.

Table 2.3 11-Point MISC (Bos, Mackinnon & Patterson, 2005)

Symptoms		**MISC**
No problems		0
Some discomfort, but no specific symptoms		1
Dizziness, cold/warm, headache, stomach/throat, awareness, sweating, blurred vision, yawning, burping, tiredness, salivation, …but no nausea	Vague	2
	Some	3
	Medium	4
	Severe	5
Nausea **7 = stop**	Some	6
	Medium	7
	Severe	8
	Retching	9
Vomiting		10

Table 2.4 Symptoms involved in MSAQ (Gianaros, Muth et al., 2001)

1. I felt sick to my stomach	9. I felt disoriented
2. I felt faint-like	10. I felt tired/fatigued
3. I felt annoyed/irritated	11. I felt nauseated
4. I felt sweaty	12. I felt hot/warm
5. I felt queasy	13. I felt dizzy
6. I felt lightheaded	14. I felt like I was spinning
7. I felt drowsy	15. I felt as if I may vomit
8. I felt clammy/cold sweat	16. I felt uneasy

2.4 Participants and Procedure*

Students and staff in Technology University of Delft were recruited to participate in our experiment. The Motion Sickness Susceptibility Questionnaire (MSSQ, Griffin & Howarth, 2000) (Appendix A) was first finished by the candidate participants for pre-screening. The MSSQ investigated the participants' travelling, illness and vomiting frequency respectively in cars, buses, coaches, small boats, ships, aeroplanes and trains in the past, and the candidates who indicated that they had never suffered from any motion sickness symptoms as a passenger in any mode of transport were excluded for this experiment. A total of 23 healthy participants participated in this experiment, with only 18 finished 2 trials with both visual conditions and 11 with available motion data. Based on the 18 participants, the MISC analysis was performed and based on the 11, motion analysis was performed. Table 2.5 shows the gender, age and susceptibility score based on MSSQ of the participants and a population reference. The participants in our experiment have relatively higher susceptibility compared with population especially in median and 75th percentile. No participant had suffered from any serious illness or injury or was under any relevant medical treatment.

Table 2.5 Participants gender, age and susceptibility
(population reference: Griffin & Howarth, 2000)

		23 participants (total)	**18 participants (MISC analysis)**	**11 participants (body motion analysis)**	**Population Reference**
Gender		Male: 17 Female: 6	Male: 14 Female: 4	Male: 9 Female: 2	Male: 333 Female: 0
Age		30.0 (SD = 128.7)	28.4 (SD = 98.9)	25.9 (SD = 7.4)	18-26
Susceptibility (MSSQ) (range: -2-	minimum	-2	-1	-1	-2
	25th percentile	5.5	5.25	5.5	4
	median	17	16	18	9
	75th percentile	25	27.25	26.5	17
	maximum	64	64	35	69

The experiment was performed at the Research lab Automated Driving Delft (RADD, www.raddelft.nl). Tests were performed at the Heertjeslaan, in Delft, which was closed to other traffic during the experiment. Prior to each trial, the participant was invited to the RADD control room in the Green Village for preparation. The experimental procedure as well as the MISC were illustrated to the participant, followed by the informed consent form being signed. Then the ECG and GSR leads1 were attached to his/her body and the MVN suit with motion trackers were put on, in the meanwhile, the vehicle was being prepared according to the specific visual condition. After calibration of the MVN trackers, the participant was asked to board the vehicle, leaving for the road and starting a 30-minute journey. There was a driver and an assistant sitting in the car during the whole journey and the latter was responsible for setting up all the recordings and asking the participant to rate their MISC ratings every minute. After each trial, the car was stopped on the road while data was saved and the assistant kept on recording the participant's MISC to acquire recovery information. Until the participant regained a low MISC (2 or 3), the car was driven back to RADD and the participant was asked to fill out the MSAQ rating their symptom levels, while the next participant was being prepared.

All the participants took part in both two conditions with each condition one and a half hour (including preparation, testing and questionnaire). To minimize the effect of environment characteristics (e.g., temperature, humidity, etc.) and individual characteristics (e.g., diet, sleep, etc.), each participant experienced both trials at approximately the same time of the two days, with an average of one-week (minimum 2 days and maximum 20 days, Fig.2.10) interval between them for refreshing and eliminating the effect of habituation. Prior to each trial, the participant was required: 1. not to intake any recreational drugs (including alcohol) for at least 24 hours; 2. having a good night's sleep; 3. not to consume excessive food for few hours preceding the experiment. Such instructions ensure the participants were in as natural physical and mental state as possible.

Up to 4 subjects per day were tested from 10 a.m. to 4 p.m., and the experiment took 3 weeks (11 days) in total. To further prevent the possible habituation and order effect, the order of the conditions that each participant experienced was randomized by Latin Square, and final results were compared within subjects.

---

[1] ECG and Galvanic Skin Resistance (GSR) were collected and will be reported in the MsC thesis of Kenny Lie

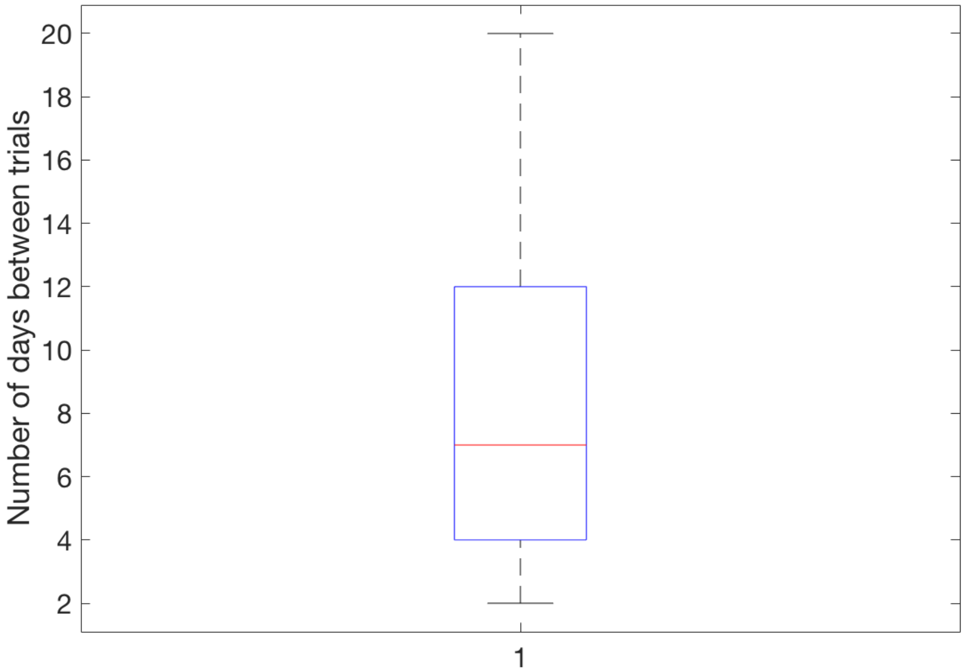

Fig.2.10 Days interval between the two trials for the same participant (mean: 8.4 days; SD: 4.8 days)

2.5 Data Analysis

Participants' body positions, velocities and accelerations were captured by the MVN system with a sampling rate of 120 Hz, and the vehicle accelerations were measured by the MTi system with a sampling rate around 90 Hz (not constant). To unify the sampling time, both data were resampled by a rate of 100 Hz (function resample in matlab), and set the exact and identical start- and end-time for each trial by checking the UNIX timestamps recorded in both systems.

The participant's MISC during the trial was recorded by an assistant every minute together with the time. The MISC could then be synchronized with the motion data. This section describes the methods that have been used in data analysis, including the quantification of motion sickness ratings, motion sickness dosage value with motion magnitude and duration, and how the motion data was processed to test the hypotheses.

MISC

MISC was the subjective illness rating recorded every minute during the trials, used for quantifying the MSI. Two indicators were used to quantify the motion sickness level for a participant in a specific trial based on the MISC he reported at every minute – 1. $MISC_{average}$; 2. $MISC_{rate}$.

For the 30-minute trials, the average MISC was calculated by dividing the total MISC of 0-30 minutes by the number of recorded MISC (31).

$$MISC_{average} = \frac{\sum_0^{30} MISC_{minute}}{31} \tag{2.1}$$

To ensure that all the trials For the trials with a duration less than 30 minutes (participants rated at 7 or quit due to illness), the $MISC_{minute}$ for the remaining minutes was defined as the maximum MISC the participant ever rated. The average MISC represents the overall illness level of a participant. The advantage of this averaging method is that the MISC information of the entire trial could be retained. Besides, compared with the maximal MISC which was often used as the illness level indicator in previous studies, the average MISC implies not only the highest level of participant's illness, but also the time he/she reached the highest level. In this experiment. For instance, most of participants in EYES-OFF-ROAD condition reached a MISC of 7 before 30 minutes, while the ones who reached 7 earlier will have a higher average MISC. However, this indicator may not contain so much information about the time someone quit. Thus the MISC rate was also examined as a more extreme indicator.

The MISC rate was the highest MISC the participant rated divided by the time of its first occurrence in minutes for a trial (Eq.2.2). This indicator keeps the information of both maximal MISC and the time a participant reached the maximal MISC, but the disadvantage is that the information on the time history of MISC across entire trial is lost.

$$MISC_{rate} = \frac{MISC_{max}}{Minute_{MISC_{max}}} \tag{2.2}$$

MSDV

After the trials, the overall motion condition of the vehicle could be integrated from the vehicle translational motion magnitude, frequency and duration by using the MSDV, which is defined in ISO 2631-1 (1997):

$$MSDV = \left[\int_{t=0}^{t=T} a_w^2(t)dt\right]^{\frac{1}{2}} \quad ms^{-1.5} \tag{2.2}$$

$a_w(t)$ is the root mean square of three frequency-weighted translational accelerations. The frequency weightings for vertical acceleration (ISO 2631-1, 1997) was used in this thesis for all the three accelerations, in order to combining the frequency characteristics with the acceleration magnitudes. The integration of the frequency-weighted accelerations determines the accumulation of motion sickness dose during time, where the square root indicates that the duration is less influential than the motion magnitude regarding motion sickness (Lawther & Griffin, 1986).

Coordinate System

The fused data from the Xsens MVN system was provided in the earth-fixed reference coordinate system defined as the right-handed Cartesian coordinate system (Fig.2.5). While the data of Xsens MTi IMU system was recorded in car local frame with the orientation to the Cartesian coordinate system provided. Therefore, the motion data of the systems should be rotated before comparing in the same coordinate frame using the orientation measurement.

The orientation recorded in the Xsens MVN system is a unit quaternion vector $\vec{q}$ at each sample, representing a rotation about a unit vector $\vec{n}$ through an angle α:

$$\vec{q} = \left(\cos\frac{\alpha}{2}, \vec{n}\sin\frac{\alpha}{2}\right) = (q_0, q_1, q_2, q_3) \quad (2.3a)$$

From the quaternion vector, a rotation matrix from body local frame to global frame can be converted:

$${}_{B}^{G}R = \begin{bmatrix} q_0^2 + q_1^2 - q_2^2 - q_3^2 & 2q_1q_2 - 2q_0q_3 & 2q_1q_3 + 2q_0q_2 \\ 2q_1q_2 + 2q_0q_3 & q_0^2 - q_1^2 + q_2^2 - q_3^2 & 2q_2q_3 - 2q_0q_1 \\ 2q_1q_3 - 2q_0q_2 & 2q_2q_3 + 2q_0q_1 & q_0^2 - q_1^2 - q_2^2 + q_3^2 \end{bmatrix} \quad (2.3b)$$

By which the translational acceleration (in terms of longitudinal, lateral and vertical acceleration) in body local frame $\vec{a}_B$, for example, could be rotated in global frame $\vec{a}_G$:

$$\vec{a}_G = {}_{B}^{G}R * \vec{a}_B \quad (2.3c)$$

Motion Data Analysis in Time Domain – filtering, quantification and windowing

In this thesis, the body lateral acceleration and roll are defined as the two dependent variables examined between conditions as they were dominant movements excited in the experiment (Fig.3.16). The motion data analysis was divided into two parts – 1) absolute motion of different body segments and 2) relative motion between head and other body segments. The absolute motion provides insight in actual postural stability in space and seat to head transmission. While the relative motion provides insight in the pelvis, lumbar and neck motion contributions to postural stability and transmission from torso to head. Both absolute and relative motion were analysed in time and frequency domain.

As for the body motion data, both lateral acceleration and roll were based on the processed data from the Xsens MVN biomechanical model calculated for the center of mass of each body segment in global frame. The processed data was then rotated in the local frame of each segment for analysis. Regarding the car motion data, however, only raw acceleration data in car local frame provided by the Xsens MTi-G system is available. The orientation data of the Xsens MTi-G system contains a large drift that could not be corrected. Therefore, for the motion analysis in time domain, the processed lateral acceleration and roll angles of body segments were used, as well as the raw lateral acceleration of the vehicle.

It was proved that motion sickness was only related to low-frequency motion below 1 Hz (Donohew and Griffin, 2004). All the motion data were bandpass filtered before time domain analysis, using a 3rd order Butterworth filter with a bandpass frequency of 0.05-1 Hz. The low cut-off frequency was to remove some system drifts observed in the original orientation data.

To quantify the lateral acceleration and roll in time domain, the root mean squares of the two signals were calculated separately representing the amplitude of the overall motion. Any non-zero acceleration in space would affect the vehicle and participants' body motion and is possible to influence the body posture and MSI, so that the root mean squares of the filtered acceleration was directly calculated that could represent the mean amplitude of non-zero acceleration. For the roll angles, on the contrary, what matters is the deviation and sway from the balance or the original position, rather than the mean magnitude. The root mean square of roll could quantify this sway in time only if the mean roll is always zero. While the original roll angle might be biased from zero due to the calibration or the usual posture of different participants. Thus, the roll data were first corrected for its non-zero mean, followed by the root mean square being calculated to indicate the body sway in angles around longitudinal axis.

Specifically, for body motion with respect to the vehicle, the root mean square of body lateral acceleration was normalized by dividing the root mean square of car acceleration (Eq.2.4). The reason is that the car was driven manually, resulting in a marginal difference in the acceleration between trials, the ratio of root mean square could provide information of the relative motion amplitude of body in the vehicle. The ratio should be always lower than 1 as the participants' body were 'thrown' to the opposite direction due to inertia when the vehicle was accelerating. If the ratio is more approaching 1, it implies that the participant was managing to synchronize their body with the car and the two had similar accelerations in space.

$$Amplitude_{body\_to\_car} = \frac{rms(a_{yB})}{rms(a_{yC})} \tag{2.4}$$

The roll movement of the participants' body was simply compared in global frame. It is assumed that the car roll movement was the same throughout all the trials, although which is hard to be proved, because there was no accurate car rolling data provided as explained before.

As for the relative motion between body segments, the head acceleration as well as roll were rotated into the sternum and pelvis local frame respectively based on the orientation data provided, and the relative acceleration $a_{head\ to\ body}$ was calculated by subtracting the acceleration of sternum or pelvis itself (Eq.2.5).

$$a_{head\ to\ body} = {}^{B}_{G}R * {}^{G}_{H}R * a_{head} - a_{body} \tag{2.5}$$

a_{head} and a_{body} are the acceleration vectors in head and body (sternum and pelvis) local frame. ${}^{G}_{H}R$ and ${}^{B}_{G}R$ are rotation matrices respectively from head local to global frame and from global to body frame (Eq.2.3b). The relative acceleration and roll was also quantified by calculating the root mean squares.

A windowing procedure was used to analyze the data throughout time to investigate the evolution of movement during exposure to the aggressive lateral motions (Stoffregen, Chen & Koslucher, 2014). 2-min non-overlapping windows have been examined throughout the time to see the overall trend of movement within trials. For each window, the ratio of root-mean-squared body-to-car acceleration (Fig.3.11a), the root mean square of body roll (Fig.3.12a) and the root mean squares of relative roll and lateral acceleration between head and other body segments (Fig.3.22a & 3.23a) were calculated and grouped in a new time series while the window moving forwards, showing the evolution of movement amplitude.

Three windows were also extracted in each trial to examine the statistical significance within and between conditions. Although the duration of each trial varied hugely – the shortest trial lasted for 6 minutes and the longest for 30 minutes as preset, it is unfair and most information will be missed if only the first 6 minutes was examined and the exposure time was set the same for all the trials (Stoffregen, Chen & Koslucher, 2014). Since no apparent difference could be observed in the window-checking throughout the entire duration for any trial (Fig.3.11a, 3.12a, 3.22a, 3.23a), the three 2 minute windows were extracted from the beginning, middle and end of each trial duration where the statistical analysis was processed (Fig.3.11b, 3.12b, 3.22b, 3.23b).

Motion Data Analysis in Frequency Domain – cumulative power, coherence and transmissibility

The motion signals were examined in frequency domain by Fourier Transform (fft in matlab). The normalized single-sided spectrum as well as the cumulative power were shown in figures (Fig.3.2, 3.16). The latter was the cumulated power for each frequency based on the spectrum, and could demonstrate how the power of signals distributed in frequencies. For examining the distribution of frequencies in time, a spectrogram was shown as well (Fig.3.17), using spectrogram in matlab with 8 segments and 50 percent of samples overlapped between segments.

To investigate how the aggressive lateral movement is transmitted from vehicle to passenger's body, transmissibility and coherence from lateral accelerations of the car to both lateral and roll accelerations of various body segments (lower-back, sternum and head) were investigated using the cross-spectra density method (CSD) (Zheng, Qiu & Griffin, 2012), which are:

$$T_{y_c y_{b_i}} = \frac{G_{a_{yc} a_{yb_i}}}{G_{a_{yc}}}, \qquad \gamma^2_{y_c y_{b_i}} = \frac{\left|G_{a_{yc} a_{yb_i}}\right|^2}{G_{a_{yc}} G_{a_{yb_i}}} \tag{2.6}$$

$$T_{y_c r_{bi}} = \frac{G_{a_{yc} \ddot{\varphi}_{b_i}}}{G_{a_{yc}}}, \qquad \gamma^2_{y_c r_{bi}} = \frac{\left|G_{a_{yc} \ddot{\varphi}_{b_i}}\right|^2}{G_{a_{yc}} G_{\ddot{\varphi}_{b_i}}}$$

$T_{y_c y_{b_i}}$, $T_{y_c r_{bi}}$ and $\gamma^2_{y_c y_{b_i}}$, $\gamma^2_{cr_{bi}}$ are transmissibility and coherence for lateral and roll accelerations from car to body segment b_i respectively. $G_{a_{yc}}$, $G_{a_{yb_i}}$ and $G_{\ddot{\varphi}_{b_i}}$ are the power spectral densities of lateral accelerations for car, body segment and roll accelerations for body segment, calculated by function pwelch in matlab. $G_{a_{yc} a_{yb_i}}$ is the cross spectral densities of lateral accelerations for car and body, and $G_{a_{yc} \ddot{\varphi}_{b_i}}$ is instead the cross spectral densities of car lateral accelerations and body roll accelerations, which are calculated by function cpsd in matlab. With the two matlab functions, the Welch's periodogram has be performed to smoothen the signals, with Hamming windows of 3000 samples (30s) and 2000 samples overlapping (20s) (The resulting frequency resolution is 0.0244Hz). The full datasets for all the trials were used for calculating the spectral densities. Although the datasets have various lengths between trials due to the different durations, the chosen Hamming Window is relatively small so that the datasets were divided into 40 to 180 segments. It is assumed the difference in length of datasets would not affect the Welch's periodogram with such a large number of segments.

The coherence indicates the linearity between input and output – seat motion and body motion in this experiment. However, the coherence calculated by Eq.2.6 using the limited number of observations is only an estimation, which means a positive estimated coherence could be false detected with a risk α, and the false positive rate will increase when there are fewer observations. Therefore, a significance threshold of coherence $\gamma^2_{th}(\alpha)$ is defined as (Gallet & Julien, 2011)

$$P\left|\hat{\gamma}^2(f) > \gamma^2_{th}(\alpha) \mid \gamma^2(f) = 0 \right| = \alpha \tag{2.7}$$

That is, we only accept the actual coherence $\gamma^2(f) > 0$ at the significance level α if the estimated coherence $\hat{\gamma}^2(f)$ larger than the threshold $\gamma^2_{th}(\alpha)$. With n observations involved for deriving the estimated coherence (the number of participants for each examined condition in this experiment), the significance threshold of coherence at level α can be calculated by (Thompson, 1979)

$$\gamma_{th}^2(\alpha) = 1 - \alpha^{\frac{1}{n-1}} \tag{2.8}$$

The Welch's periodogram method with overlapping samples has been used in calculating the spectral densities, which is said to influence the significance threshold by increasing number of degree of freedoms (Gallet & Julien, 2011). By using Welch's method, although the number of divided segments of motion signals varies between different trials with different number of samples, it is comparatively large for all of the trials with the window of 3000 samples and overlapping of 2000 samples (40-180 segments). Large number of Welch segments makes the significance threshold small enough within each trial and could be ignored (Gallet & Julien, 2011). So, the significance threshold for coherence was simply estimated by Eq.2.8 in this thesis only depending on the number of trials/participants in each condition.

2.6 Statistical Methods

The normality of data was examined by plotting the distribution as well as QQ-plot, and the results of Shapiro-Wilk test were also considered (an example is shown in Appendix B). If the data is regarded normal distributed, the parametric tests were used, or the nonparametric tests were used instead. All the statistical tests were performed in SPSS.

Parametric Test

Paired t-test

The paired t-test was used to test the difference in means between two dependent groups. In this experiment, for example, it has been used to test the normally distributed head or body motion amplitudes between EYES-ON-ROAD condition and EYES-OFF-ROAD condition which was performed by the same participant.

Repeated Measures ANOVA

As for more than two dependent observations, for example, comparing the head and body motion in time windows which were extracted separately at the beginning, middle and end of the same trials (Fig.3.14, 3.15, 3.24, 3.25). The three time windows for each trial were dependent on each other since only one participant was measured. The Repeated Measured ANOVA was applied if the dependent variables were normally distributed, which is an extension of paired t-test also detecting the overall difference between the related means.

Nonparametric Test

Mann-Whitney U-test

Mann-Whitney U-test is a non-parametric statistical analysis which has been also used to find differences between different groups assuming independent variables. The advantage of Mann-Whitney U-test is that the normal distribution is not required, but it is less powerful than t-test. In this experiment, it is used to test the difference between sensitive and non-sensitive groups where all the trials were assumed to be independent.

Wilcoxon Signed Rank Test

Wilcoxon signed rank test is also a non-parametric statistical analysis which could replace the paired t-test for testing the difference between the dependent trials with two visual conditions when the data was not normally distributed.

Friedman Test

The Friedman test was to replace the repeated measures ANOVA if normality was not found, testing the difference between three time windows.

Levene's Test

Levene's test was used to test the equality of variance between populations, which was performed between both visual conditions and sensitivity groups in terms of absolute and motion data. For normal distributions, the parametric Levene's test was realized in SPSS by ANOVA procedure. While for non-normal distributions, the nonparametric Levene's test was also realized in ANOVA procedure, but after calculating the data deviations from group mean ranks, where the data was normalized by ranking.

Pearson's Product-Moment Correlation Coefficient

Pearson's product-moment correlation coefficient has been used to check the correlation between two signals. The coefficient ρ is between -1 and 1 – 1 means a total positive linear correlation; -1 means a total negative linear correlation; 0 means no correlation.

Bonferroni Correction

Since various null hypotheses were statistically tested between the two visual conditions or between sensitive or non-sensitive group in this thesis. For example, the motion of pelvis, sternum and head were all compared in both lateral and roll direction – 6 hypotheses were tested simultaneously between two datasets (two conditions or two sensitivities). To avoid the multiple testing problem – the more inferences are made simultaneously, the probability of false rejection of a single true null hypothesis (Type I error, α) increases, the Bonferroni Correction was applied to this multiple comparison for correcting the significance level for each individual hypothesis:

$$\alpha_{correction} = \frac{\alpha}{n} \tag{2.6}$$

In this thesis, the original significance level α is always set 0.05, and the n is the number of hypotheses simultaneously being tested, which is 6 in the example. So, if only the critical value for an individual hypothesis is lower than $\frac{\alpha}{n}$, the critical value for the entire experiment could be lower than α.

3. Results

3.1 Car Motion*

The car orientation and linear acceleration were continuously measured by Xsens MTi-G located under the passenger's seat. During each trial, the driver was managing to keep the car lateral frequency around 0.2 Hz guided by a metronome with frequency of 12 bpm (beats per minute). Except the trials for himself, only one driver was driving for all of the trials, ensuring the similar vehicle motion throughout the experiment.

An example of the car three-direction longitudinal accelerations in a 6-minute trial is shown in Fig.3.1. As the Xsens MTi-G sensor was not located horizontally under the vehicle seat, a gravity component has been included in the longitudinal direction, which was corrected using rotation matrix (see red lines in Fig.3.1). After correction, the root mean squares of the longitudinal, lateral and vertical (gravity included) acceleration in this trial are respectively 0.68 m/s^2, 2.20 m/s^2 and 9.75 m/s^2, including 7 slaloms and 7 U turns that were necessary due to the limitation of road length. No difference was observed in car motion between the trials (see Fig. 3.3).

Fig. 3.2 shows the three accelerations in frequency domain - the normalized magnitude after Fourier transform together with the cumulative power (the estimated value of gravity, 9.8 m/s^2, in vertical direction was removed to show better comparison). It suggests that only lateral acceleration was excited drastically around 0.2 Hz – the frequency has been proved most effective in evoking motion sickness for all kinds of transports. Therefore, most of the motion sickness symptoms resulted from vehicle lateral motion in this experiment, only which will be considered in the following analysis.

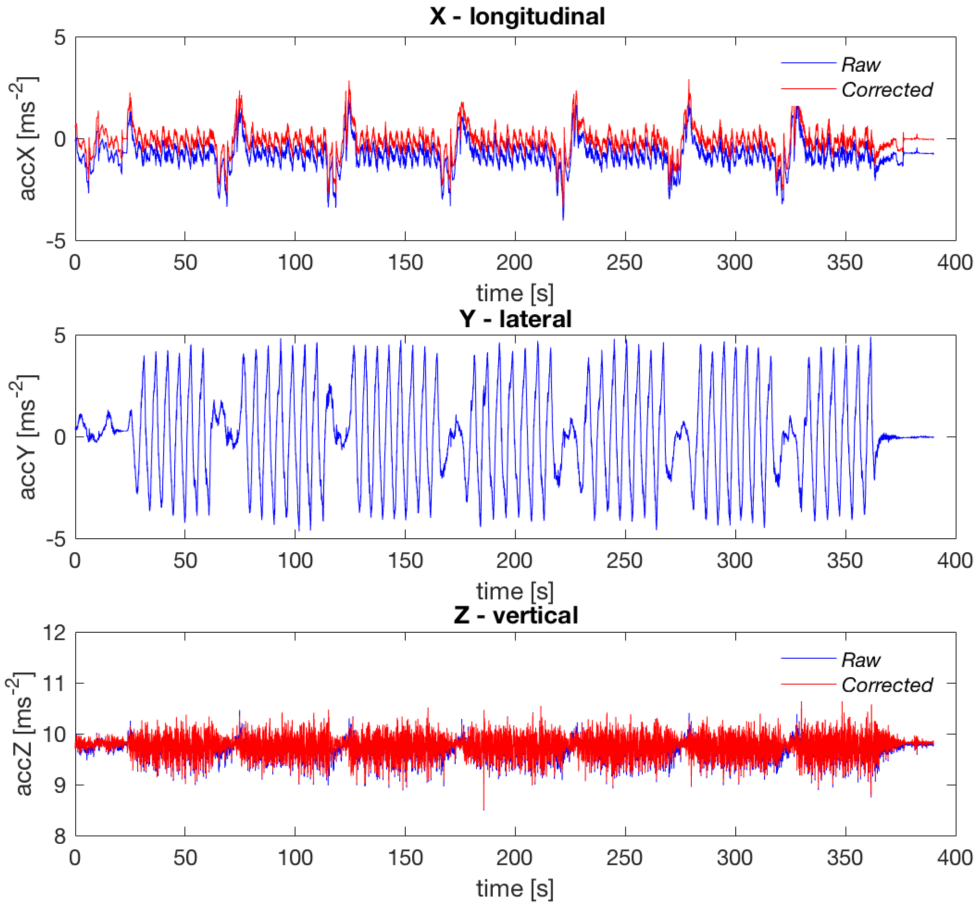

Fig.3.1 Car longitudinal, lateral and vertical acceleration in time for a 6-min trial (blue –raw data; red – corrected for gravity components in longitudinal and vertical direction)

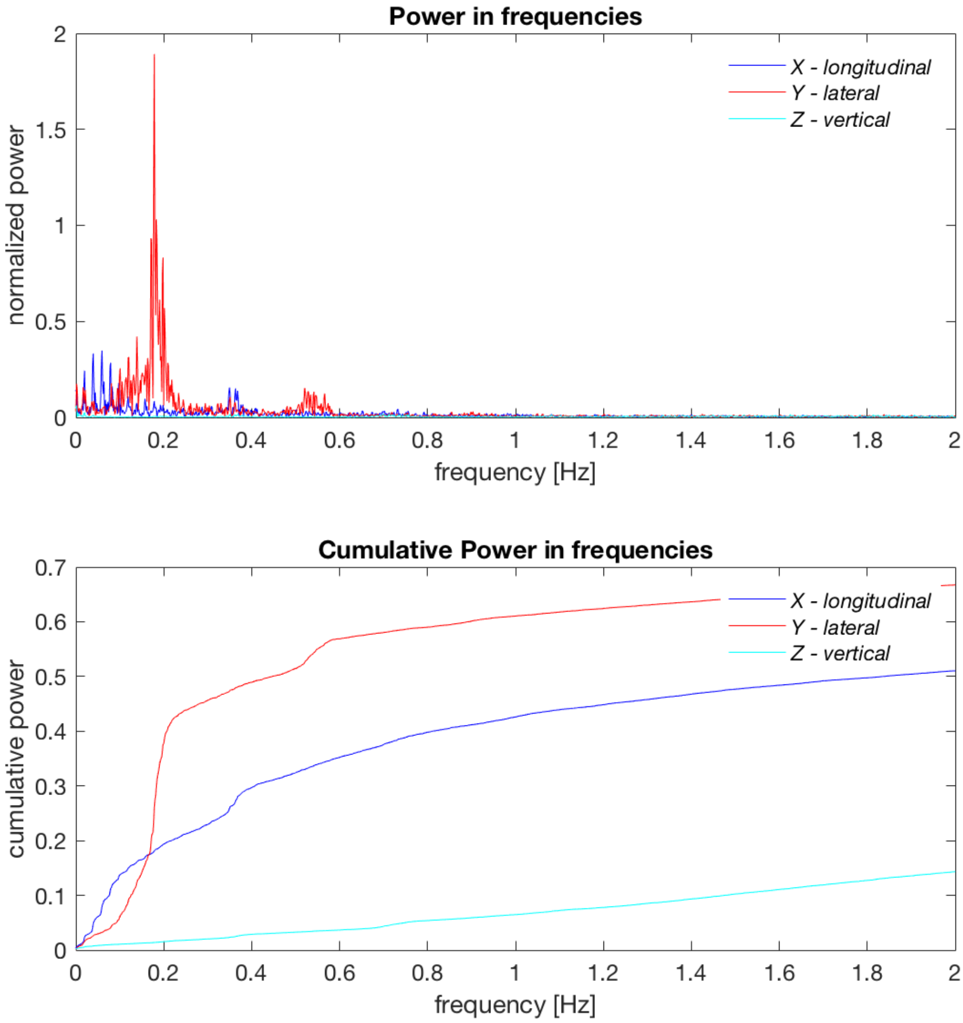

Fig.3.2 Power and cumulative power of car longitudinal, lateral and vertical accelerations in frequency for a 6-min trial

MSDV

The motion sickness does value (MSDV) of car motion was calculated for 18 participants who finished the trials for both visual conditions. The MSDV combines the frequency-weighted acceleration and exposure duration to indicate the potential possibility for a specific motion in inducing motion sickness (see section 2.5). Fig.3.3 shows how the MSDV developed in time for the 36 trials with 18 participants. According to the definition, MSDV is quadratic to the frequency-weighted acceleration magnitude but only half in the power of exposure time (Eq.2.2). Observed in Fig.3.3, the MSDV grew in time in a square function, implying the acceleration magnitude was remained generally constant during the whole journeys. To test the similarity of MSDV between trials, duration for the shortest trial, 6 minutes, was extracted for statistical test. Specifically, mean MSDV of the first 6 minutes of all the trials were compared between conditions using Mann-Whitney U test, and no difference was found in vehicle MSDV between the two visual conditions (p = 0.27).

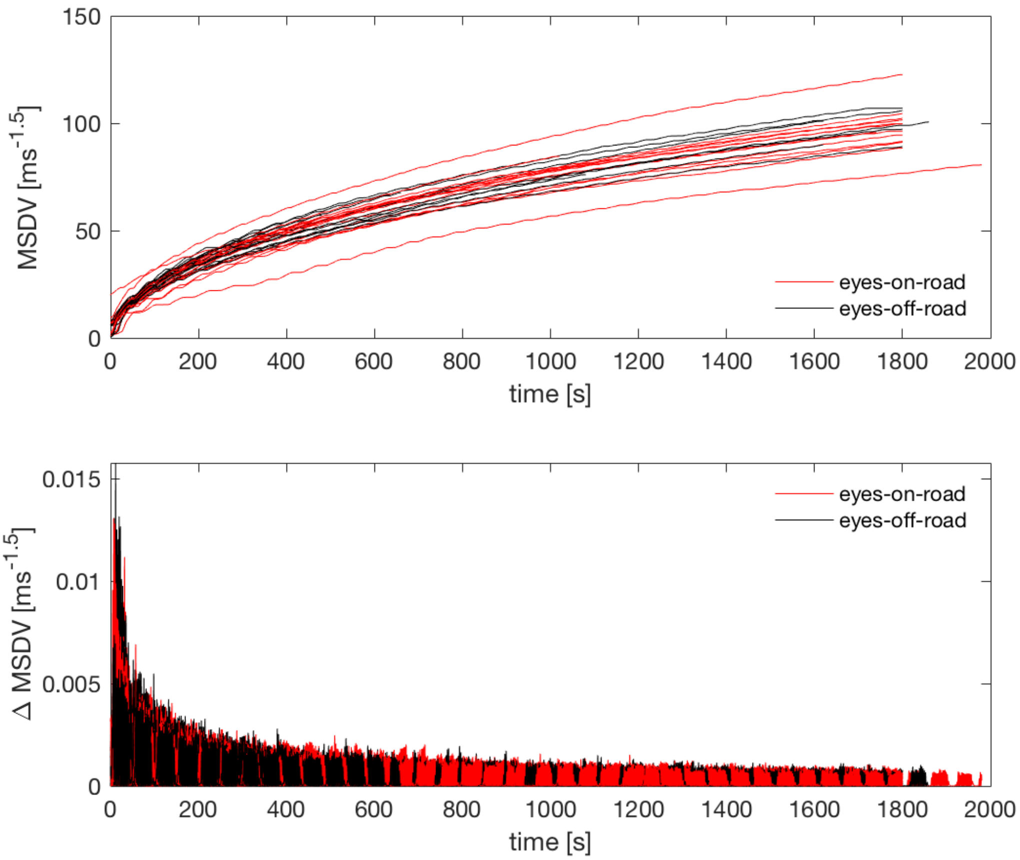

Fig.3.3 Car MSDV and its gradient in time for 18 participants in two visual conditions

3.2 Motion Sickness Between Visual Conditions

In this section, the level of motion sickness reported by the participants has been checked between the EYES-ON-ROAD and EYES-OFF-ROAD condition. MISC was used as the main quantitative method compared within participants, in time and in vehicle motion to show the effect of vision on motion sickness. And the results of MSAQ were also compared between visual conditions to investigate the effect of vision on the occurrence of different symptoms. The predictability of MSSQ in the actual MISC has been checked in both conditions to validate the reliability of this questionnaire. Finally, the three subjective motion sickness scores (MISC, MSAQ and MSSQ) were compared to see the correlation of different methods.

MISC within Participants

The $MISC_{average}$ as well as $MISC_{rate}$ (see section 2.5) was compared between the two visual conditions within 18 participants who finished both trials (Fig.3.4). Among the participants, both $MISC_{average}$ as well as $MISC_{rate}$ indicates that 16 had higher illness level in EYES-OFF-ROAD condition, and 2 have different results using the two indicators. Specifically, 5 of the participants reached a MISC of more than 6 (6 or 7) and quit before finishing 30-minutes trial with EYES-ON-ROAD, however, there were 12 of them quit during the EYES-OFF-ROAD trials due to the high MISC. No one has quit with a MISC of less than 6 in either conditions. It is observed that $MISC_{rate}$ could maintain more variance between participants normalized by the mean (Fig.3.4, Table 3.1), especially for those reached 7. So that $MISC_{rate}$ could be a better indicator if considering individual characteristics. Significant difference is found in both $MISC_{average}$ and $MISC_{rate}$ for all the 18 participants between conditions (Table 3.1).

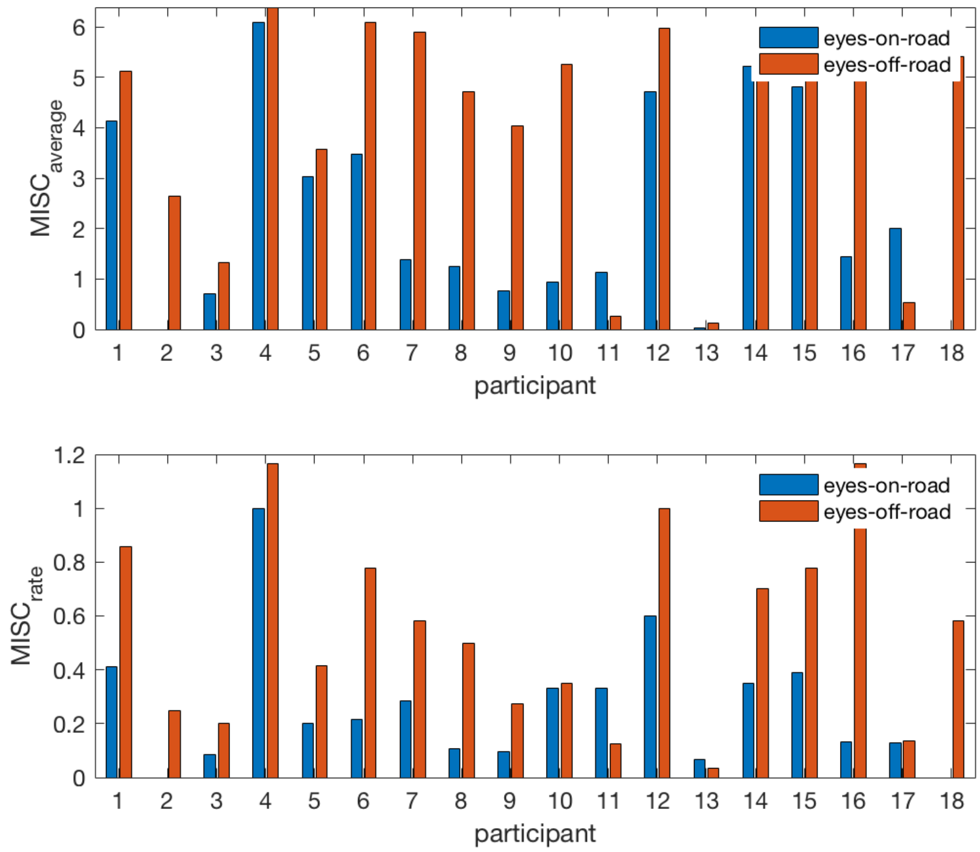

Fig.3.4 $MISC_{average}$ and $MISC_{rate}$ rate for 18 participants in two visual conditions

Table 3.1 Mean, SD and significance of $MISC_{average}$ and $MISC_{rate}$ rate for 18 participants in two visual conditions (Wilcoxon signed rank test)

		$\boldsymbol{MISC_{average}}$	$\boldsymbol{MISC_{rate}}$
EYES-ON-ROAD	mean	2.28	0.26
	SD	1.98	0.24
EYES-OFF-ROAD	mean	4.18	0.55
	SD	2.22	0.36
Sig. (p value)		0.002	0.001

MISC in Time

Fig.3.5 shows the percentage of participants reached a MISC of 7 (quit),6 and 5 separately at every minute in trials for both visual conditions. For the entire 30-minutes trial, around 30% of the 18 participants quit half-way with a MISC of 7, and 40% reached a MISC of 5 in EYES-ON-ROAD condition. However, for the EYES-OFF-ROAD condition, 70% participants quit before 30 minutes, most of which quit between 5th and 15th minutes, and almost 90% participants reached a MISC of 5. The growth of MISC in time for the two visual conditions was averaged for all 18 participants (Fig.3.6). The MISC rating was rapidly growing at the first 10 minutes in both EYES-ON-ROAD and EYES-OFF-ROAD conditions, which was almost constant in gradient for the former, while for the latter, a leap was seen at around 5th minute and $\Delta MISC$ reached 1. Since the participants who quit were considered to rate their maximal scale for the remaining duration of the experiment, it is noticed in Fig.3.5 that 40% participants rated MISC of 7 and quit in the first 10 minutes for EYES-OFF-ROAD condition (10% for EYES-ON-ROAD condition), resulting in the mean MISC climbing more slowly after 10 minutes, where the two conditions have similar $\Delta MISC$. For better comparing the MISC in the two conditions after those sensitive ones quit, the MISC increasing in time is also showed for each individual (Fig.3.7, the participants order is the same as Fig.3.4). It is found that for most of the participants, the MISC in EYES-OFF-ROAD condition grew much more rapidly in time.

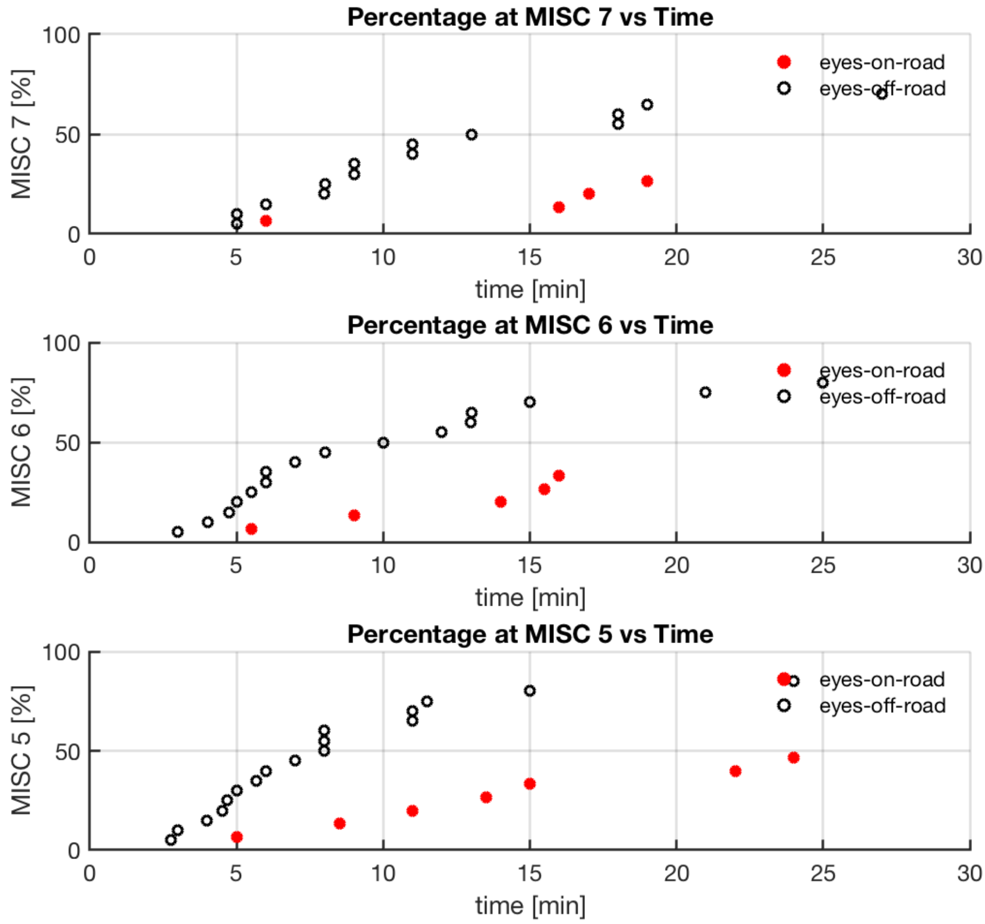

Fig.3.5 Percentage of participants reached MISC of 7,6 and 5 in time with two conditions

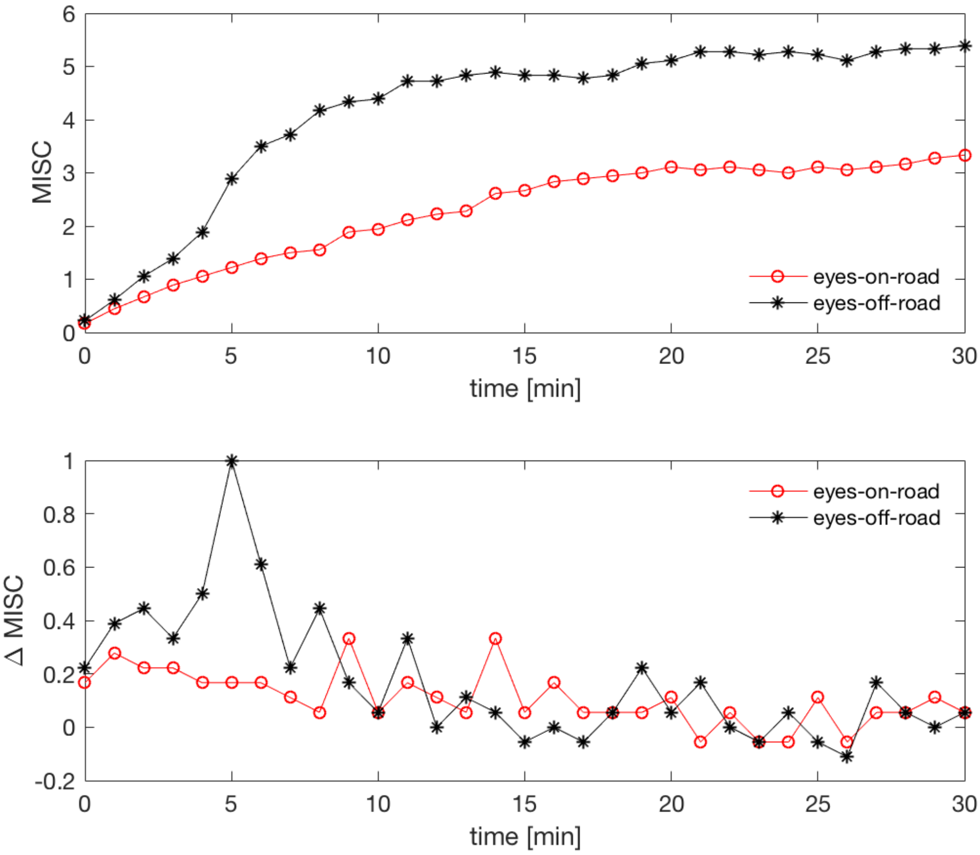

Fig.3.6 Participants mean MISC growth in time with two conditions

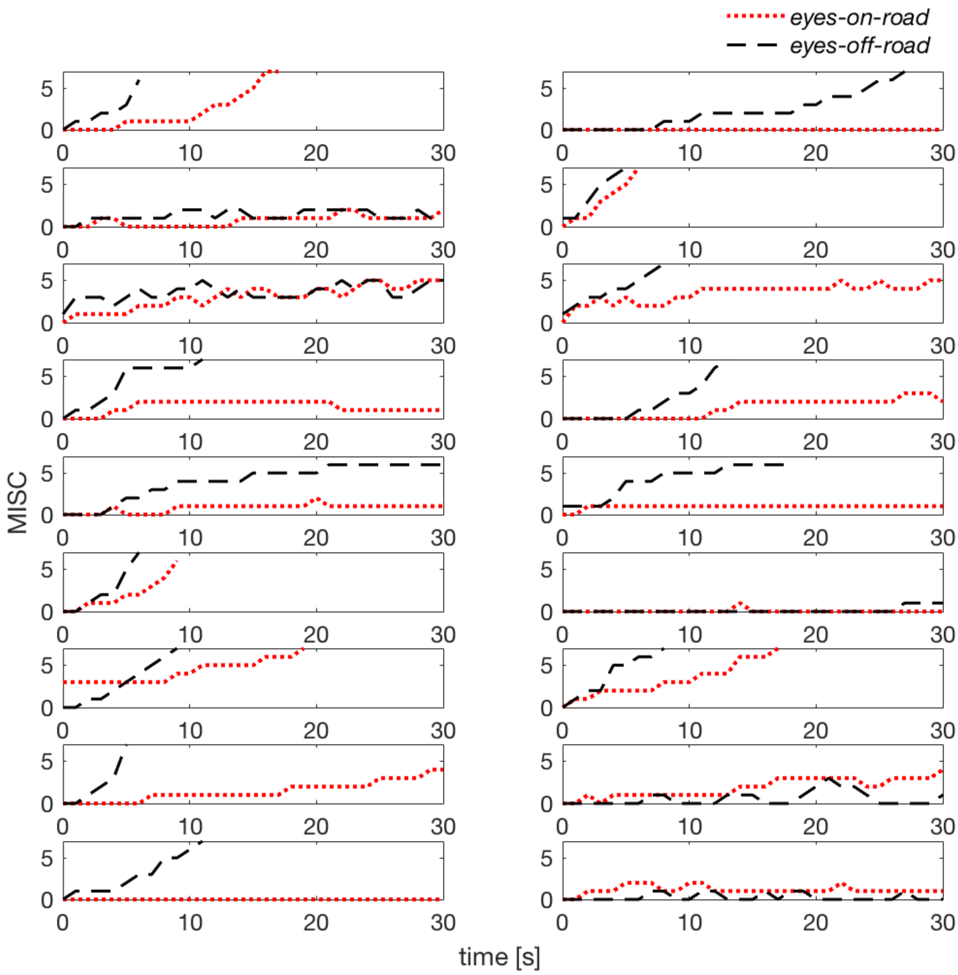

Fig.3.7 MISC in two visual conditions for 18 participants

MISC with Vehicle Motion

The growth of MISC and vehicle stimulus accumulation (MSDV) was compared within the 18 participants in both visual conditions. Mean of the MISC for all participants is shown in Fig.3.8a with bold line. Because the MISC rating for each minute was strictly synchronized with the MSDV duration by using the real timestamps for each trial, it is hard to anticipate the time of remaining MSDV for the participants who quit before 30 minutes. The MISC average method by filling the maximal MISC for remaining minutes in Fig.3.6 cannot be applied here. The mean MISC in Fig.3.8 was only averaged within the participants who were still in the journeys while the ones quit were excluded. The drawback of this method is that the mean MISC will show a decrease after the sensitive participants quit, so that the sensitive participants who reached a MISC of 7 were separated from those who finished 30-minutes trial and the means MISC of the two groups are shown in Fig.3.8b which could better reveal the MISC evolution for both conditions.

For EYES-ON-ROAD condition, the mean MISC for all participants is linearly climbing with the increase of the car MSDV, especially before the first participant quit at 17 minute (MSDV around 50), although the mean MISC for non-sensitive group was almost maintained 0. However, in the EYES-OFF-ROAD condition, both groups showed a rapidly increased MISC with respect to car MSDV, when the non-sensitive group showed a bit delay compared with sensitive one. According to the Pearson's product-moment correlation test, the MISC correlates with MSDV in both condition for both groups (ρ = 0.93, $p < 0.001$ for sensitive group in EYES-ON-ROAD; ρ = 0.74, $p < 0.001$ for non-sensitive group in EYES-ON-ROAD; ρ = 0.97, $p < 0.001$ for both sensitive and non-sensitive group in EYES-OFF-ROAD).

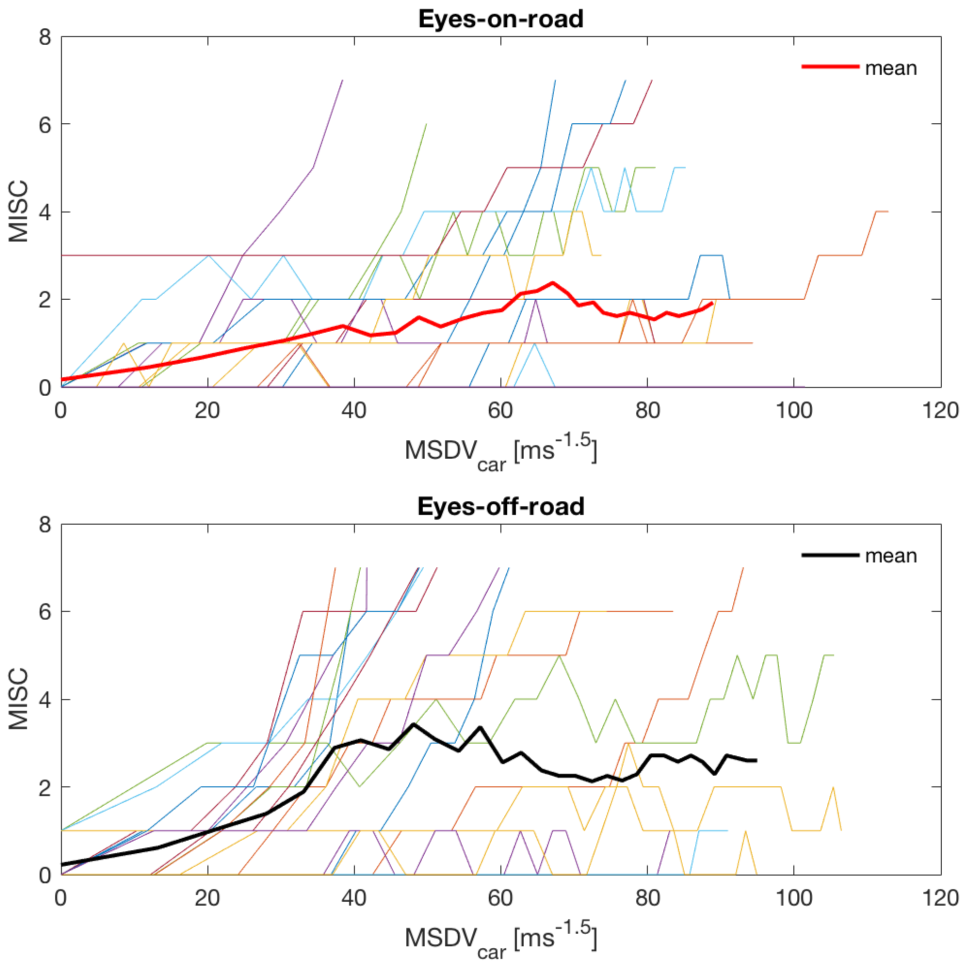

(a)

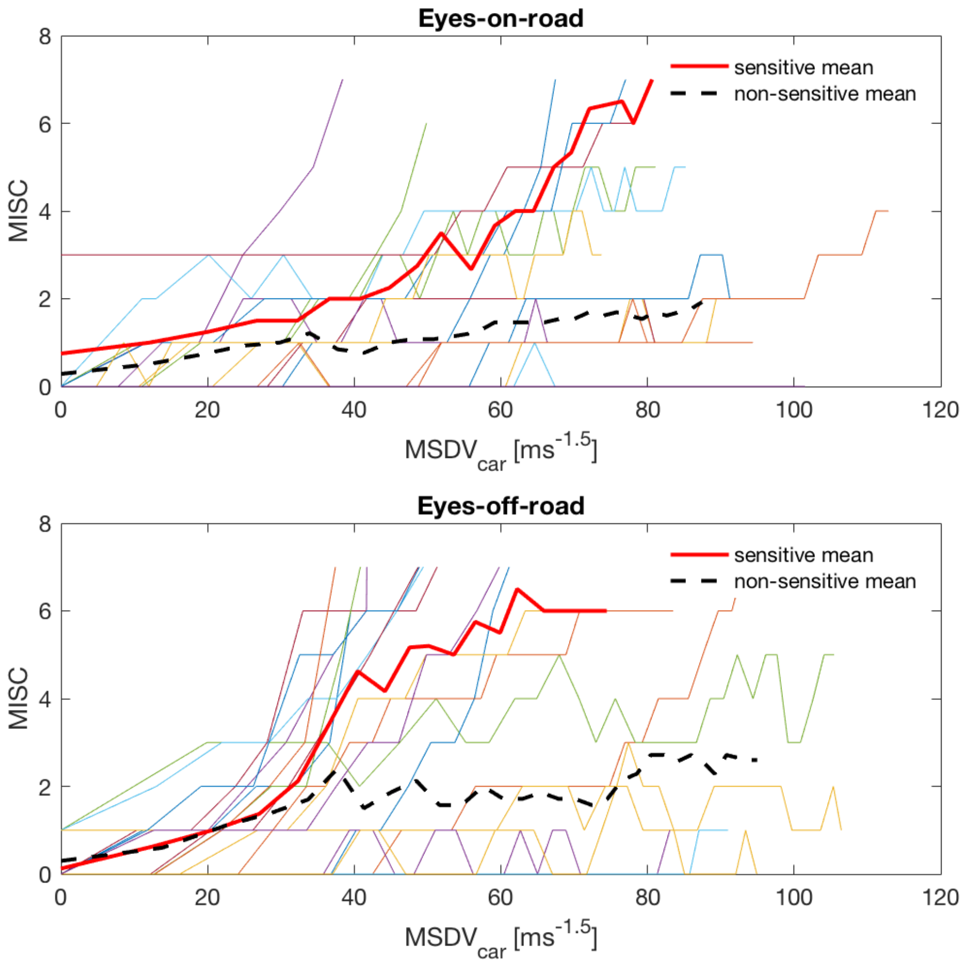

(b)

Fig.3.8 Relation between participants MISC and car MSDV per trial in two visual conditions – (a) Mean MISC over all participants in each condition; (b) Mean MISC over sensitive group (reached 7) and non-sensitive group (not reached 7) separately in each condition

Specific Sickness Symptoms as a Function of Vision

MSAQ was used as the symptom checklist finished by the participants after each trial, indicating their most affected systems. The results of MSAQ for the 18 participants finishing two visual conditions is shown in Fig.3.9 (using the same number as Fig.3.4). Sensitivity to each dimension of symptoms varies significantly between individuals, nevertheless, the MSAQ scores were found significantly higher in EYES-OFF-ROAD condition for overall ($p < 0.001$, $z = -3.5$), gastrointestinal ($p = 0.0012$, $z = -3.2$), central ($p < 0.001$, $z = -3.6$) and peripheral ($p = 0.0020$, $z = -3.1$) scores, but no significant difference was found for sopite-related score (p = 0.019, z = -2.3). (Wilcoxon signed rank test, α=0.05, Bonferroni correction: $\alpha_{correction}$=0.01).

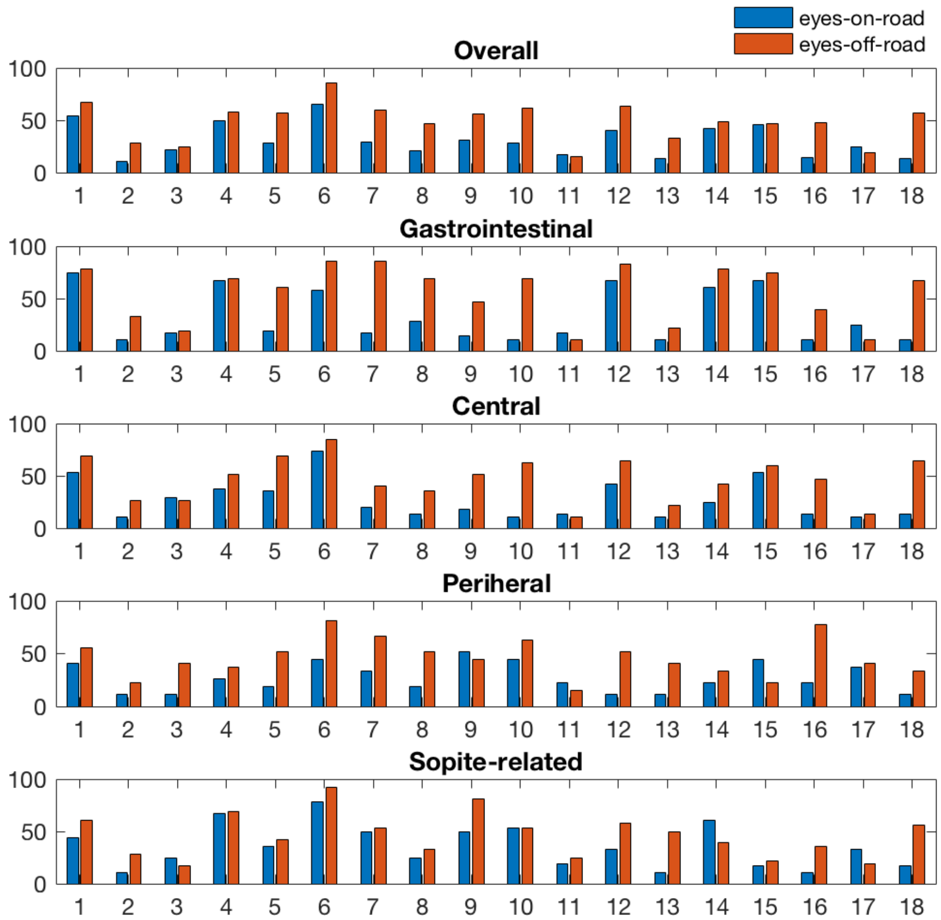

Fig.3.9 Results of MSAQ for 18 participants in EYES-ON-ROAD and EYES-OFF-ROAD condition

Within the participants, the $MISC_{average}$ and $MISC_{rate}$ were compared with the results of MSAQ, and correlation for both visual conditions was shown in Fig.3.10. As shown in Table 3.2, both the $MISC_{average}$ and $MISC_{rate}$ correlate with the overall MSAQ score, gastrointestinal symptoms score and central symptoms score (except for $MISC_{rate}$ with central symptoms) at a significance level of 0.01. It implies that participants with high-level of discomfort for gastrointestinal or central nervous system tend to rate a high MISC during the trials. However, for MSAQ score about peripheral and sopite-related symptoms, only marginal significance at a level of 0.05 or no significance was found in correlation with the $MISC_{average}$ and $MISC_{rate}$.

$MISC_{average}$ is more correlated with MSAQ scores for all symptoms, compared with $MISC_{rate}$. No difference was found in these correlations for either indicator between the two visual conditions (Wilcoxon signed rank test: p = 0.47 both $MISC_{average}$ and $MISC_{rate}$).

It was noticed that peripheral symptoms include sweaty or hot feelings, which may result from high temperature rather than carsickness (the experiment was executed in summer when the highest outside temperature was around 35℃). Although we were turning on the car air-condition all the time during trials and the car inside temperature was controlled constant, wearing the Xsens suit might cause extra hot feelings for some of participants. Similar uncontrollable variables could be involved in sopite-related symptoms such as drowsiness – tiredness of participants may arise prior to the trials though they were instructed to have a good sleep before the experiment.

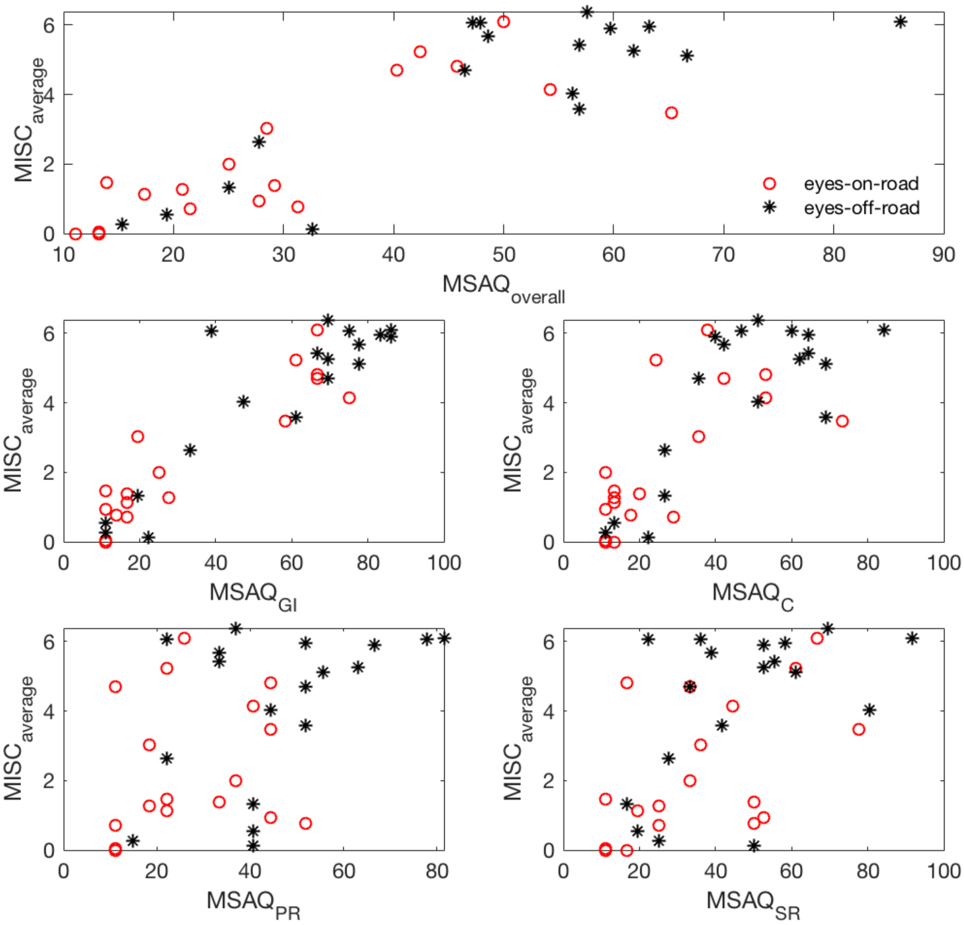

(a)

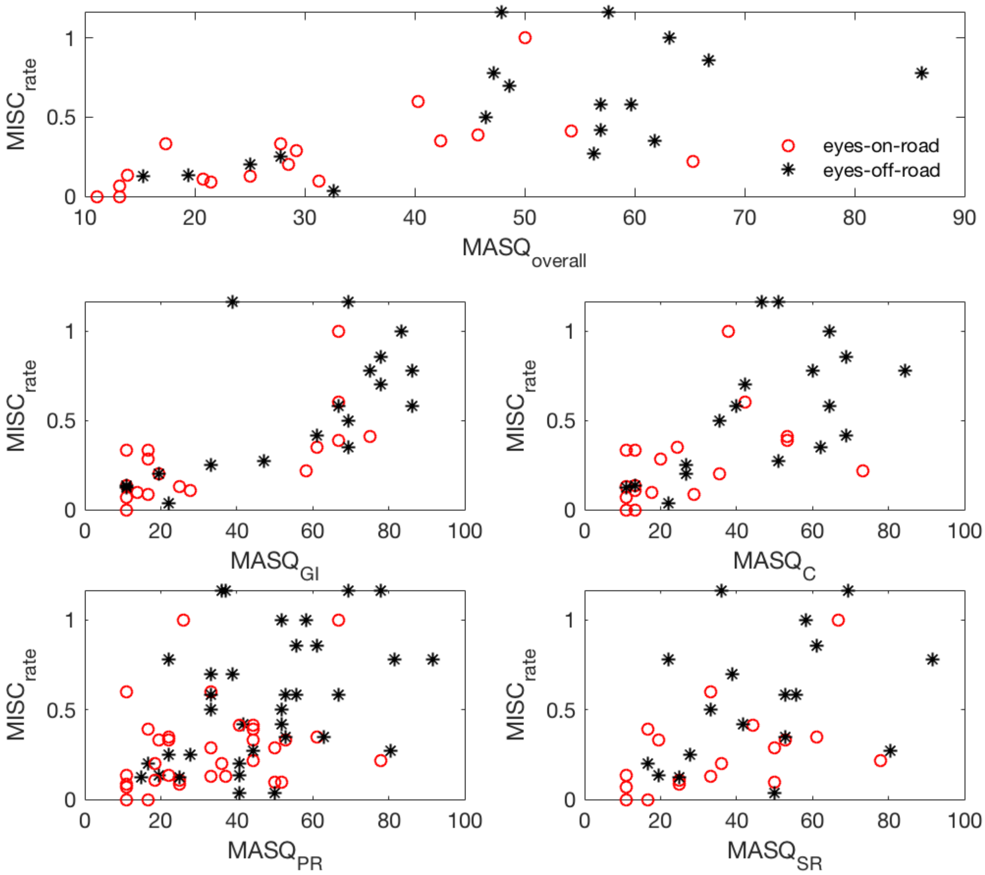

(b)

Fig.3.10 Correlation between MISC and MSAQ ratings for overall, gastrointestinal (GI), central (C), peripheral (PR) and sopite-related (SR) symptoms respectively, for 18 participants in two visual conditions –

(a) $MISC_{average}$; (b) $MISC_{rate}$

Table 3.2 Correlation between (1) $MISC_{average}$ and MSAQ; (2) $MISC_{rate}$ and MSAQ, for overall, gastrointestinal (GI), central (C), peripheral (PR) and sopite-related (SR) symptoms respectively, for 18 participants in two visual conditions (Pearson's product-moment correlation coefficient, two-tailed)

		$MISC_{average}$		$MISC_{rate}$	
		Correlation coefficient (ρ)	Sig. (p value)	Correlation coefficient (ρ)	Sig. (p value)
EYES-ON-ROAD	$MSAQ_{overall}$	0.82	<0.001[1]	0.62	0.007[1]
	$MSAQ_{GI}$	0.92	<0.001[1]	0.70	0.001[1]
	$MSAQ_{C}$	0.70	0.001[1]	0.43	0.073
	$MSAQ_{PR}$	0.23	0.36	0.16	0.53
	$MSAQ_{SR}$	0.54	0.02[2]	0.50	0.035[2]
EYES-OFF-ROAD	$MSAQ_{overall}$	0.82	<0.001[1]	0.62	0.006[1]
	$MSAQ_{GI}$	0.89	<0.001[1]	0.66	0.003[1]
	$MSAQ_{C}$	0.77	<0.001[1]	0.61	0.008[1]
	$MSAQ_{PR}$	0.46	0.06	0.39	0.11
	$MSAQ_{SR}$	0.50	0.03[2]	0.37	0.14

[1] *correlation is significant at the 0.01 level;*
[2] *correlation is significant at the 0.05 level.*

For EYES-ON-ROAD condition, a correlation was found between the participants' $MISC_{average}$ and the score of MSSQ they filled out (indicating their susceptibility) before the experiment (Pearson's product-moment correlation coefficient: ρ = 0.54, p = 0.02, α = 0.05). However, no correlation was found between $MISC_{rate}$ and MSSQ score (ρ= 0.28, p = 0.26). For EYES-OFF-ROAD, no correlation was found for either indicators with the MSSQ (ρ= 0.27, p = 0.29 for $MISC_{average}$; ρ= 0.30, p = 0.22 for $MISC_{rate}$) (figure 3.11). The MSSQ investigated the participants' susceptibility based on their history experience in all types of transports, where was more natural with vision provided. So for EYES-ON-ROAD condition, the less susceptible population would be less sensitive, although this susceptibility could only predict the average MISC. Nevertheless, motion sickness under vision-blocked situation was more unnatural and hard to predict by previous susceptibility. For example, for the participants with score under 10 in MSSQ (less susceptible than the median in population, Griffin and Howarth, 2000), they rated a comparatively low MISC in the journey with vision, however, all except 2 of these 7 participants reported an extremely high MISC when there was no external vision in the car.

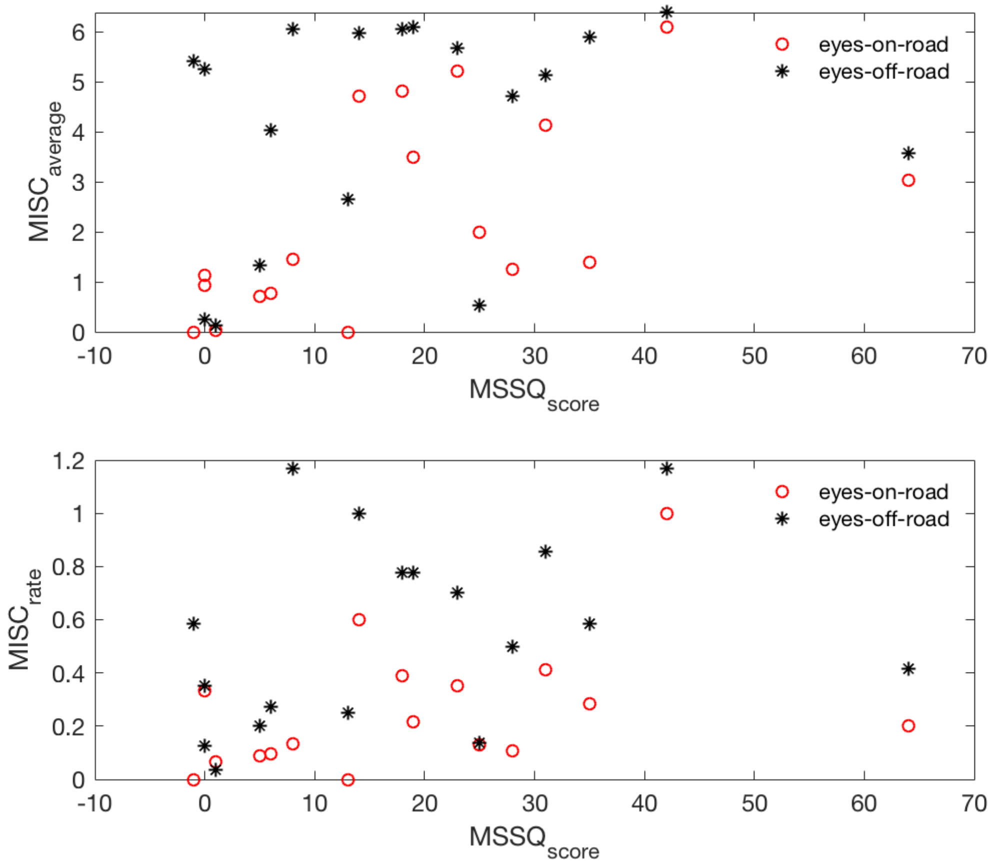

Fig.3.11 Correlation between (1) $MISC_{average}$ and MSSQ; (2) $MISC_{rate}$ and MSSQ total susceptibility score, for 18 participants in two visual conditions

3.3 Head and Body Motion in Time Domain

To reveal the regularity of participants' upper-body motion, motion of three body positions were studied – pelvis, sternum and head, from the closest to the farthest away from the car seat where car motion was measured. Body motion of 11 participants (No. 1, 3, 7, 8, 9, 10, 12, 14, 15, 17, 18 in figure 3.4) were captured successfully for both visual conditions by the Xsens MVN system, on whom the body motion analysis was based.

In this section, the participants' head and body motion was first checked with respect to the vehicle, followed by investigating the relative motion between different body segments. Since only the lateral acceleration was excited at 0.2 Hz, the dominant motion inducing motion sickness for both car and human body includes lateral translational motion, roll and yaw. However, we had informed the participants that they should always sit straight and look forward during the trials, so that the yaw motion of the participants was supposed to be the same as vehicle and could not vary between conditions. Therefore, only lateral acceleration and roll motion will be analyzed. Both lateral acceleration and roll angles were quantified by root mean squares and compared in time by windowing procedure (see section 2.5).

Head and Body Motion in Time Domain Overview

An example of participant head motion in three translational directions, for the same 6-minute trial as Fig.3.1, is shown in Fig.3.12. Comparing with the car and head motion in time, similar lateral accelerations can be observed, while body motion contained a small amount irregularities and noise resulting from voluntary movement. To remove the system noises as well as unexpected drifts (mainly in orientation data), and focus on the low frequencies related to motion sickness, the motion signals were processed through a band-pass filter with order of 3 and bandpass frequency from 0.05 Hz to 1 Hz. The filtered signal is shown in red lines together with the original signal (blue) lines (Fig.3.12), where the basic movement was kept and high-frequency noise was removed by the filter. To avoid the disturbances of noises, the filtered data (for both lateral acceleration and roll in body and car) was used in all the time domain analyses.

Fig.3.13 shows an example of the comparison for filtered lateral acceleration and roll between car, pelvis, sternum and head observed in three slaloms. As mentioned before, there are some drifts in the car rotational data, however, which are not apparent if only three slaloms were checked. So, the car roll was only plotted here for visualized comparison that was not used in following data analysis. It is found the lateral acceleration for all the body segments were extremely synchronized with the car acceleration, since the latter was the dominant motion excited, compared to which the information about body lateral motion within the vehicle was hidden. However, the body rolls in space were comparatively large and irregular in comparison with vehicle, especially for head. What is interesting is the head roll was even comparatively larger at the U turns which might induce extra sickness.

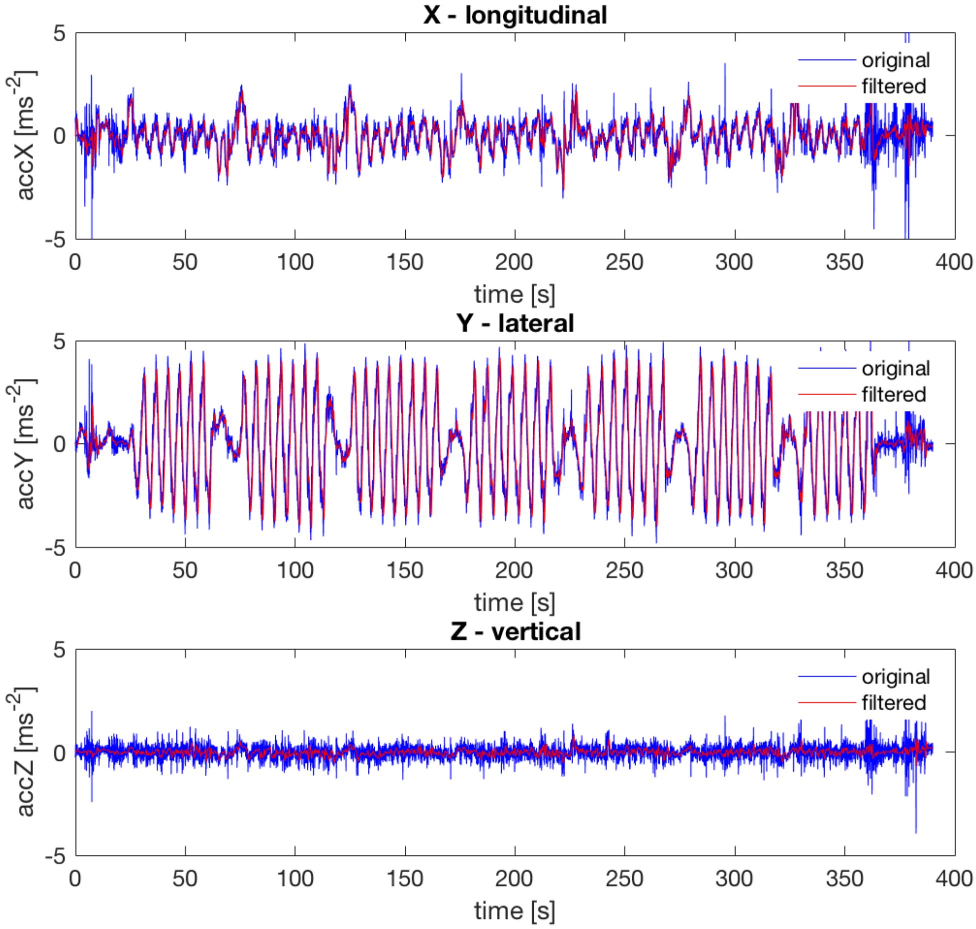

Fig.3.12 Head longitudinal, lateral and vertical accelerations in time for a 6-minute trial (blue – original data; red – low-pass filtered data with cut-off frequency of 1 Hz)

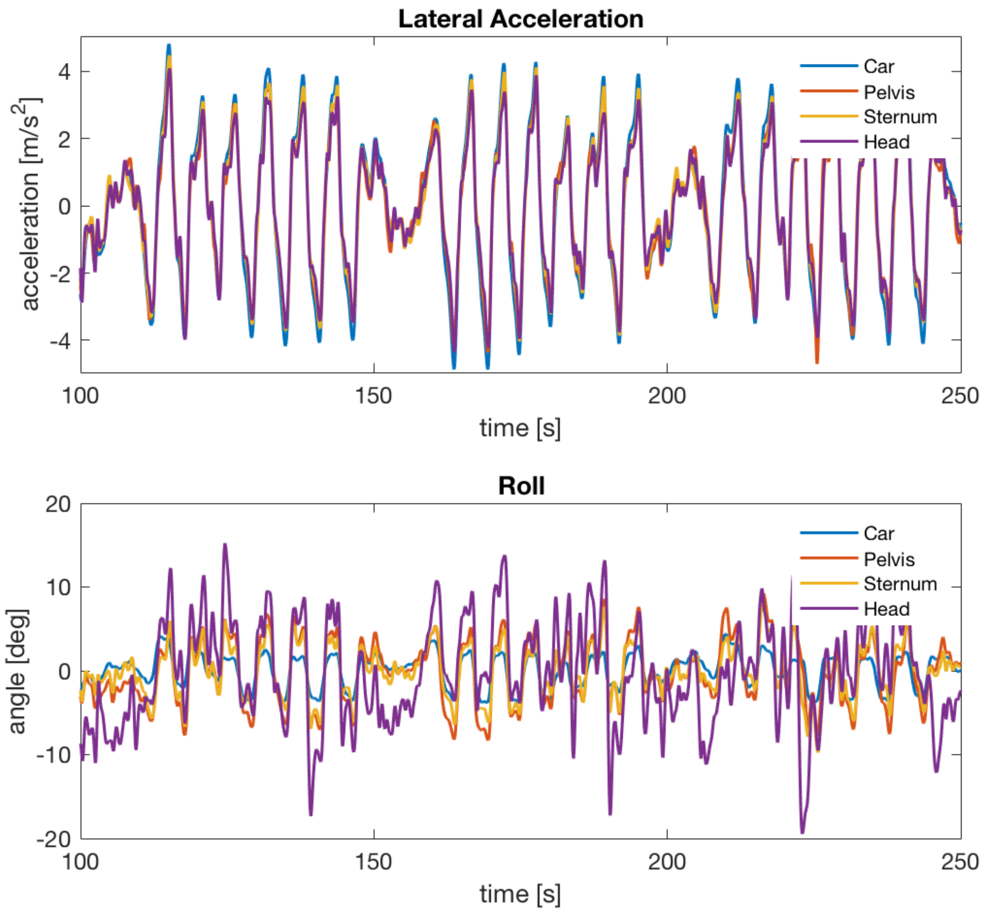

Fig.3.13 Comparison of lateral acceleration and roll angles for car, pelvis, sternum and head in 3 slaloms (all band-pass filtered with 0.05-1Hz)

Head and Body Motion with respect to Car

Fig.3.14a shows the ratio of root mean squared lateral acceleration respectively for head, sternum and pelvis in the vehicle for both visual conditions, where a windowing procedure has been used to examine the movement evolution over time. Specifically, the ratio was calculated for every two minute and throughout the entire duration for each trial. It is observed that the ratio of the lateral acceleration of all three body segments in car lateral acceleration was always below 1 and around 0.9 for most of the trials in either visual condition. No significant change was found in time, although there was only one participant gradually reducing his sternum and pelvis acceleration in the EYES-ON-ROAD trial.

As no apparent difference was observed for the body relative acceleration in time (Fig.3.14a), three of the windows were selected for a double check using statistical analysis – at the beginning, middle and end of the exposure for each trial (Fig.3.14b). No statistical difference was found for all the three body segments in either conditions (Table 3.1).

Fig 3.14 shows that the standard deviation between different individuals was higher in eye-on-road condition for the lateral acceleration of all the three body segments, especially of head, which might suggest that for the conditions with vision, people were trying to control their body motion with different control strategies which resulted in more 'irregular' body motion compared with the conditions without vision, where people were just 'thrown' by the vehicle.

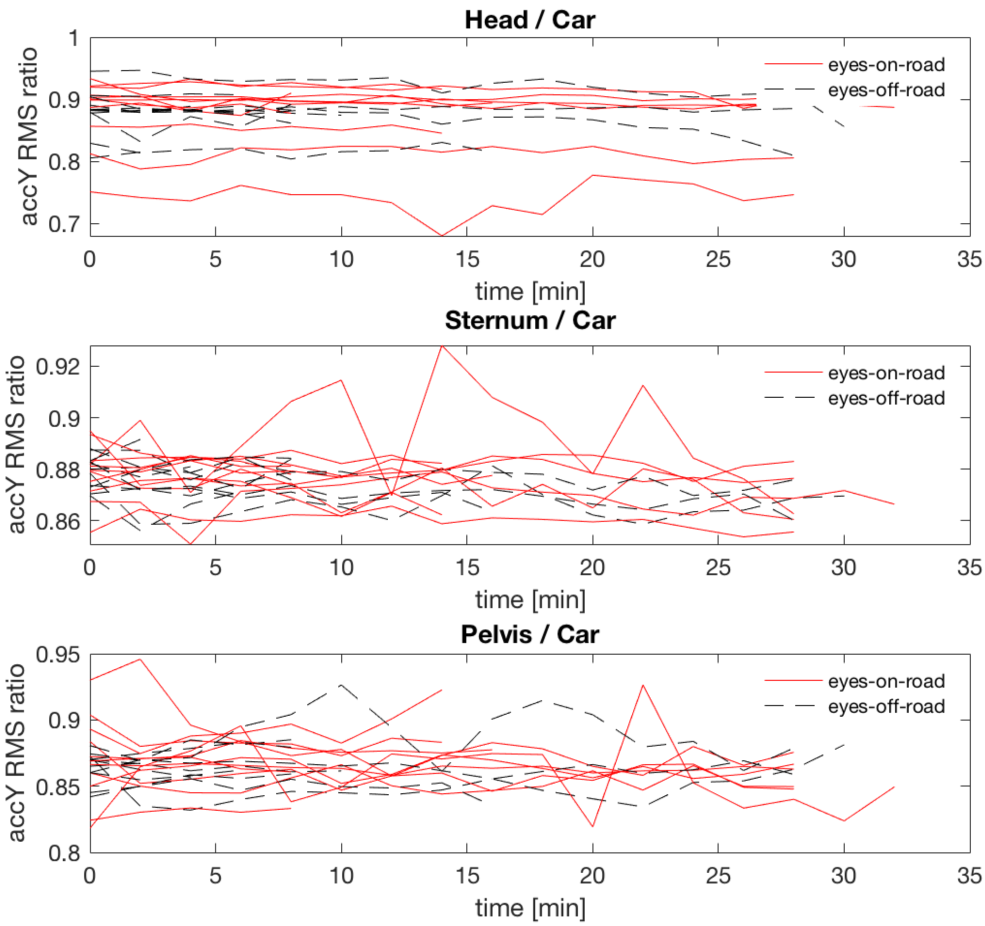

(a)

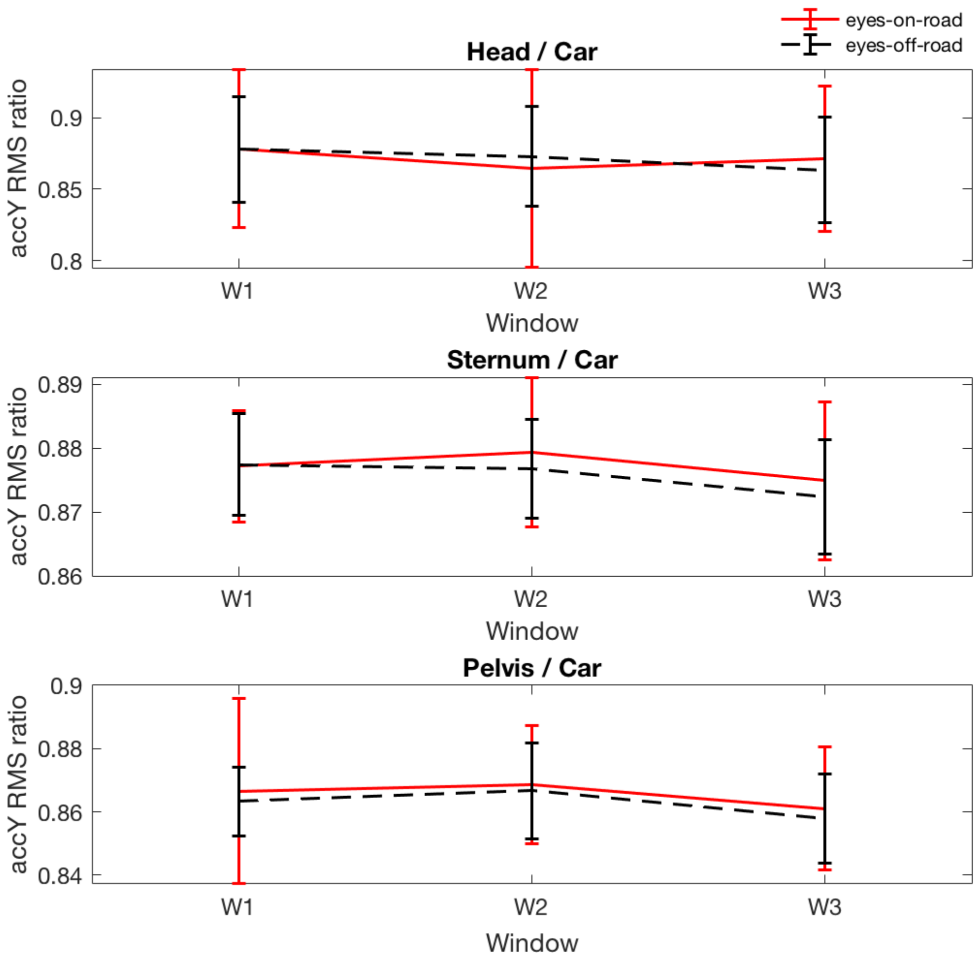

(b)

Fig.3.14 Ratio of root mean squared head, sternum and pelvis lateral acceleration to car lateral acceleration (after 0.05-1 Hz band-pass filtering) throughout time in two visual conditions – (a) with 2-minute window over the entire duration for all the 22 trials with 11 participants in two conditions; (b) the mean ratio for all participants at W1 (beginning), W2(middle) and W3(end) of the trials in two conditions, whiskers indicate the standard deviation.

Table 3.1 Difference in lateral acceleration RMS (normalized by dividing car lateral acceleration RMS) between three time windows – beginning, middle and end of trials (Repeated Measures ANOVA or Field test*, α=0.05, Bonferroni Correction was used)

CONDITION	POSITION	SIG.	EFFECT SIZE	POWER
EYES-ON-ROAD	Head*	0.441	-	-
	Sternum	0.166	0.329	0.337
	Pelvis**	0.346	0.097	0.183
EYES-OFF-ROAD	Head	0.184	0.167	0.266
	Sternum	0.191	0.308	0.309
	Pelvis	0.139	0.355	0.373

** Non-normal distribution (Shapiro-Wilk test). Tested by Fieldman test.*
*** Sphericity was violated, where Huynh-Feldt method was used as correction.*

The $MSDV_{head}$ was calculated as well using the three translational accelerations of head and compared with the $MSDV_{car}$ calculated from car motion. It is found that $MSDV_{head}$ was always lower than $MSDV_{car}$, consistent with that the RMS ratio of lateral accelerations was below 1 for the entire duration (Fig.3.14a). This reduction in acceleration amplitude showed a delay in predicting MISC for both visual conditions (Fig.3.17), while no apparent difference in this delay was observed between the conditions.

The windowing procedure was also examined for the root mean square of roll angles of the three parts of body (Fig.3.15). It is found the rolls of all the three body segments having an increase tendency in EYES-ON-ROAD condition especially during the first-half of total duration (Fig.3.15b), which was opposite to the lateral accelerations (Fig.3.14b). Nevertheless, no statistical difference was found between the three windows in time, except for the pelvis roll in EYES-OFF-ROAD condition (Table 3.2).

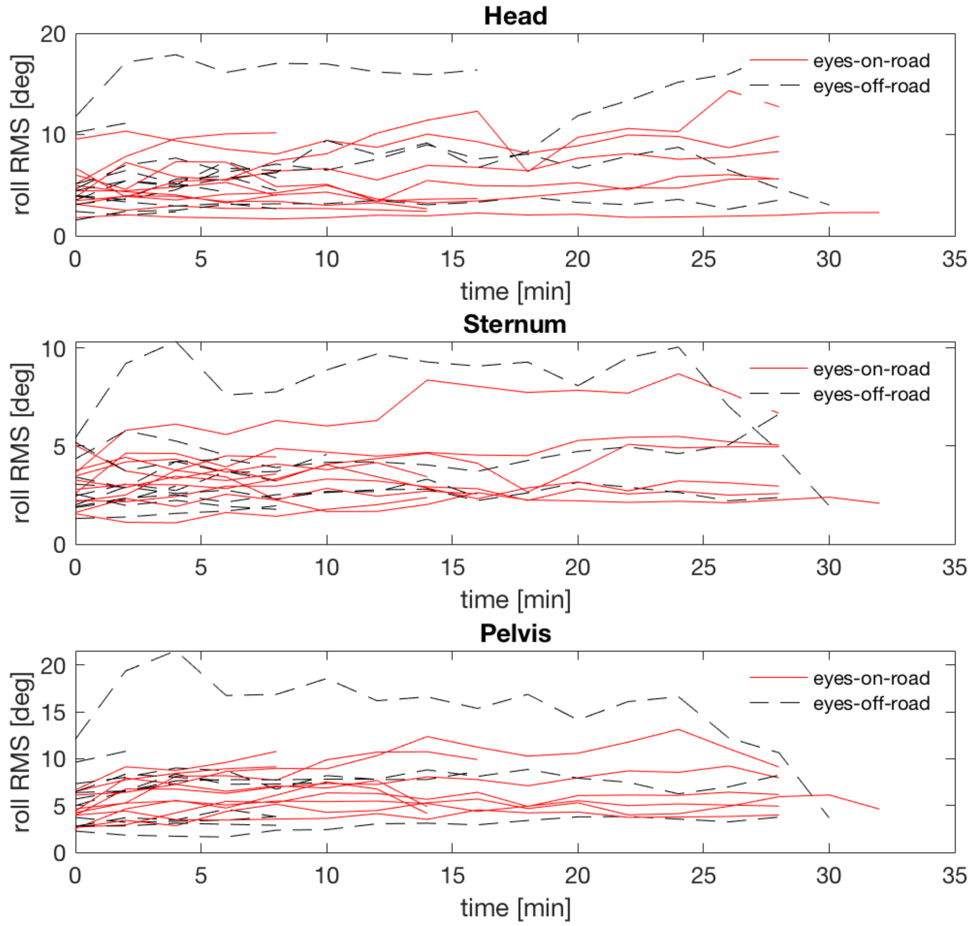

Head
roll RMS [deg]
time [min]
eyes-on-road
eyes-off-road
Sternum
roll RMS [deg]
time [min]
eyes-on-road
eyes-off-road
Pelvis
roll RMS [deg]
time [min]
eyes-on-road
eyes-off-road

(a)

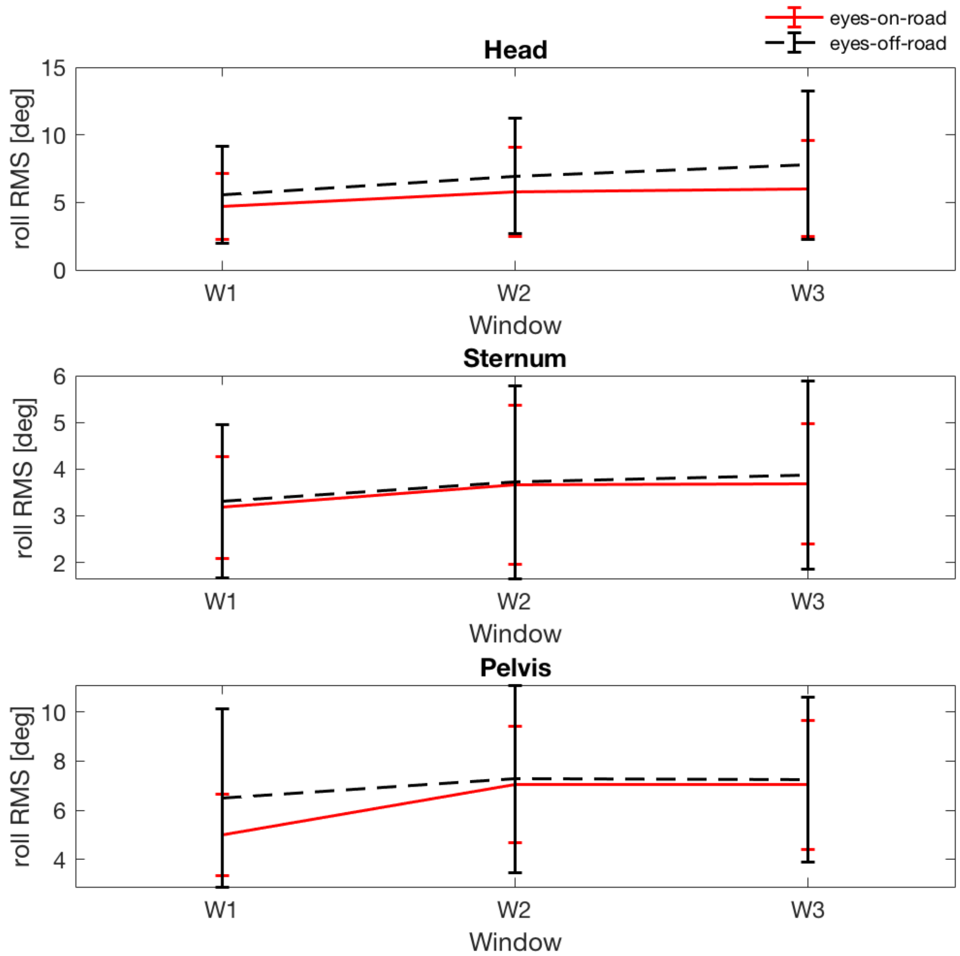

(b)

Fig.3.15 Root mean squares of head, sternum and pelvis roll (after 0.05-1 Hz band-pass filtering) throughout time in two visual conditions – (a) with 2-minute window over the entire duration for all the 22 trials with 11 participants in two conditions; (b) the mean ratio for all participants at W1 (beginning), W2(middle) and W3(end) of the trials in two conditions.

Table 3.2 Difference in roll RMS between three time windows – beginning, middle and end of trials (Repeated Measures ANOVA, α=0.05, Bonferroni Correction was used)

CONDITION	POSITION	SIG.	EFFECT SIZE	POWER
EYES-ON-ROAD	Head*	0.177	0.170	0.287
	Sternum	0.100	0.400	0.441
	Pelvis	**0.025**	0.559	0.720
EYES-OFF-ROAD	Head*	0.142	0.197	0.320
	Sternum	0.133	0.361	0.382
	Pelvis	**0.015**	0.606	0.804

** Sphericity was violated, where Huynh-Feldt method was used as correction.*

The relative stationarity of both the lateral accelerations and roll angles in time (only one significant difference was found) makes it possible to investigate the difference between conditions using the overall root mean squares value throughout all the time. Table 3.3 shows the RMS ratio of the lateral accelerations and the RMS of the roll angles for the three body positions, together with the results of Mann-Whitney U test comparing the difference between trials in different visual conditions. No significant difference was found in the amplitude of either lateral accelerations or roll angles between the EYES-ON-ROAD condition and EYES-OFF-ROAD condition for any body positions.

Instead of visual conditions, the trials were also divided into groups depending on the participants' susceptibility. 'Sensitive' group (12 of 22) includes the trials where participant reached 7 as the maximal MISC or quit due to motion sickness, while other trials lasting for 30 minutes were defined as 'non-sensitive' group (10 of 22). Extreme division by whether MISC of 7 has been reached was possible to separate the participants who are really susceptible and suffered from nausea and extreme sickness during the experiment, that is more convincing rather than using lower MISC as threshold due to the different identities to the 'slight sick' for different individuals. In other words, participants could have different standards for rating MISC of 2, 3 or 4, while being level 7 could be more similar to everyone indicating that they could not continue. The means and standard deviations of normalized lateral acceleration RMS and roll RMS for 'sensitive' group and 'non-sensitive' group are shown in Table 3.3, followed by the results of Mann-Whitney U test, while the latter shows no difference between groups.

According to the MSAQ, we know the severity of different types of symptoms related to motion sickness for each participant. Whether motion amplitude of different body segments affected the severity of symptoms arising in different dimensions (gastrointestinal, central, peripheral, and sopite-related) was investigated. Participants' sensitivity in the two main dimensions of motion sickness symptoms – gastrointestinal system and central nervous system are also shown in Table 3.3, with the three body motion amplitudes. Peripheral and sopite-related symptoms are comparatively slight and include many uncontrolled variables (such as temperature, participant's sleep quality etc.) which could not perfectly indicate the MSI and was excluded. Nevertheless, the participants' MSAQ scores highly correlated on their illness level indicated by MISC (figure 3.8), as well as the scores in the subordinate dimensions. To avoid the highly individual-dependent overall illness level, the ratio of scores in each dimension towards the MSAQ overall score was used as the indicator for the degree that participants were influenced by a specific dimension of symptoms. Still, difference was found in body motion amplitude between neither 'gastrointestinal-sensitive' group and 'gastrointestinal-non-sensitive' group nor 'central-sensitive' group and 'central-non-sensitive' group according the Mann-Whitney U test.

Although no body-movement difference was detected with respect to vision and multi-dimensional motion sickness sensitivity, it is observed that for lateral acceleration amplitude, the means of the three body positions examined are very similar – around 87 percent of the car lateral acceleration, however, the mean roll of the sternum was found only around half of that for head or pelvis, while the latter two are similar. The smaller roll of the sternum may suggest some human posture control strategies when exposed to a large passive horizontal motion, which will be discussed further by the relative motion investigation.

Table 3.3 Difference of lateral acceleration RMS and Roll RMS for head, sternum and pelvis between trials separated by vision, MISC sensitivity, gastrointestinal sensitivity and central sensitivity (mean significance: for visual conditions – 1. Paired t-test; 2. Wilcoxon Signed Rank Test; for sensitivities – Mann-Whitney Test; SD significance: Levene's nonparametric test; α=0.05, Bonferroni Correction, $\alpha_{correction}$=0.0083).

			LATERAL ACCELERATION RMS* (M/S^2)			**ROLL SD (DEG)**		
			Head	**Sternum**	**Pelvis**	**Head**	**Sternum**	**Pelvis**
VISION	EYES-ON-ROAD	mean	0.87	0.88	0.87	5.5	3.6	6.8
		SD	0.053	0.0089	0.017	2.6	1.4	2.0
	EYES-OFF-ROAD	mean	0.87	0.88	0.86	6.8	3.6	6.9
		SD	0.034	0.007	0.013	4.1	1.9	3.8
	Mean Sig. (p value)		**0.37**[2]	**0.65**[1]	**0.76**[1]	**0.098**[1]	**0.93**[2]	**0.91**[1]
	SD Sig. (p value)		**0.52**	**0.73**	**0.53**	**0.72**	**0.52**	**0.28**
MISC**	SENSITIVE	mean	0.87	0.87	0.87	6.2	3.0	6.6
		SD	0.033	0.006	0.012	3.9	0.99	2.3
	NON-SENSITIVE	mean	0.87	0.87	0.86	6.2	4.3	7.2
		SD	0.055	0.0096	0.016	2.9	2.0	3.7
	Mean Sig. (p value)		**0.45**	**0.31**	**0.22**	**0.82**	**0.11**	**0.92**
	SD Sig. (p value)		**0.57**	**0.80**	**0.71**	**0.61**	**0.40**	**0.61**
GASTRO-INTESTINAL***	SENSITIVE	mean	0.88	0.88	0.87	5.5	3.2	6.7
		SD	0.03	0.0058	0.016	2.4	1.1	2.5
	NON-SENSITIVE	mean	0.87	0.87	0.86	6.9	4.0	7.0
		SD	0.055	0.0093	0.013	4.2	2.0	3.5
	Mean Sig. (p value)		**0.95**	**0.15**	**0.24**	**0.60**	**0.55**	**0.90**
	SD Sig. (p value)		**0.61**	**0.54**	**0.81**	**0.048**	**0.34**	**0.71**
CENTRAL***	SENSITIVE	mean	0.88	0.88	0.86	6.4	3.9	7.8
		SD	0.040	0.0092	0.014	4.1	2.1	3.4
	NON-SENSITIVE	mean	0.87	0.87	0.87	6.0	3.3	5.9
		SD	0.047	0.0066	0.016	2.8	1.1	2.3
	Mean Sig. (p value)		**0.26**	**0.32**	**0.32**	**0.90**	**0.90**	**0.17**
	SD Sig. (p value)		**0.15**	**0.020**	**0.82**	**0.61**	**0.80**	**0.78**

** Lateral Acceleration r.m.s. – the r.m.s was normalized by dividing car lateral acceleration r.m.s.*

*** MISC – the sensitivity was separated by whether or not the MISC reached 7 in the trial.*

**** Gastrointestinal, central – the sensitivity was separated by the score of MSAQ relative items normalized by dividing the overall score for each participant (half of the trials were defined as sensitive).*

Head Motion with respect to Other Body Segments

Apart from the relative motion between body and vehicle, the motion between different body positions could also vary in various situations. The head roll relative to sternum or pelvis was derived from the rotation matrix of head local frame rotating to the sternum or pelvis local frame, and the relative lateral accelerations were calculated by Eq.2.5. Both accelerations and Euler angles were filtered before rotations, by the same band-pass filter used in the previous section (bandpass frequency of 0.05 Hz to 1 Hz).

Fig.3.16 and Fig.3.17 shows the root mean squares of head lateral acceleration and roll angles relative to sternum and pelvis in both visual conditions. The same windowing procedure (see section 3.4) was used to show the variables changing in time. No significant difference was found between the three time windows for either relative lateral acceleration or relative roll (Table 3.4).

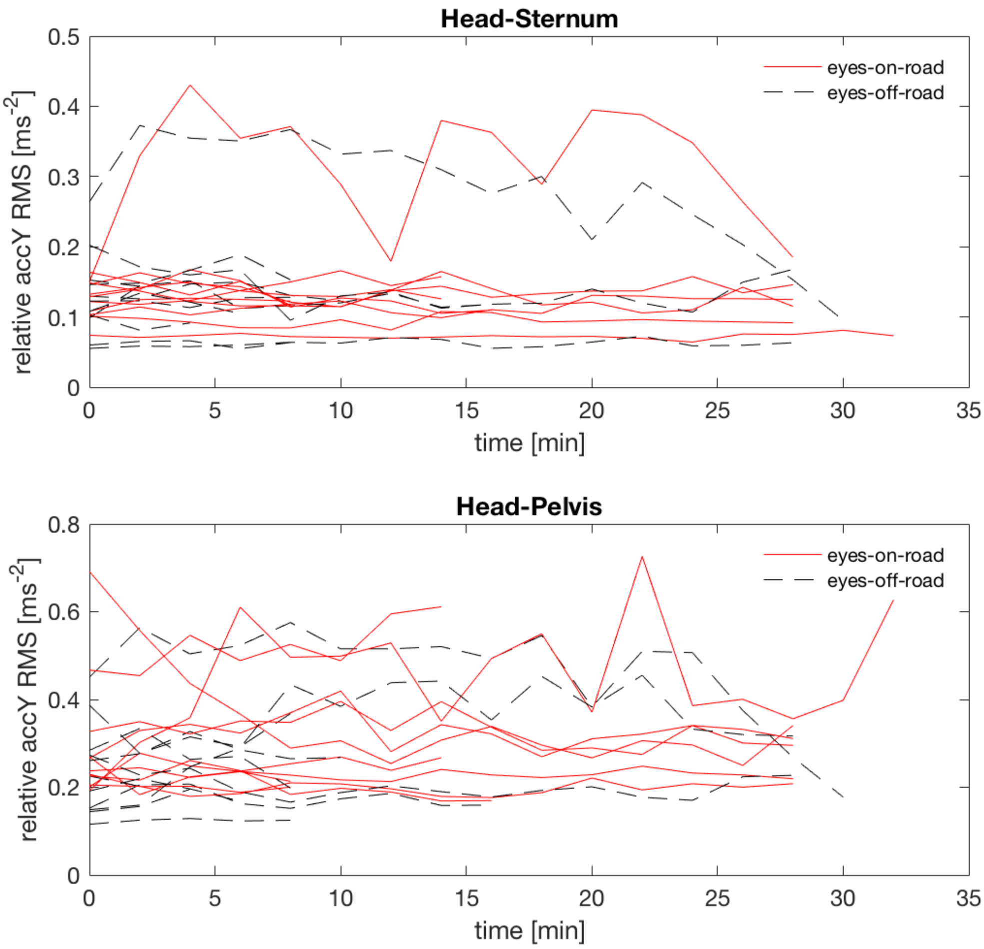

(a)

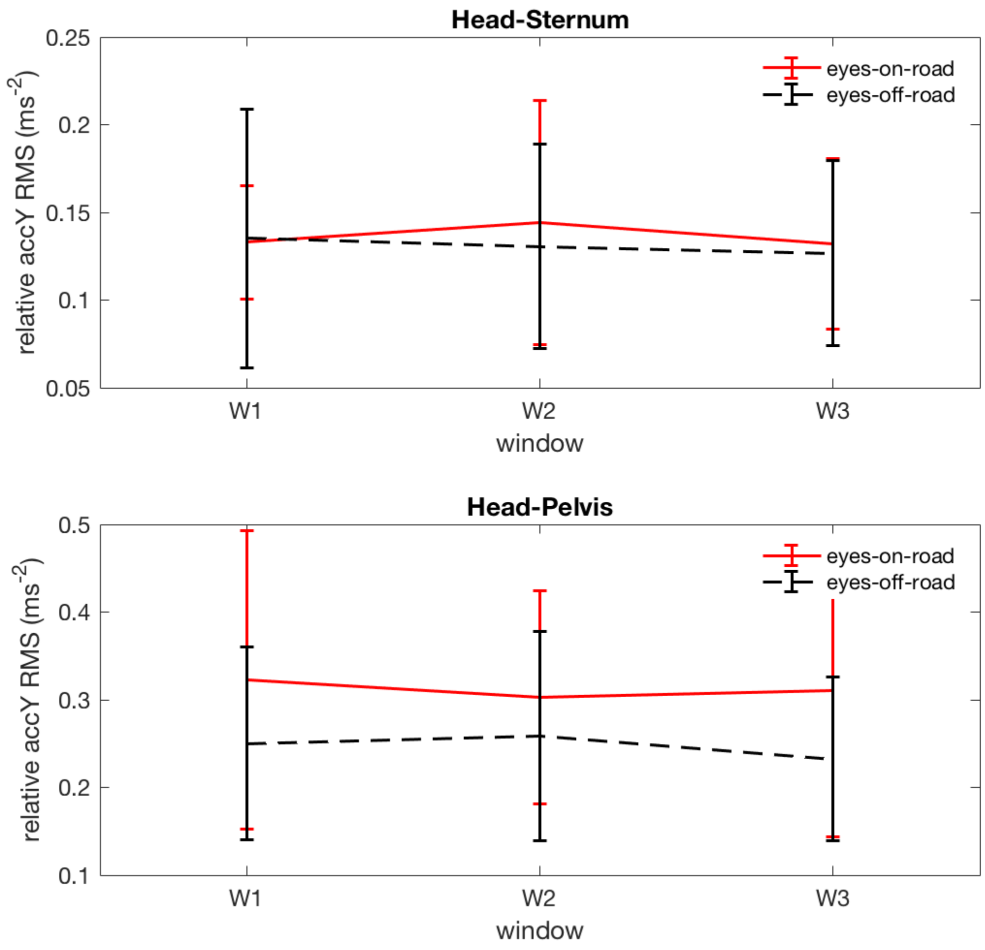

(b)

Fig.3.16 Relative head lateral acceleration RMS with respect to sternum and pelvis (after 1 Hz low-pass filtering) throughout time in two visual conditions – (a) with 2-minute window over the entire duration for all the 22 trials with 11 participants in two conditions; (b) the mean RMS for all participants at W1 (beginning), W2(middle) and W3(end) of the trials in two conditions.

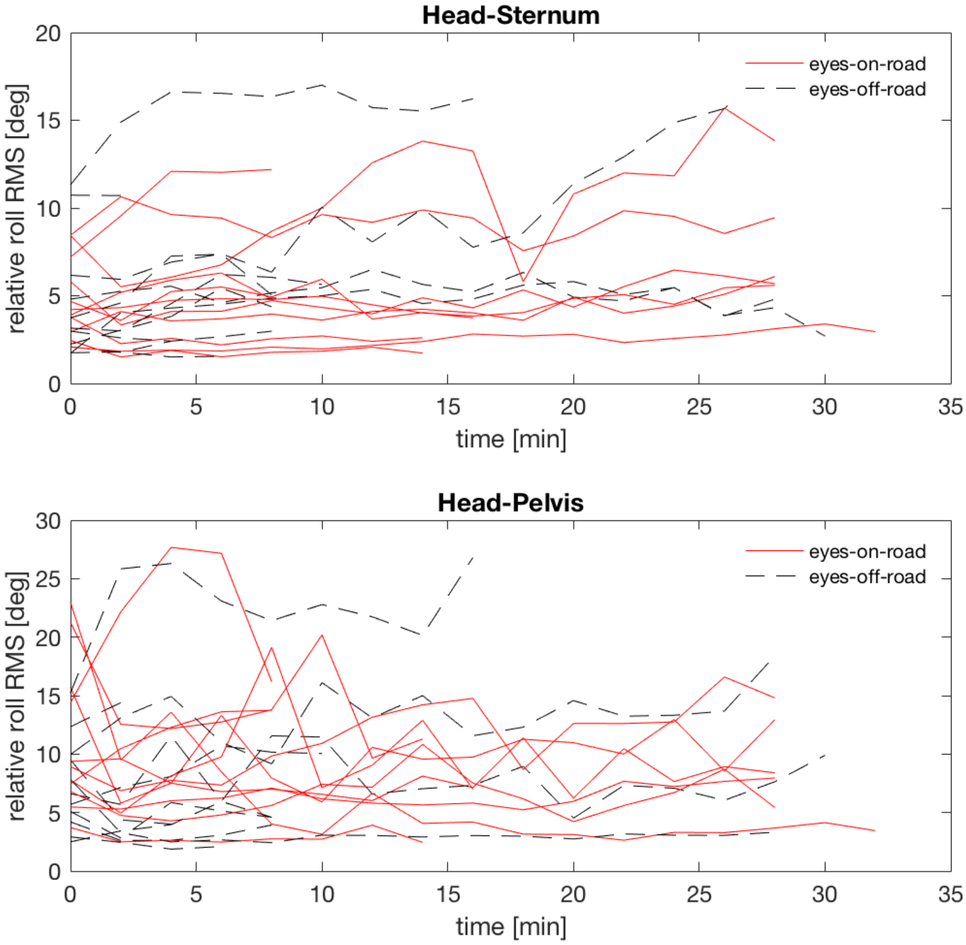

Head-Sternum
eyes-on-road
eyes-off-road
relative roll RMS [deg]
time [min]
0
5
10
15
20
25
30
35
Head-Pelvis
eyes-on-road
eyes-off-road
relative roll RMS [deg]
time [min]

(a)

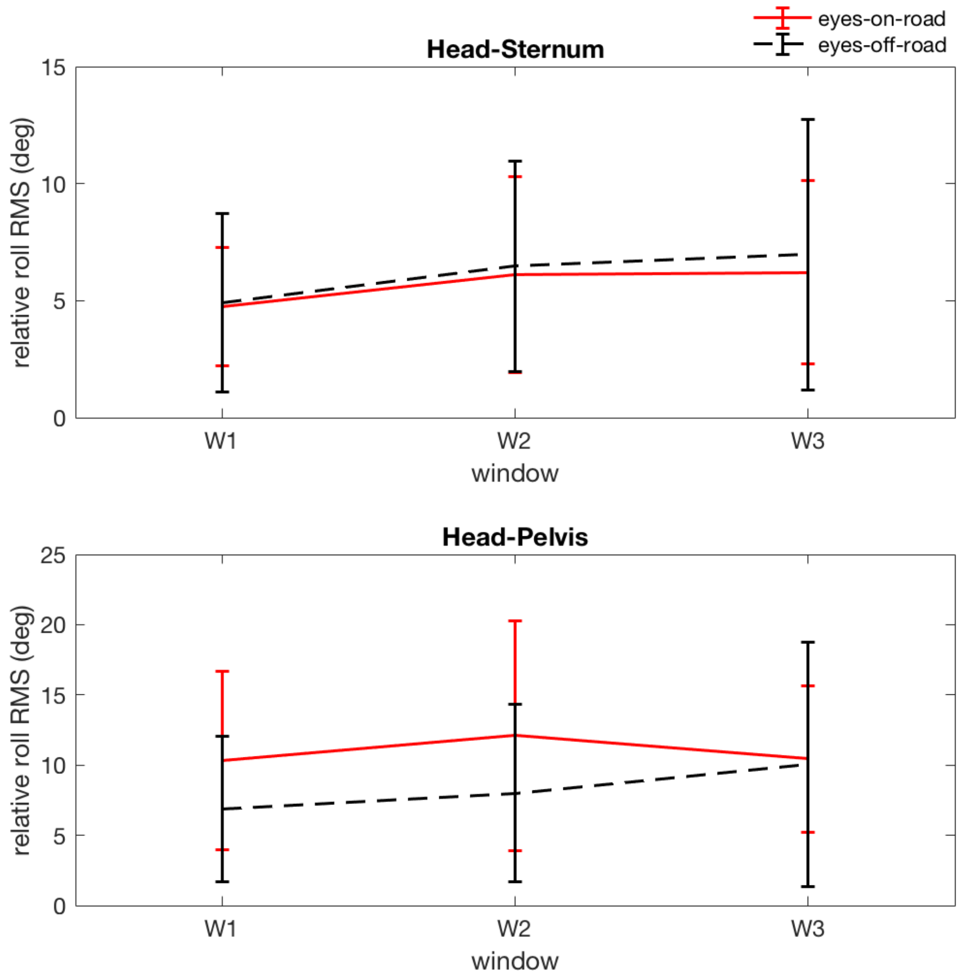

(b)

Fig.3.17 Relative head roll RMS with respect to sternum and pelvis (after 1 Hz low-pass filtering) throughout time in two visual conditions – (a) with 2-minute window over the entire duration for all the 22 trials with 11 participants in two conditions; (b) the mean STD for all participants at W1 (beginning), W2(middle) and W3(end) of the trials in two conditions.

Table 3.4 Significance of Difference in roll RMS between three time windows – beginning, middle and end of trials (Friedman test*, α=0.05, Bonferroni Correction was used)

SIG. (P VALUE)	RELATIVE LATERAL ACCELERATION		RELATIVE ROLL	
	Head-Sternum	Head-Pelvis	Head-Sternum	Head-Pelvis
EYES-ON-ROAD	0.441	0.178	0.529	0.695
EYES-OFF-ROAD	0.529	0.148	0.441	0.103

** Friedman test was used since no normal distribution was found.*

Table 3.5 shows mean and standard deviation of relative lateral acceleration and roll between body segments over all the durations, together with the results of Mann-Whitney U test, for different visual conditions – EYES-ON-ROAD and EYES-OFF-ROAD, different multidimensional sensitivities – MISC sensitive and MISC non-sensitive, gastrointestinal sensitive and gastrointestinal non-sensitive, central sensitive and central non-sensitive respectively. No statistical difference was found between any groups. Nevertheless, the higher standard deviation was observed again in EYES-OFF-ROAD, MISC NON-SENSITIVE and GASTROINTESTINAL NON-SENSITIVE group compared with the opposite observations (as observed in Table 3.3), especially for head-to-sternum relative lateral accelerations.

Table 3.5 Relative lateral acceleration root mean squares and roll standard deviations between head and sternum and pelvis for different vision and multidimensional sensitivity groups (mean significance: for visual conditions – Wilcoxon Signed Rank Test; for sensitivities – Mann-Whitney Test; SD significance: Levene's nonparametric test; α=0.05, Bonferroni Correction, $\alpha_{correction}$=0.0125)

			LATERAL ACCELERATION R.M.S. (M/S^2)		ROLL SD (RAD)	
			Head-Sternum	Head-Pelvis	Head-Sternum	Head-Pelvis
VISION	EYES-ON-ROAD	mean	0.63	1.3	6.9	13.8
		SD	0.58	0.91	3.3	7.4
	EYES-OFF-ROAD	mean	0.52	0.96	7.4	12.0
		SD	0.22	0.62	4.6	6.9
	Mean Sig. (p value)		**0.37**	**0.59**	**0.33**	**0.33**
	SD Sig. (p value)		**0.63**	**0.47**	**0.70**	**0.61**
MISC*	SENSITIVE	mean	0.47	0.95	6.3	12.0
		SD	0.073	0.74	4.5	6.9
	NON-SENSITIVE	mean	0.7	1.3	7.4	14.3
		SD	0.63	0.81	3.4	6.9
	Mean Sig. (p value)		**0.82**	**0.34**	**0.28**	**0.34**
	SD Sig. (p value)		**0.060**	**0.85**	**0.13**	**0.51**
GASTRO-INTESTINAL**	SENSITIVE	mean	0.47	0.98	5.7	12.0
		SD	0.077	0.76	3.4	8.6
	NON-SENSITIVE	mean	0.68	1.2	8.0	13.8
		SD	0.6	0.79	4.4	5.1
	Mean Sig. (p value)		**1**	**0.43**	**0.24**	**0.29**
	SD Sig. (p value)		**0.25**	**0.90**	**0.77**	**0.27**
CENTRAL**	SENSITIVE	mean	0.71	0.98	6.9	12.6
		SD	0.59	0.73	4.5	7.4
	NON-SENSITIVE	mean	0.44	1.2	7.4	13.2
		SD	0.079	0.83	3.6	6.9
	Mean Sig. (p value)		**0.15**	**0.6**	**0.55**	**0.84**
	SD Sig. (p value)		**0.84**	**0.41**	**0.29**	**0.36**

** MISC – the sensitivity was separated by whether or not the MISC reached 7 in the trial.*

*** Gastrointestinal, central – the sensitivity was separated by the score of MSAQ relative items normalized by dividing the overall score for each participant (half of the trials were defined as sensitive).*

3.4 Head and Body Motion in Frequency Domain

For frequency domain, both lateral and roll acceleration of body segments will be discussed in terms of coherence and transmissibility from the vehicle seat or other body segments. The coherence implying linearity and causality between input and output (from vehicle to body or from torso to head). And the transmission gain and phase indicates the transmissibility and delay between the input and output. Since only the motion around frequency of 0.2 Hz was excited in the car as well as body (see figure 3.2, 3.18, 3.19), the signals with bandwidth from 0.15 to 0.25 Hz were statistically compared in frequency domain; the motion in other frequencies contained mostly noise which has little effects on motion sickness.

Head and Body Motion in Frequency Overview

Head translational accelerations and rotational angles of the same trial in Fig.3.1, 3.2, 3.12, 3.13 are shown in frequency domain (Fig.3.18). Compared with the car acceleration (Fig.3.2), head longitudinal acceleration was slightly excited at the 0.2 Hz which is the dominant frequency in lateral direction. It possibly resulted from the rotational movements caused by car steering such as pitch and roll. Nevertheless, the head longitudinal acceleration at 0.2 Hz is still comparatively mild and can be ignored in comparison to the lateral one, but roll, as the dominant rotational motion in discussed frequency, will be considered in the following frequency analysis.

The spectrogram of head lateral and roll accelerations was also checked. The dominant frequency of the signal, 0.2 Hz, was not changing over the whole trial, so the following analysis of transmissibility and coherence were based on the entire trials.

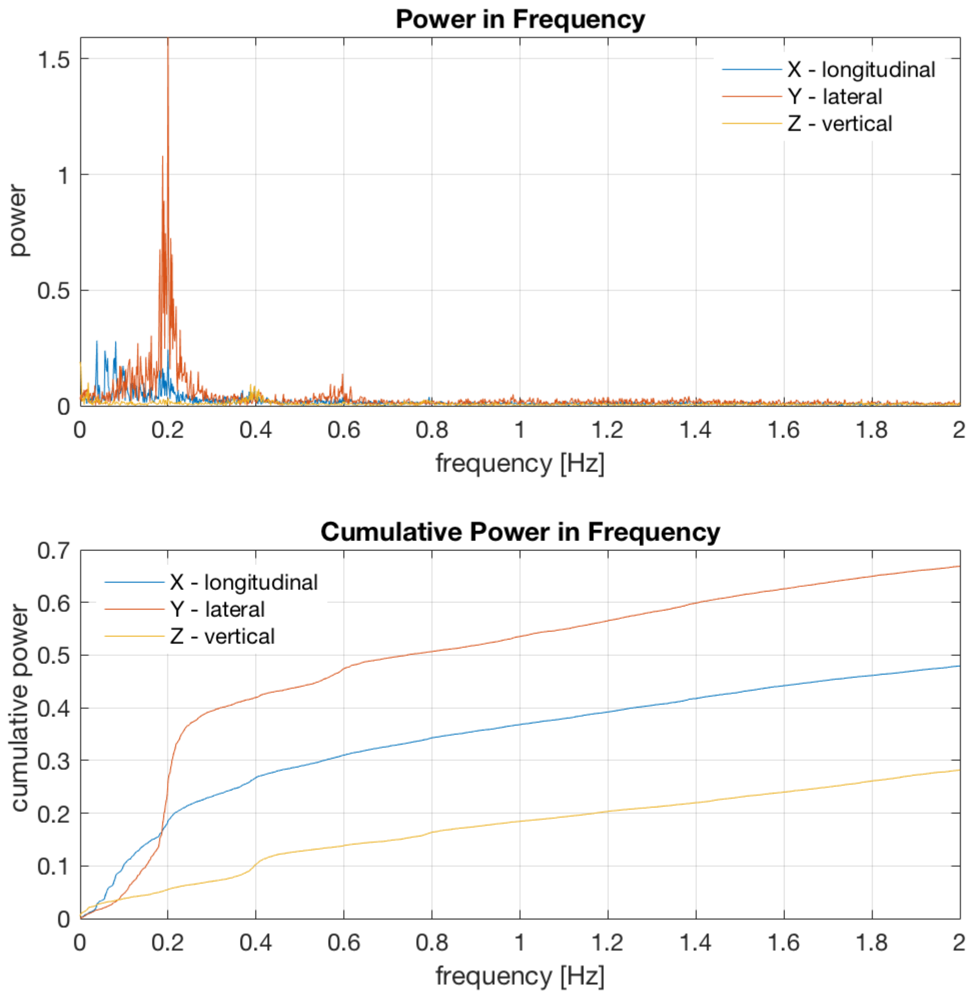
Power in Frequency
power
frequency [Hz]
X - longitudinal
Y - lateral
Z - vertical
0
0.5
1
1.5
0.2
0.4
0.6
0.8
1.2
1.4
1.6
1.8
2
Cumulative Power in Frequency
cumulative power
frequency [Hz]
X - longitudinal
Y - lateral
Z - vertical
0.1
0.2
0.3
0.4
0.5
0.6
0.7

(a)

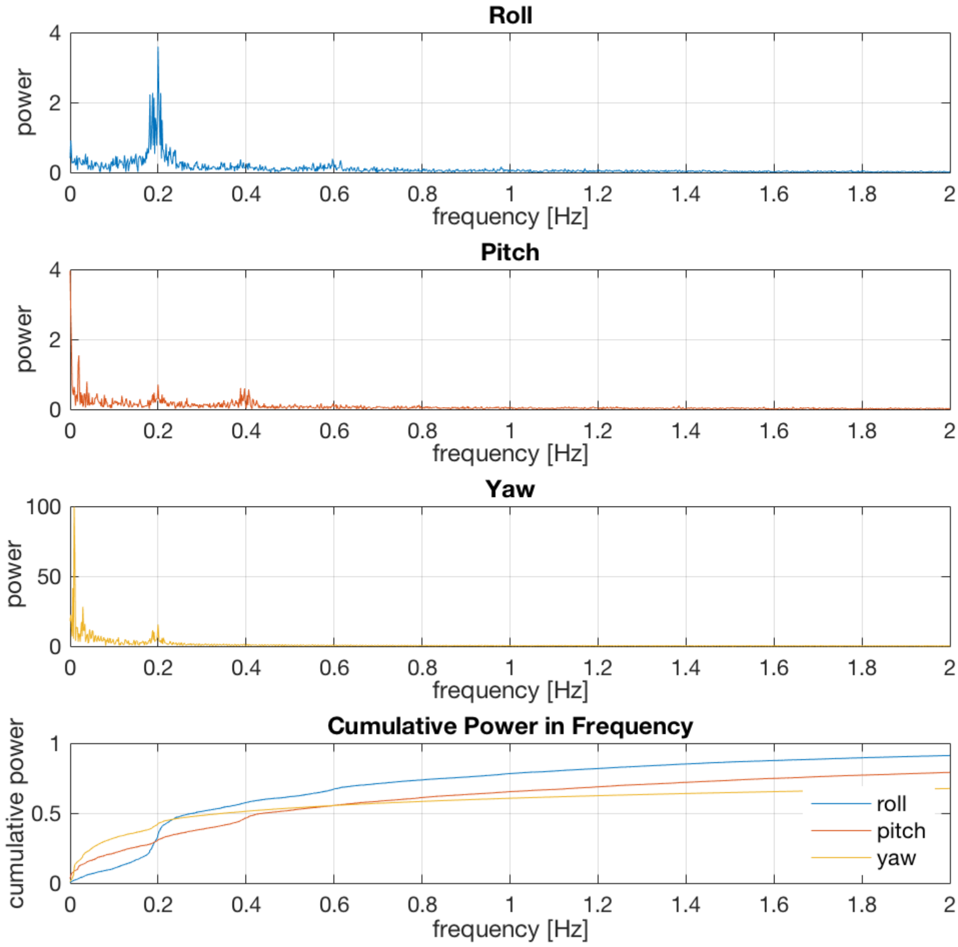

(b)

Fig.3.18 Head accelerations in time for an 8-minute trial – (a) longitudinal, lateral and vertical; (b) roll, pitch and yaw (power normalized to the sample size; cumulative power normalized to 1)

Head and Body Motion with respect to Car

Coherence

The coherence between seat and body segments indicates the linearity and causality between the input (seat) and the output (body). In other words, if the body movement was completely caused by the car movement, and if this relation is linear, the coherence between the two motion signals should be 1, however, any voluntary tension or control generated by the participants per se could reduce the coherence.

The coherence of head lateral and roll accelerations were considered together with respect to the car lateral acceleration input in both conditions (Fig.3.19). Two peaks were found around 0.17 Hz and 0.55 Hz for both lateral and roll accelerations – the former was caused by the dominant 0.2 Hz input motion while the latter might result from resonance. With 11 participants in each visual condition, the significance threshold for coherence is 0.26 for significance level $\alpha = 0.05$ (Eq.2.8). That means the mean coherence in Fig.3.19 will not be considered below 0.26.

The coherence was also checked from car seat to other body segments (pelvis and sternum), which is compared with that for head by the mean for all the 11 participants (Fig.3.20). With respect to lateral acceleration at around 0.2 Hz, it is found the coherence significantly varied between seat to head, sternum and pelvis for both visual conditions (Friedman's test: p = 0.020 for EYES-ON-ROAD; p = 0.006 for EYES-OFF-ROAD), and the three coherence in EYES-OFF-ROAD condition was closer to 1. For roll acceleration, however, the coherence between the seat and head, sternum and pelvis was not found significantly different in EYES-ON-ROAD condition (Friedman's test: p = 0.18). The head coherence was found lower than the torso in EYES-OFF-ROAD condition (Friedman's test: p = 0.029), though all the three coherences were relatively higher than EYES-ON-ROAD condition. The different coherence observed in different body positions could be explained by the body control. When external vision was provided, for instance, the passengers were able to control their body roll and lateral movement based on the anticipatory information. While stabilizing head roll would be easier than controlling the lateral acceleration when the latter was following the car motion, and it increases the nonlinearity in the head and torso roll with respect to the car acceleration. Without the visual information provided, the passengers lacked the expectation and body motion would be more coherent with the car.

According to the dominant frequency and significance threshold, only the coherence averaged only from 0.15 Hz to 0.25 Hz of lateral and roll accelerations was compared between groups (Table 3.6) – EYES-ON-ROAD and EYES-OFF-ROAD condition; MISC sensitive and non-sensitive group; gastrointestinal sensitive and non-sensitive group; central sensitive and non-sensitive group. No statistical difference was found in both mean and standard deviation of coherence with a significance level after Bonferroni correction ($\alpha_{correction}$=0.0083), although there was some significance being found with α=0.05.

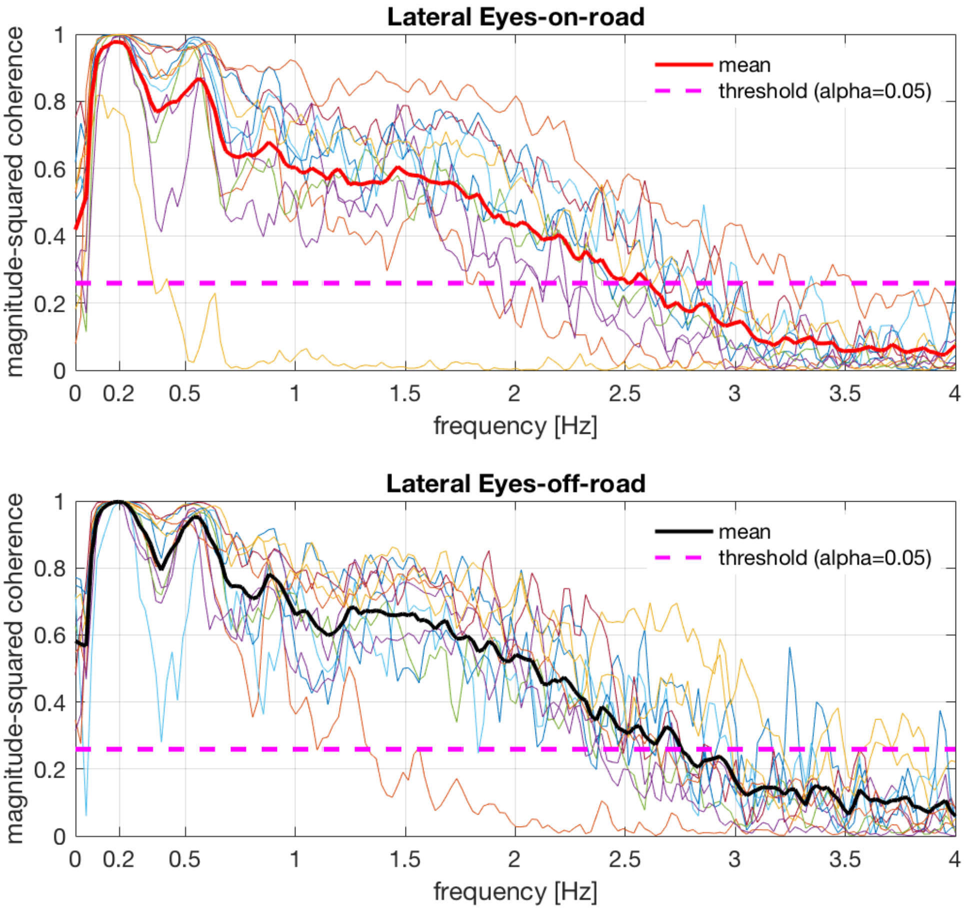
Lateral Eyes-on-road
mean
threshold (alpha=0.05)
magnitude-squared coherence
frequency [Hz]
Lateral Eyes-off-road
mean
threshold (alpha=0.05)
magnitude-squared coherence
frequency [Hz]

(a)

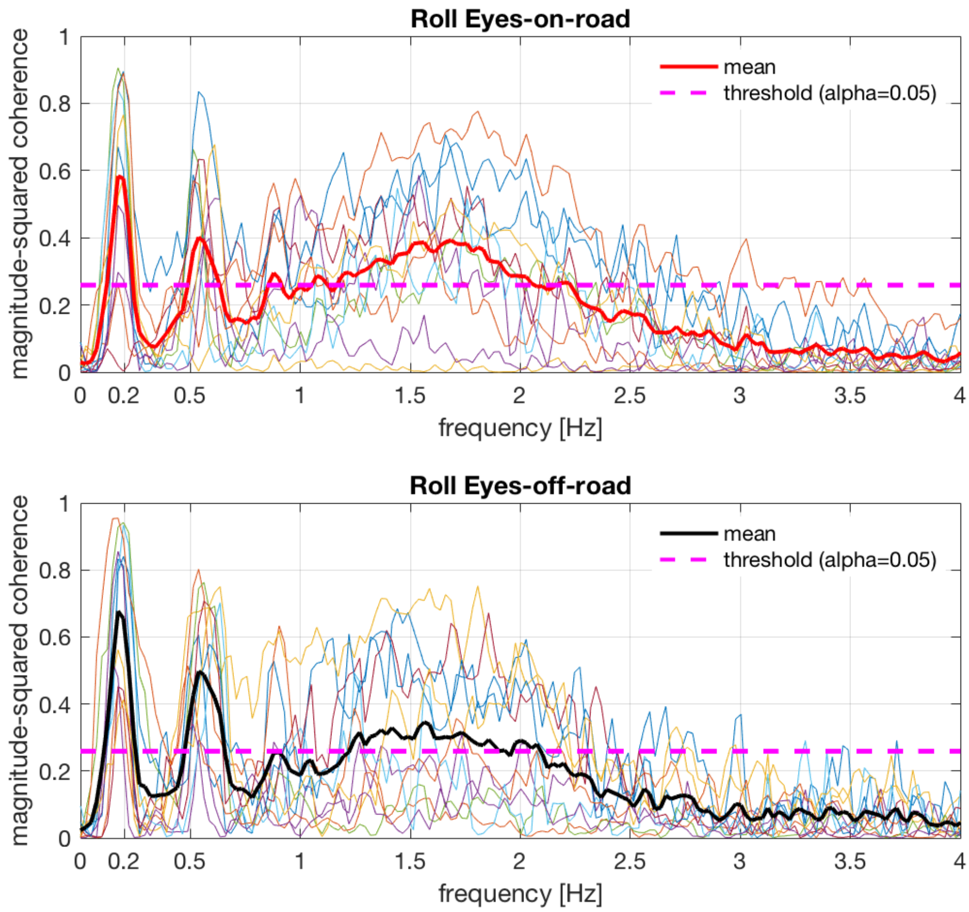

(b)

Fig.3.19 Magnitude-squared coherence of lateral and roll acceleration from car seat to head for 11 participants in both visual conditions – (a) lateral acceleration; (b) roll acceleration. (mean and significance threshold are shown together)

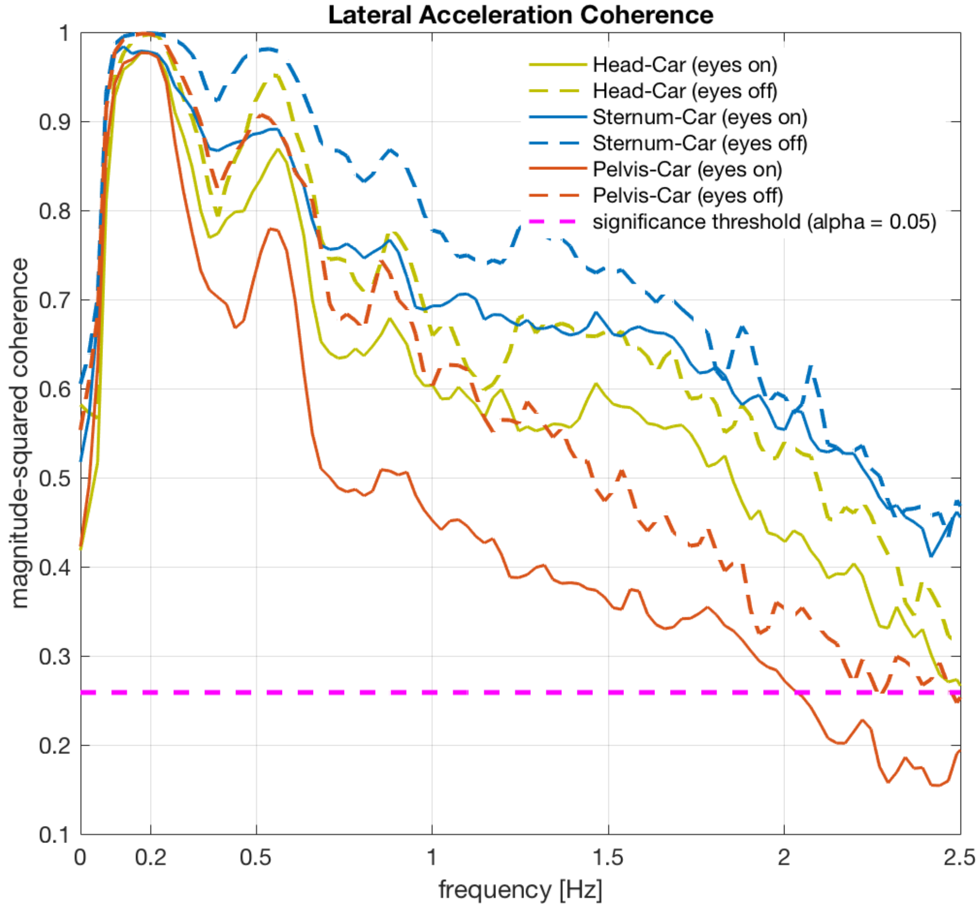
Lateral Acceleration Coherence
Head-Car (eyes on)
Head-Car (eyes off)
Sternum-Car (eyes on)
Sternum-Car (eyes off)
Pelvis-Car (eyes on)
Pelvis-Car (eyes off)
significance threshold (alpha = 0.05)
magnitude-squared coherence
frequency [Hz]
0.1
0.2
0.3
0.4
0.5
0.6
0.7
0.8
0.9
1
0
0.2
0.5
1
1.5
2
2.5

(a)

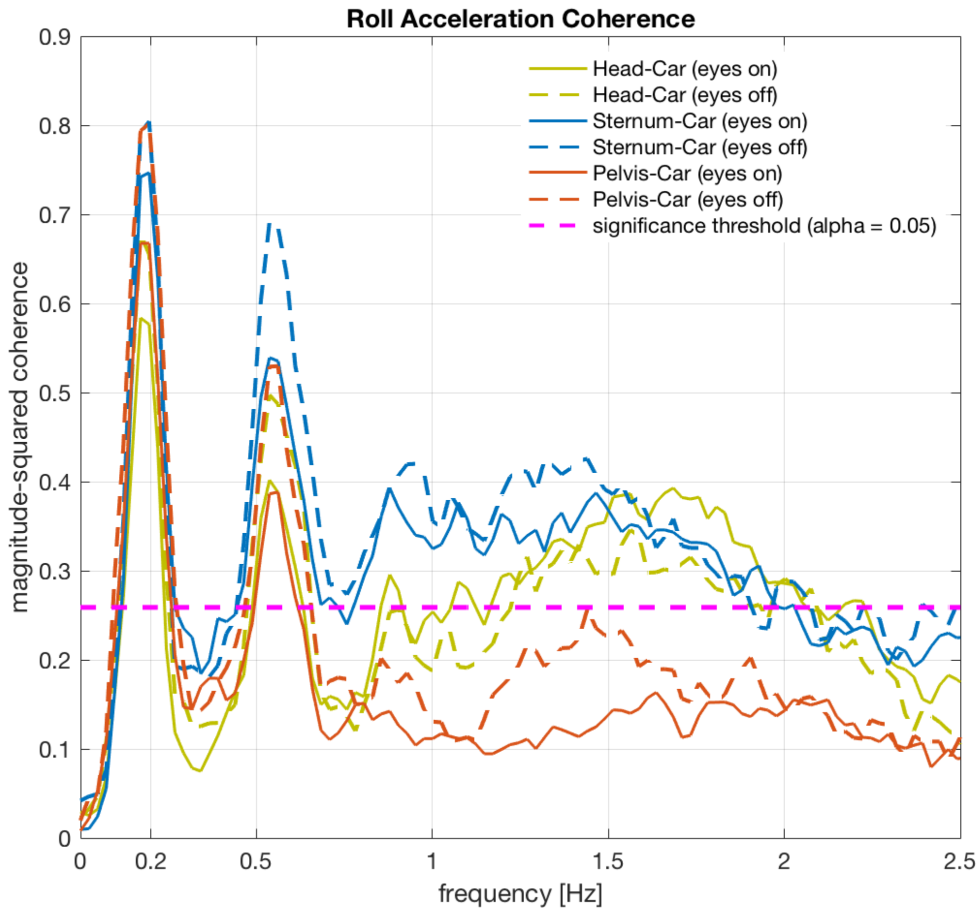

(b)

Fig.3.20 Mean Magnitude-squared coherence of lateral and roll acceleration from car seat to head, sternum and pelvis for 11 participants in both visual conditions – (a) lateral acceleration; (b) roll acceleration (with significance threshold)

Table 3.6 Coherence integrated from 0.15 Hz to 0.25 Hz for lateral and roll accelerations comparison between visual and sensitive groups (mean significance: for visual conditions – Wilcoxon Signed Rank Test; for sensitivities – Mann-Whitney Test; SD significance: Levene's nonparametric test; α=0.05, Bonferroni Correction, $\alpha_{correction}$=0.0083).

			LATERAL ACCELERATION COHERENCE			**ROLL ACCELERATION COHERENCE**		
			H-C*	S-C	P-C	H-C	S-C	P-C
VISION	EYES-ON-ROAD	mean	2.95	2.96	2.95	1.91	2.36	2.09
		SD	0.12	0.12	0.11	0.70	0.49	0.77
	EYES-OFF-ROAD	mean	2.99	3.00	2.99	2.12	2.42	2.43
		SD	0.0089	0.0014	0.0091	0.58	0.29	0.59
	Mean Sig. (p value)		**0.59**	**0.29**	**0.021**	**0.29**	**0.66**	**0.33**
	SD Sig. (p value)		**0.53**	**0.092**	**0.90**	**0.69**	**0.61**	**1**
MISC**	SENSITIVE	mean	2.99	2.998	2.99	2.10	2.52	2.49
		SD	0.0036	<0.001	0.0054	0.65	0.24	0.52
	NON-SENSITIVE	mean	2.95	2.96	2.95	1.91	2.23	1.98
		SD	0.12	0.12	0.12	0.62	0.49	0.79
	Mean Sig. (p value)		**0.093**	**0.059**	**0.036**	**0.35**	**0.23**	**0.14**
	SD Sig. (p value)		**0.14**	**0.31**	**0.44**	**0.43**	**0.23**	**0.50**
GASTROINTESTINAL***	SENSITIVE	mean	2.99	2.998	2.99	1.96	2.60	2.49
		SD	0.0038	<0.001	0.0057	0.66	0.19	0.55
	NON-SENSITIVE	mean	2.95	2.96	2.95	2.07	2.19	2.03
		SD	0.11	0.12	0.11	0.63	0.44	0.77
	Mean Sig. (p value)		**0.19**	**0.056**	**0.034**	**0.75**	**0.016**	**0.15**
	SD Sig. (p value)		**0.13**	**0.75**	**0.70**	**0.45**	**0.72**	**0.89**
CENTRAL***	SENSITIVE	mean	2.99	2.99	2.99	2.19	2.36	2.49
		SD	0.0042	0.0093	0.0057	0.55	0.43	0.51
	NON-SENSITIVE	mean	2.95	2.96	2.95	1.84	2.42	2.03
		SD	0.12	0.12	0.11	0.69	0.36	0.79
	Mean Sig. (p value)		**0.33**	**0.22**	**0.15**	**0.17**	**0.75**	**0.19**
	SD Sig. (p value)		**0.25**	**1**	**0.63**	**0.80**	**0.62**	**0.39**

** H – Head; S – Sternum; P – Pelvis; C – Car.*

*** MISC – the sensitivity was separated by whether or not the MISC reached 7 in the trial.*

**** Gastrointestinal, central – the sensitivity was separated by the score of MSAQ relative items normalized by dividing the overall score for each participant (half of the trials were defined as sensitive).*

Transmissibility and Phase

Transmissibility and phase are widely used to check the seat-to-head motion transmission and delay between input (seat) and output (head) signal (Eq.2.6). In this experiment, the seat-to-head transmissibility in lateral acceleration peaked at 1.5 Hz for both visual conditions (Fig.3.21) – the frequency was hardly excited though. The area from 0.15 to 0.25 Hz was calculated as the quantification of the transmissibility, and was compared between conditions. Apart from lateral acceleration, head roll was also a dominant motion affected by the car horizontal movement, the transmissibility for which was calculated from the car lateral acceleration to head roll acceleration (Eq.2.6). Unlike the relatively coincident seat and head lateral accelerations, head roll acceleration resulted from translational acceleration is much lower at low frequencies for both conditions (Fig.3.22) and varied significantly between different individuals, suggesting that head roll movement was highly dependent on individual behavior that could be controlled as well. Table 3.7 shows the integrated lateral and roll transmissibility from 0.15 to 0.25 Hz for the two visual conditions. No difference was observed in seat-to-head transmissibility between EYES-ON-ROAD and EYES-OFF-ROAD.

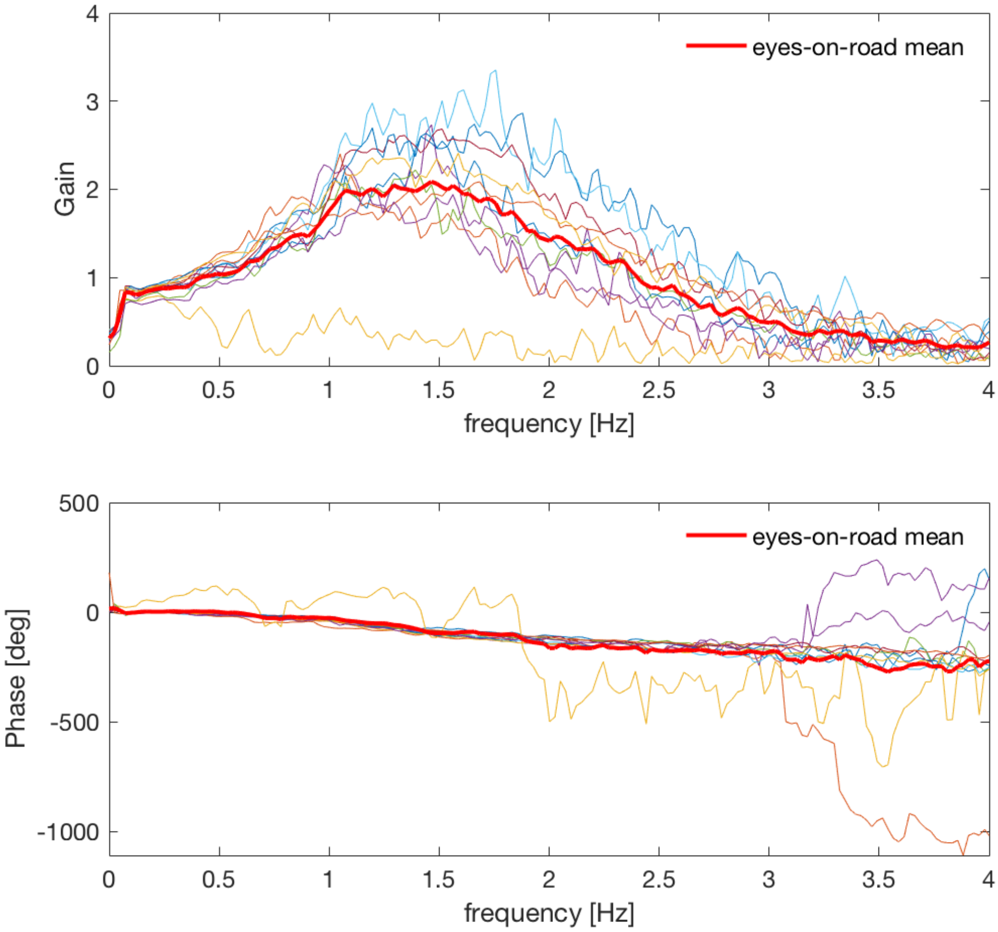

(a)

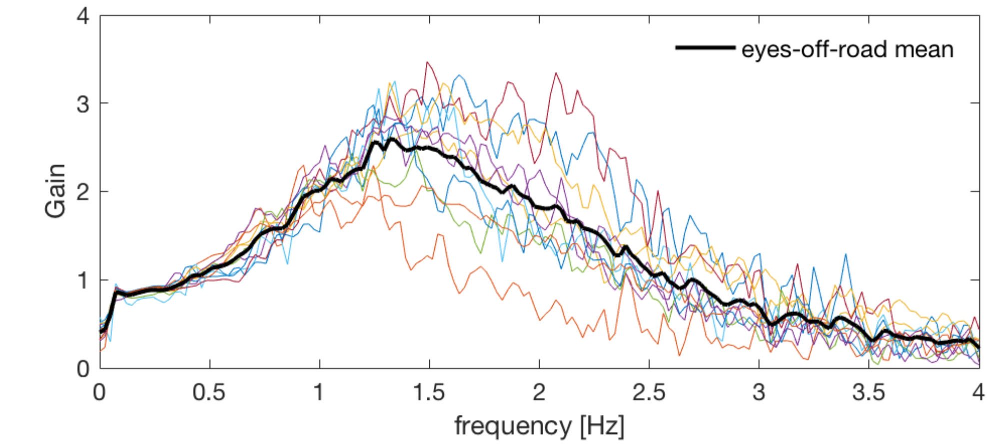

eyes-off-road mean
Gain
frequency [Hz]
0
1
2
3
4
0.5
1.5
2.5
3.5

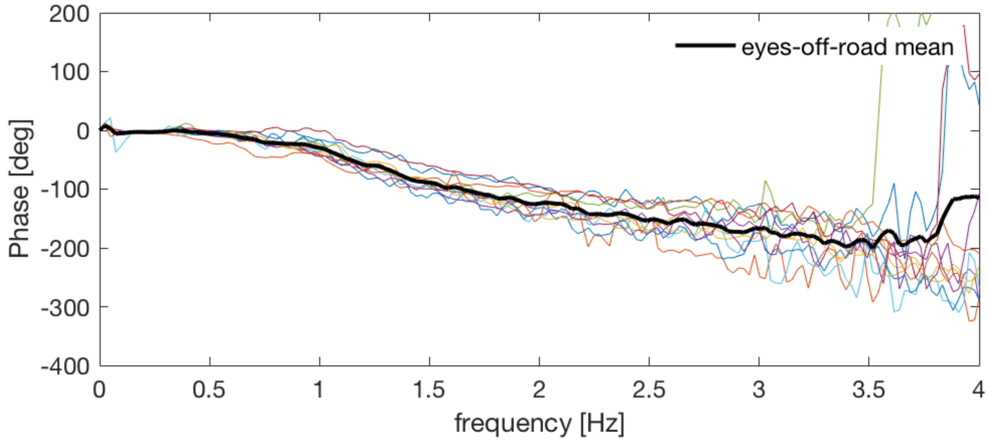

eyes-off-road mean
Phase [deg]
frequency [Hz]
200
100
0
-100
-200
-300
-400

(b)

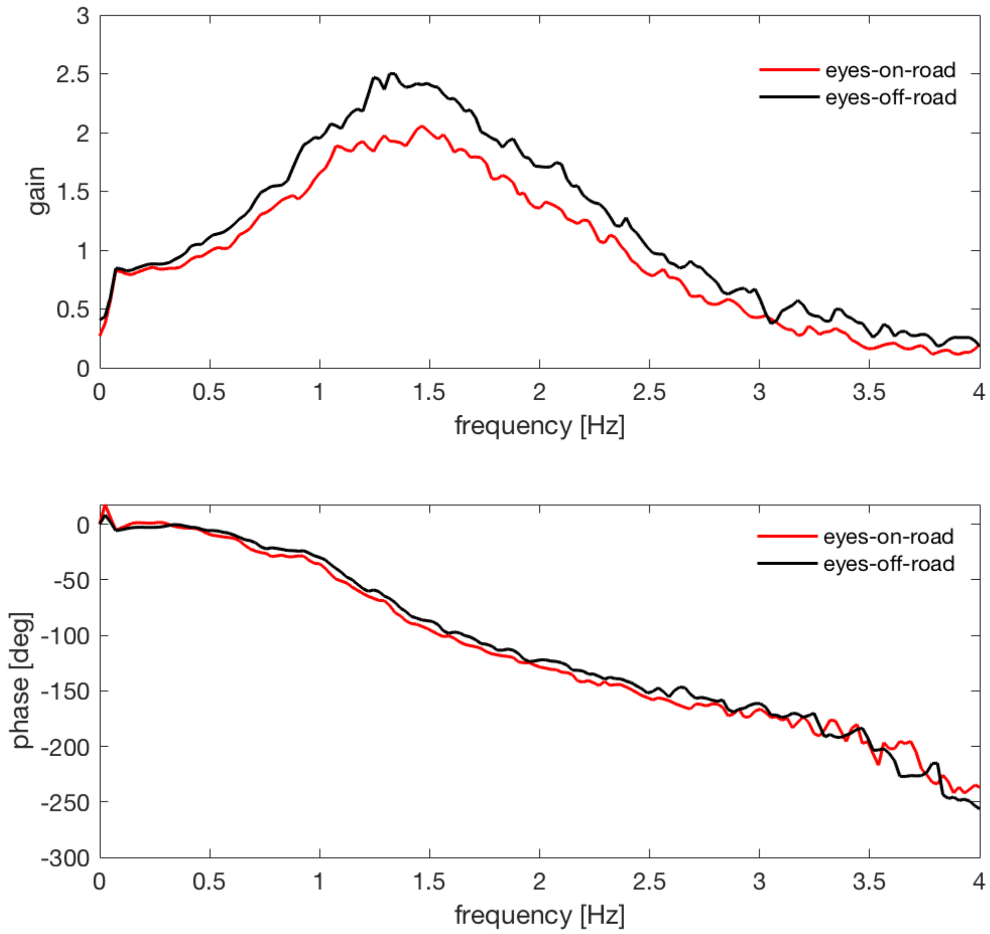

(c)

Fig.3.21 Lateral acceleration seat-to-head transmissibility gain and phase for 11 participants in both visual conditions – (a) EYES-ON-ROAD; (b) EYES-OFF-ROAD; (c) EYES-ON-ROAD and EYES-OFF-ROAD (bold line is mean of all the participants)

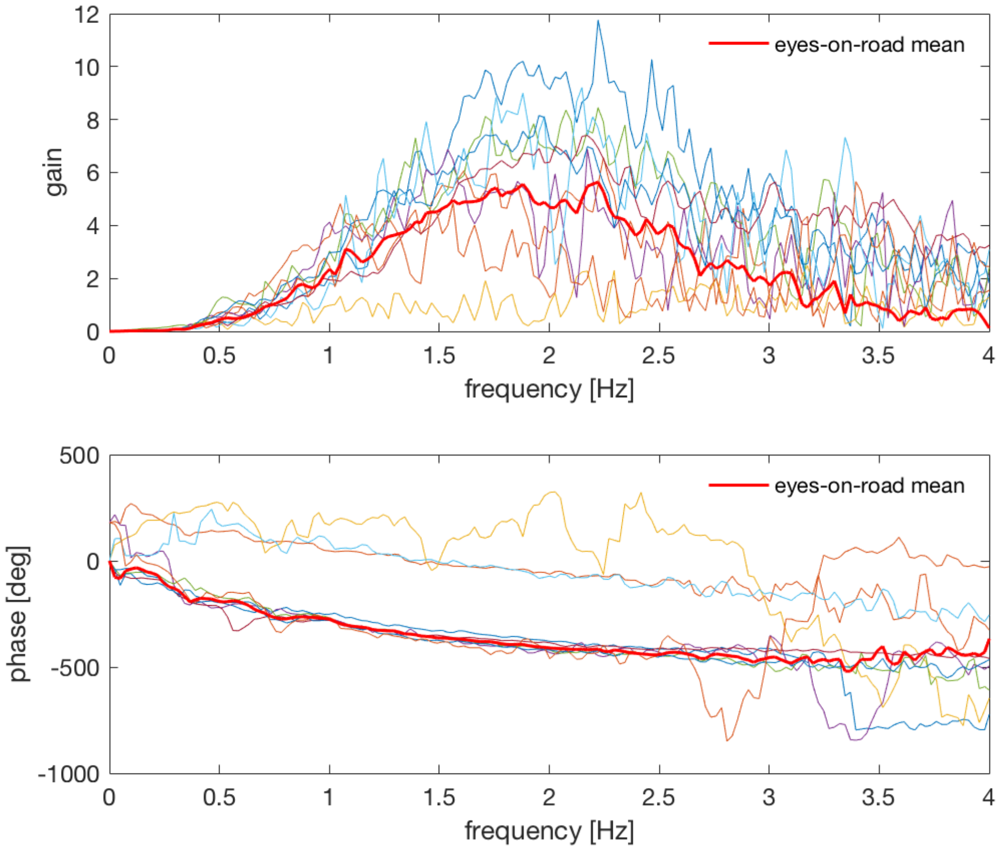
eyes-on-road mean
gain
frequency [Hz]
eyes-on-road mean
phase [deg]
frequency [Hz]

(a)

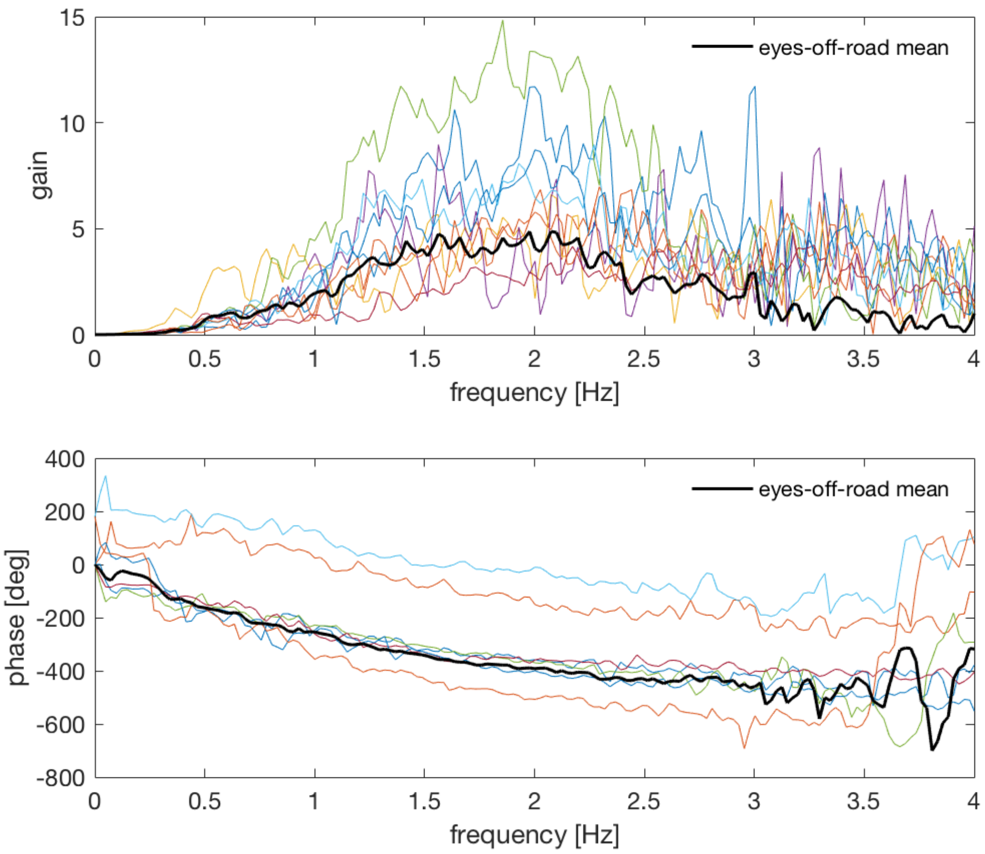
eyes-off-road mean
gain
15
10
5
0
0
0.5
1
1.5
2
2.5
3
3.5
4
frequency [Hz]
eyes-off-road mean
phase [deg]
400
200
0
-200
-400
-600
-800
0
0.5
1
1.5
2
2.5
3
3.5
4
frequency [Hz]

(b)

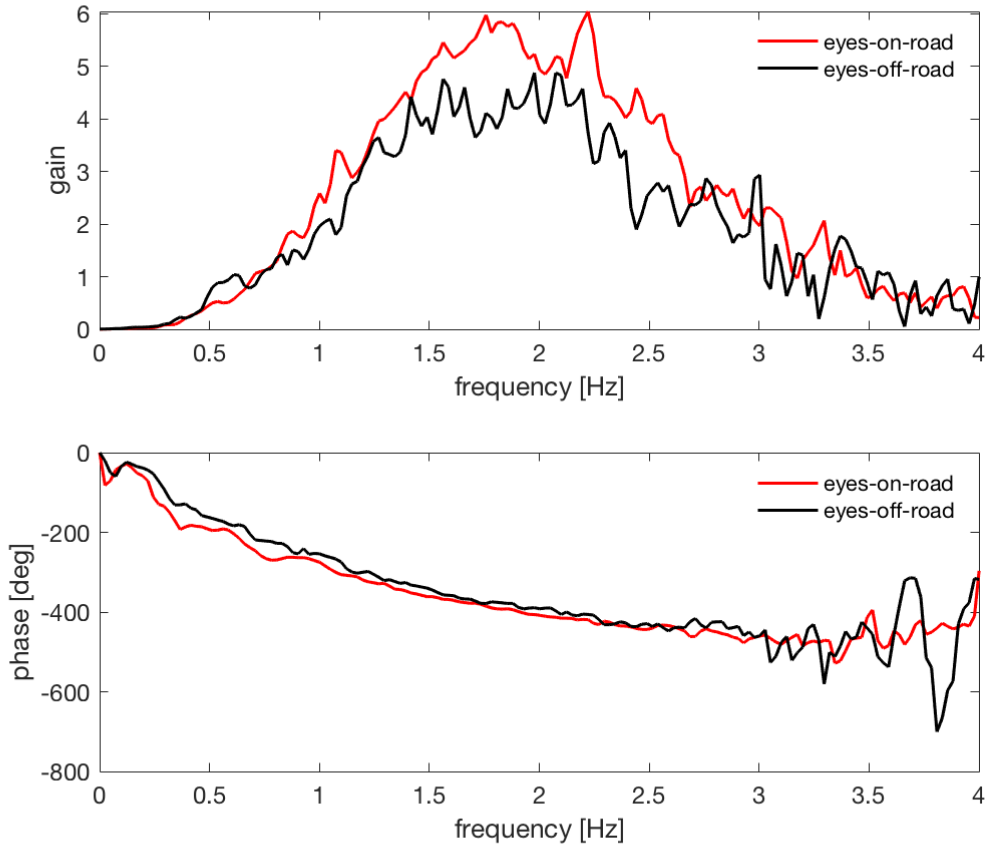

(c)

Fig.3.22 Roll acceleration seat-to-head transmissibility gain and phase for 11 participants in both visual conditions – (a) EYES-ON-ROAD; (b) EYES-OFF-ROAD; (c) EYES-ON-ROAD and EYES-OFF-ROAD (bold line is mean of all the participants)

Table 3.7 Transmission gain and phase integrated from 0.15 Hz to 0.25 Hz for lateral and roll accelerations comparison between visual conditions (mean significance: Wilcoxon Signed Rank Test; SD significance: Levene's nonparametric test; α=0.05, Bonferroni Correction, $\alpha_{correction}$=0.0125).

		LATERAL ACC		ROLL ACC	
		gain	phase	gain	phase
EYES-ON-ROAD	mean	3.4	-2.9	0.19	-58.4
	SD	0.25	0.96	0.12	100.6
EYES-OFF-ROAD	mean	3.5	-3.0	0.27	-13.8
	SD	0.15	1.2	0.22	98.1
MEAN SIG. (P VALUE)		**0.86**	**0.65**	**0.13**	**0.18**
SD SIG. (P VALUE)		**0.14**	**0.23**	**0.78**	**0.90**

Head Motion with respect to Other Body Segments

The coherence within the body – from torso to head and from pelvis to sternum was also examined (Fig.3.23). Similar to the coherence from seat to body, both lateral and roll coherence within the body was all lower in EYES-ON-ROAD condition at low frequencies according to the figures, suggesting the passenger's head would be more linearly correlated with torso without external vision in the vehicle. It is noticed that the coherence from pelvis to head had the largest discrepancy between the two conditions for both lateral and roll acceleration, compared with the coherence between pelvis and sternum or sternum and head.

Likewise, the lateral and roll coherence from 0.15 Hz to 0.25 Hz was statistically tested between visual and sensitive groups (Table 3.8). Two significant differences were found between the participants reached MISC of 7 and those did not – both the lateral and roll coherence from pelvis to head. Furthermore, the pelvis-to-head roll coherence was also found significant between the groups sensitive to central nervous symptoms and who were non-sensitive.

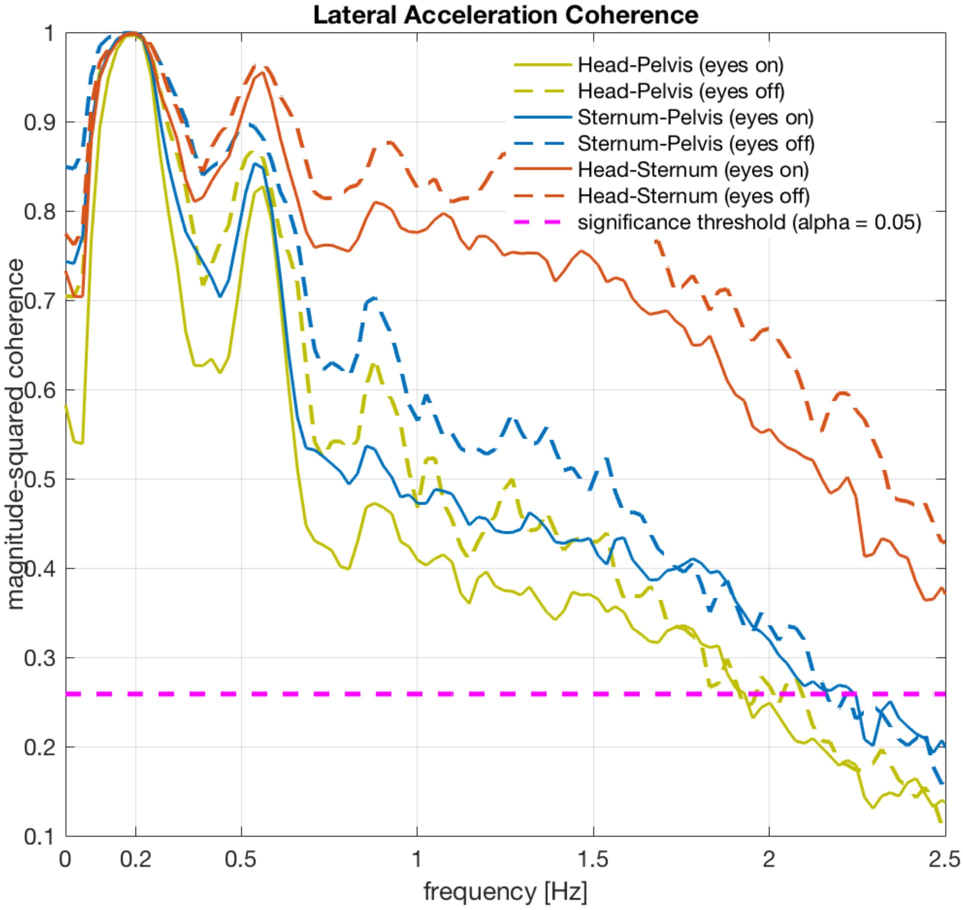
Lateral Acceleration Coherence
Head-Pelvis (eyes on)
Head-Pelvis (eyes off)
Sternum-Pelvis (eyes on)
Sternum-Pelvis (eyes off)
Head-Sternum (eyes on)
Head-Sternum (eyes off)
significance threshold (alpha = 0.05)
magnitude-squared coherence
frequency [Hz]
1
0.9
0.8
0.7
0.6
0.5
0.4
0.3
0.2
0.1
0
0.2
0.5
1
1.5
2
2.5

(a)

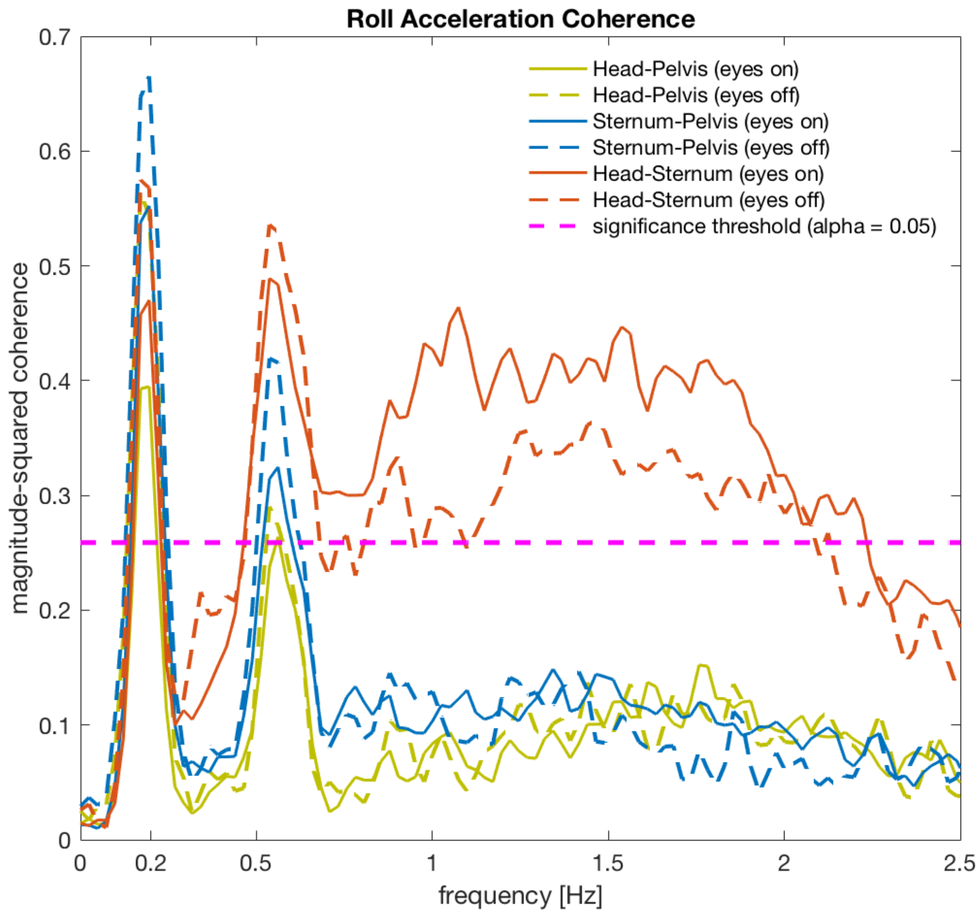

(b)

Fig.3.23 Magnitude-squared coherence from pelvis to head, pelvis to sternum and sternum to head respectively, together with significance threshold – (a) lateral acceleration; (b) roll acceleration

Table 3.8 Coherence integrated from 0.15 Hz to 0.25 Hz for lateral and roll accelerations comparison between visual and sensitive groups (mean significance: for visual conditions – Wilcoxon Signed Rank Test; for sensitivities – Mann-Whitney Test; SD significance: Levene's nonparametric test; α=0.05, Bonferroni Correction, $\alpha_{correction}$=0.0083).

			LATERAL ACCELERATION COHERENCE			ROLL ACCELERATION COHERENCE		
			H-P*	S-P	H-S	H-P	S-P	H-S
VISION	EYES-ON-ROAD	mean	2.98	2.99	2.99	1.46	1.80	1.63
		SD	0.021	0.016	0.013	0.65	0.81	0.71
	EYES-OFF-ROAD	mean	2.99	2.99	2.99	1.85	2.11	1.88
		SD	0.012	0.0093	0.0087	0.68	0.62	0.50
	Mean Sig. (p value)		**0.33**	**0.30**	**0.48**	**0.24**	**0.48**	**0.48**
	SD Sig. (p value)		**0.90**	**0.61**	**0.80**	**0.92**	**0.32**	**0.32**
MISC**	SENSITIVE	mean	2.99	3.00	3.00	1.89	2.20	1.89
		SD	0.0060	0.0056	0.0030	0.67	0.53	0.64
	NON-SENSITIVE	mean	2.97	2.98	2.99	1.37	1.66	1.59
		SD	0.021	0.017	0.014	0.61	0.83	0.57
	Mean Sig. (p value)		**0.014**	**0.12**	**0.080**	**0.043**	**0.16**	**0.25**
	SD Sig. (p value)		**0.45**	**0.35**	**0.16**	**0.97**	**0.17**	**0.87**
GASTROINTESTINAL***	SENSITIVE	mean	2.99	3.00	3.00	1.74	2.24	1.84
		SD	0.0060	0.0059	0.0033	0.62	0.57	0.67
	NON-SENSITIVE	mean	2.98	2.98	2.99	1.58	1.68	1.67
		SD	0.022	0.017	0.014	0.75	0.77	0.56
	Mean Sig. (p value)		**0.10**	**0.076**	**0.27**	**0.39**	**0.088**	**0.56**
	SD Sig. (p value)		**0.082**	**0.89**	**0.20**	**0.13**	**0.53**	**0.47**
CENTRAL***	SENSITIVE	mean	2.99	2.99	2.99	1.99	2.06	1.85
		SD	0.0073	0.012	0.011	0.61	0.57	0.62
	NON-SENSITIVE	mean	2.98	2.99	2.99	1.32	1.85	1.66
		SD	0.022	0.015	0.011	0.59	0.87	0.61
	Mean Sig. (p value)		**0.12**	**0.65**	**0.65**	**0.019**	**0.75**	**0.48**
	SD Sig. (p value)		**0.29**	**0.63**	**0.90**	**0.97**	**0.12**	**0.44**

** H – Head; S – Sternum; P – Pelvis*

*** MISC – the sensitivity was separated by whether or not the MISC reached 7 in the trial.*

**** Gastrointestinal, central – the sensitivity was separated by the score of MSAQ relative items normalized by dividing the overall score for each participant (half of the trials were defined as sensitive).*

4. Discussions

4.1 Motion Sickness with Vision

Two visual conditions were investigated during the experiment: EYES-ON-ROAD with vehicle external vision and EYES-OFF-ROAD with vehicle internal vision. 18 participants experienced both visual conditions in separate trials so that the MSI could be compared within participants. According to the results of both MISC and MSAQ, the subjective motion sickness ratings by most participants were comparably higher in EYES-OFF-ROAD condition. After being exposed to the nauseogenic motion for 5 minutes, the mean MISC reported by the participants with internal vision at every subsequent minute was almost twice that of the external visual condition (Fig.3.6), and 70% of the participants failed to finish the 30-minute trial quitting with medium nausea (Fig.3.5).

The superiority of external vision has been reported in previous field studies. Griffin and Newman (2004) investigated five different visual fields including external vision and internal vision which was realized similar to our experiment – the participants were located at the central rear seat in a petro car; the external vision was normal vision and the internal vision was realized by positioning panels to block forward view as well as side views. The comparison of Griffin and Newman’s experiment and ours is shown in Table 4.1.

Table 4.1 Experiment comparison between Griffin and Newman (2004) and the present study

		GRIFFIN AND NEWMAN (2004)	THE PRESENT STUDY
PARTICIPANTS		100 participants in 5 groups (20 participants each group); Results were compared between groups	18 participants performed both conditions; Results were compared within participants
VISUAL CONDITIONS		Normal vision; Internal vision; Side view only; Narrow forward view; Blindfold	Normal vision; Internal vision
MOTION SCENARIO	Type	Natural driving on suburban roads, with several corners and junctions	Slalom driving on a straight road, with U turns after every 5-6 slaloms
	Maximal Speed (km/h)	48	25
	Duration (mins)	30	30
MSDV (AVERAGED FOR 30 MINS) ($\boldsymbol{m \cdot s^{-1.5}}$)		22.4	83.9
MOTION SICKNESS RATING		7-points illness rating	11-points MISC

Griffin and Newman also found significant difference in motion sickness ratings between external vision and internal vision. The average motion sickness ratings of our experiment were compared with theirs with respect to the car MSDV (derived from vehicle accelerations) in the two visual conditions (Fig.4.1). Since the performed car MSDV in our experiment was comparatively larger than that in Griffin and Newman's experiment, the MSDV as well as corresponding MISC in Griffin and Newman's result were doubled and the final MSDV of 30-minute trials was adjusted as 45 $m \cdot s^{-1.5}$. This MSDV can maintain half information in our experiment where the maximal MSDV was 83.9 $m \cdot s^{-1.5}$. The corresponding MISC in Griffin and Newman's experiment could be doubled as well since it is assumed that the MISC is linearly correlated with MSDV when the latter is under 40 $m \cdot s^{-1.5}$ (Fig.3.8). Because a different illness rating method (7-points scale) was used in Griffin and Newman's experiment, the MISC value has been converted to a percent of the maximal points in the two illness rating scales respectively (the maximal points one possibly reaches are respectively 6 and 7 in the two scales, both representing moderate nausea). Fig.4.1 reveals that our result is consistent in the increase trend of MISC with Griffin and Newman's for a MSDV of 25-45 in EYES-ON-ROAD condition and 35-45 in EYES-OFF-ROAD condition, while the MISC in Griffin and Newman's experiment showed an earlier skip when the MSDV was only 20-25 $m \cdot s^{-1.5}$. The discrepancy possibly results from the not fulfilled assumption that MISC is linearly correlated with the MSDV or there was slight bias between the MISC ratings by difference scales.

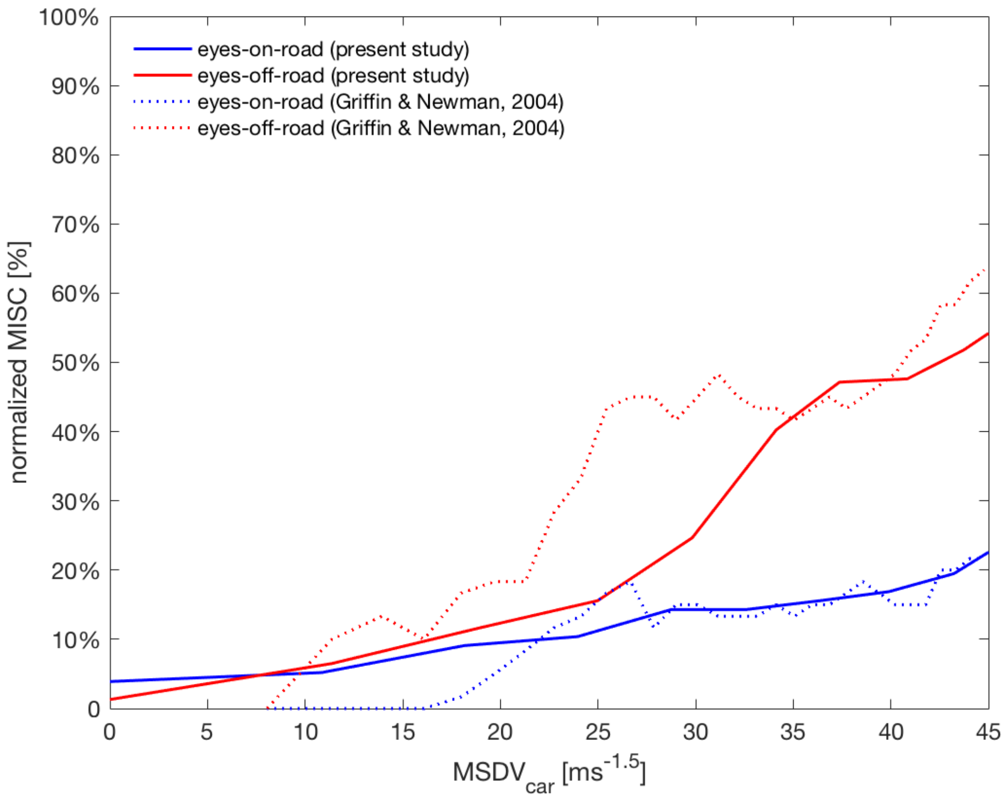

Fig.4.1 MISC increasing with car MSDV in EYES-ON-ROAD and EYES-OFF-ROAD condition (comparison with results of Griffin and Newman (2004))

(The MSDV as well as corresponding MISC in Griffin and Newman's result were doubled in scale. The MISC percentage is the percent of MISC in maximal MISCs of the two illness rating scales that both indicate moderate nausea)

Turner and Griffin (1999a) related the superiority of forward view to motion amplitude during the study of coach passengers, suggesting the motion sickness difference between normal view and internal view could be only found when dosage value of lateral acceleration was above 12 $m \cdot s^{-1.5}$. To validate this, the relationships between average MISC and car MSDV in two visual conditions were plotted together (Fig.4.2). As the lateral motion was the dominant motion in our slaloms journey, the overall car MSDV can be estimated as the 'dosage value of lateral motion' mentioned by Turner and Griffin. In Fig.4.2, it is found that the difference in MISC between external- and internal-visual conditions was not apparent before the car reached a MSDV of 12 $m \cdot s^{-1.5}$ – the MISC of EYES-ON-ROAD condition was even higher than that of EYES-OFF-ROAD condition when the car motion was below 10 $m \cdot s^{-1.5}$ (only the first minute in this experiment). However, as soon as the car reached a MSDV of 15 $m \cdot s^{-1.5}$, the variation in motion sickness ratings was significantly increasing until nausea was induced in passengers. Therefore, as Turner and Griffin reported, the benefit of external vision in carsickness is dependent on the magnitude of car motion – the external vision will be more beneficial when the car motion is more aggressive.

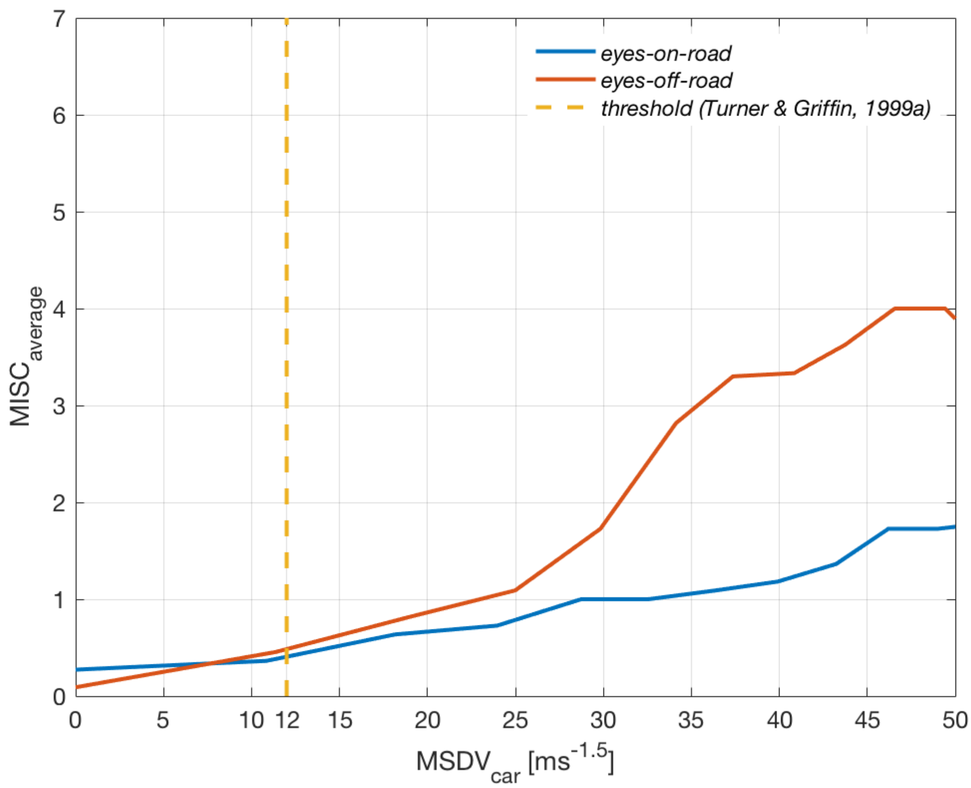

Fig.4.2 Average MISC with respect to car MSDV compared in two visual conditions

The superiority of external vision has been reported by field studies like Griffin and Newman (2004), Wada and Yoshida (2016), Turner and Griffin (1999a) and found in the present study. Nevertheless, no difference was found between external and internal vision in several previous simulator experiments or studies on other transports (e.g., Bos, Mackinnon & Patterson, 2005, Butler & Griffin, 2006). There are two main differences between car field tests and motion simulator experiments:

- The motion stimulus of a simulator is isolated to a singular direction, frequency and amplitude. For instance, Butler and Griffin (2006) only stimulated sinusoidal fore-and-aft oscillation at 0.1 Hz with an acceleration magnitude of 0.89 $m \cdot s^{-2}$ in their simulator motion sickness experiment. However, our present field test involved more complex motions with the limitations of car, road as well as driver. Such complex motion might be more unpredictable and provide a wider range of visual cues due to rotation of the vehicle.

- The visual environment of a simulator may be monotonous. If the 'external vision' in a simulator was mimicked and shown by a display (Feenstra Bos and van Gent, 2011), the graphical quality of the scenery and thus the associated visual information may be low when compared to that offered by the real external view. For some of the laboratory studies, the view of laboratory was simply provided as the external vision in a motion simulator, where the participants can only view the laboratory with no anticipatory information about the simulator motion. It could be the reason that the simulator studies by Bos, Mackinnon and Patterson (2005) and Butler and Griffin (2006) found blindfolded participants had lower motion sickness ratings compared with those had external or internal vision. On the contrary, an external vision in a real car involves all the information about external environment – earth-fixed reference and anticipation, from which the passengers can simply infer the car motion as well as their own body motion. Besides, the vision of real environment might polychrome and informative that makes the journey less boring and influence the passenger's self-mood.

According to the internal model of sensory conflict theory (Fig.1.2), the motion sickness is induced by the conflict between spatial senses (mainly by vestibular system and visual system), which can be either concurrent senses, such as that one is experiencing a physical motion but view at stable scenes, or the estimated senses, such as that one is experiencing a motion which is not expected by his/her central nervous system. As suggested in previous studies, the advantage of viewing external in road transports could be explained in two aspect. On one hand, visual information in earth-fixed frame of reference makes passengers possible to deduce their current head motions (e.g., ego-acceleration) that is stimulating their vestibular systems, and the simultaneous visual-vestibular conflict is supposed to be reduced. On the other hand, the forward vision could provide anticipatory information for the passengers to expect the car future motion. Such expectation is helpful in updating the internal model in our central nervous system and reducing the conflict between present senses and the expectation.

Comparing the visual conditions in simulator and field experiments, both external scenes (laboratory scene and environment scene) are able to provide earth-fixed frame of reference for current motion being estimated. However, the laboratory could not provide anticipation like passengers viewing the forward road and knowing the coming turns and crosses. That benefits of external vision were not found in laboratory tests suggests that this anticipatory information plays an important role in the superiority of external vision in real cars. The importance of anticipation was also validated in previous studies – the anticipatory information can be helpful in reducing motion sickness even it is artificial (Feenstra, Bos & van Gent, 2011).

Apart from the motion sickness ratings by MISC, the severity of each symptom during the trials was also reported by participants (Fig.3.9) – the gastrointestinal symptoms (e.g., stomach illness, nausea etc.), the central symptoms (e.g., dizziness, lightheaded feeling etc.) and the peripheral symptoms (e.g., feeling hot, cold sweat etc.) were found significantly different between external- and internal-visual conditions. Correlation was also found between participants MISC and their ratings for gastrointestinal and central symptoms, possibly because the MISC was highlighting symptoms like nausea. All dimensions of motion sickness symptoms were aggravated by internal vision except for sopite-related symptoms, implying that internal vision in the vehicle was irritative to the overall motion sickness rather than specific symptoms. Relatively less affected peripheral and sopite-related symptoms, as mentioned before, might resulted from uncontrolled variables like temperature and the participant's mental state, and less correlated with motion sickness per se.

Individual characteristics is the most influencing factor to speculate if one is sensitive to motion sickness in specific environment (Lackner, 2014), which was investigated by the MSSQ capturing susceptibility in other (previous) conditions. In present experiment, the variation in motion sickness susceptibility between participants were very significant as well. Interestingly, the participants' motion sickness ratings in EYES-ON-ROAD condition were quite linearly correlated with their reported susceptibility, however, the correlation was not seen in EYES-OFF-ROAD condition (Fig.3.11). It suggests that one's carsickness occurrence in a new journey can be predicted by his/her previous susceptibility (scores of MSSQ) only if external vision is provided. Compared with normal driving with EYES-ON-ROAD, the internal vision situation is more unnatural but quite frequent in our natural life, especially when autonomous driving is developing rapidly. In the near future, most of time of passengers in vehicles must be occupied by internal-visual activities such as reading or communicating. Therefore, the failure of current MSSQ in predicting motion sickness for EYES-OFF-ROAD journey indicates that some new susceptibility investigation methods need to be developed.

Two indicators based on MISC were compared in this thesis – $MISC_{average}$ for the entire duration and $MISC_{rate}$ dividing the maximal MISC by the time it was first reported. It was found that $MISC_{rate}$ could maintain more information about the time participants got severe sick if most of participants reached a relatively high MISC (5 or more), and $MISC_{average}$ is more dependent on the highest score participants rated. Both indicators show a linear correlation with the ratings of gastrointestinal and central symptoms by MSAQ. That means the 11-point MISC is more related to the scale of participants' gastrointestinal or central symptoms rather than peripheral or sopite-related symptoms. It might result from that 'nausea' was used as a higher scale than other symptoms, or participants suffered from gastrointestinal or central symptoms more tend to believe that they were motion sick, compared with those who only felt hot or drowsy.

4.2 Head and Body Motion with Vision

Visual and vestibular sensory signals were shown to be integrated in the dorsal medial superior temporal area (MSTd) of the macaque visual cortex (Angelaki et al., 2011). When the two sensory cues were provided simultaneously and congruently, monkeys were found to be more sensitive and accurate in heading judgement compared with when either of them was solely reliable. Similar advantage of sensory integration was found in humans – reliable visual information was suggested to increase semicircular feedback which helps minimize head rotation in space (Happee et al., 2017). With external vision provided in the vehicle in combination with their vestibular senses, the passengers could be more sensitive to their orientation and informative at their actual motion in space. Such information is supposed to be beneficial for passengers to control their body posture.

When visual and vestibular information is contradictory, humans are expected to adjust their relative weighting of the two sensory cues (Angelaki et al., 2011). For instance, Fetsch et al. (2009) verified that visual and vestibular cues dynamically reweighted to form optimal weightings that are proportional to their reliabilities in a multisensory heading discrimination task. The actual weights of contradictory cues were found consistent with the weights predicted from the single-cue conditions using Bayesian probability theory. In our experiment, when only internal vision is available in the vehicle, the visual cue was supposed to be ineffective in providing motion perception and head-in-space stabilization, the reliability of visual system could reduce, followed by decreased weighting of visual cues when integrated with vestibular cues, where the participants were likely to judge their body motion more relying on their vestibular perception.

According to the previous studies, passengers sensitivity to self-motion would be higher in EYES-ON-ROAD condition where the visual and vestibular perception were both reliable and combined, compared with EYES-OFF-ROAD condition where passengers would mainly rely on the vestibular perception which is less reliable than the combined senses. Nevertheless, no significant difference was found between the two visual conditions in the amplitude of lateral acceleration and roll for head, sternum and pelvis over the entire trials (Table 3.3). It suggests that although the participants motion perception was more reliable, their head and body motion amplitude in space was not adjusted. Similar phenomenon was observed by Keshner, Cromwell & Peterson (1995), and they found the neck velocities were similar in gain as well as phase whether the vision was provided or not. With sensory weightings and integration, a passenger could adjust the reliability about vestibular and visual system so that the body could be better controlled no matter the vision was reliable.

As for the motion in frequency domain, however, the coherence of participants' motion with respect to the vehicle was observed to be slightly affected, though not significant (Fig.3.20). The coherence from car to the body segments indicates the linearity as well as causality between the two motions, in other words, the coherence will be higher if the output signal (head or body motion) is caused by the input signal (car motion) linearly in a higher degree. Any disturbances that could influence the output signal would reduce the coherence level, which, in this case, could be the voluntary body control – a higher degree of active body control would decrease the coherence.

In this experiment, the mean coherence of both lateral accelerations and rolls in the bandwidth of 0.15-0.25 Hz for head, sternum and pelvis with car appeared to be slightly higher in EYES-OFF-ROAD condition (Table 3.6), although no statistical difference was found. It is consistent with the hypothesis that visual cues would help participants increase semicircular feedback and improve effort in voluntary body control subsequently to minimize head and body motion (Happee et al., 2017), though this effort was not apparently shown in the overall amplitude of head or body motion in space as discussed above. Active body control was supposed to delay the body motion in space with respect to the vehicle and shown in the phase plot of seat-to-body transmission (Fig.3.21 & 3.22), which was not seen instead. It could result from that the seat-to-body transmissibility was too low at the low frequencies (0.15-0.25 Hz) compared with higher frequencies, while the peak was accordance with previous studies (around 1.5 Hz for lateral accelerations and around 2 Hz for roll accelerations, Paddan & Griffin, 1988).

4.3 Head and Body Motion with Motion Sickness

Head and Body Motion in Time

Considering the head and body movements with respect to the car in time, the RMS lateral acceleration for sternum and pelvis were found slightly decreasing in the last 2 minutes (W3) compared with the first and middle 2 minutes (W1, W2) in each trial (Fig.3.14), though no statistical significance was found (Table 3.1). Since the RMS lateral acceleration for body segments was normalized by dividing the car lateral acceleration RMS to remove the uncontrolled difference in car motion between trials. The ratio of RMS can be explained as the relative motion of body segments in the car – with a smaller ratio below 1, the body segments are supposed to have larger accelerations in the opposite direction with respect to the car, so that the body sway inside the car is supposed to increase. Similar increase in body relative motion was found in roll direction – the RMSs of roll for head, sternum and pelvis were observed increasing in the middle and last 2 minutes (W2, W3) compared with the first 2 minutes (Fig.3.15), where the statistical significance was found in pelvis roll in EYES-OFF-ROAD trials. Nonetheless, neither lateral acceleration nor roll angle was found changing in time as for relative motion between head and other body segments.

Lackner (2014) pointed out that increased body sway, in other words, postural instability, could be elicited by some of the motion sickness symptoms such as ‘feel like spinning’ or impaired concentration. If it is validated, the head and body lateral acceleration as well as roll angles with respect to the vehicle should be found increasing in time when the motion sickness level was continuously increasing. The slight difference observed in the time windows (Fig.3.14 & 3.15) could more or less indicate the effect of motion sickness severity on postural control, nevertheless, statistical difference was not shown. Whereas, the power of repeated measures ANOVA was not high due to the relatively small sample size, which could be the reason that significant difference of body motion was not found in time. Besides, the 3-windowing procedure was not rigorous enough in this experiment, since the duration of trials varied so large that it was impossible to ensure that every participant was exposed to same duration of the aggressive stimulus in each sampling window. For example, if everyone has finished the 30-minute trial, the three windows can be extracted from 0-2 minutes, 14-16 minutes and 28-30 minutes. On the contrary, some of our participants were only exposed to the motion for 6 minutes where the three windows were extracted continuously from the start to the end. This is an inevitable drawback of the relatively high-irritative motion scenario that we have used in the experiment, which instead was necessary to separate the sensitive and non-sensitive participants and see the apparent difference in motion sickness ratings. To figure out the precedence relationship between postural stability and motion sickness symptoms, more rigorous windowing procedure in time domain could be designed in future studies to test if someone’s postural instability is increasing when his/her motion sickness symptoms is getting severe.

Head and Body Motion between Groups

Although the trials with internal vision have significantly higher MSI than those with external vision, there were still some participants feeling no symptoms in EYES-OFF-ROAD condition and some others feeling extremely bad in EYES-ON-ROAD condition. Therefore, apart from the visual conditions, the participants' head and body motion were also compared between sensitive group and non-sensitive group by statistical test of independent trials.

According to the ecological theory (Riccio & Stoffregen, 1991), motion sickness results from postural instability when someone is lacking body control strategies in specific situation. Two characteristics of this 'instability' hypothesized by Riccio and Stoffregen have been investigated in this thesis:

1. Riccio and Stoffregen indicated that increasing body sway in horizontal plane indicates more postural instability that could result in higher degree of motion sickness (Fig.4.3). According to the body sway in lateral and roll directions (quantified by lateral acceleration RMS and roll RMS) with respect to the vehicle in this experiment (Table 3.3), no statistical difference was found between sensitive and non-sensitive groups that reported highly differently in the severity of sickness. An example is shown Fig.4.4, where the left figure shows the head lateral acceleration and roll of a relatively sensitive participant (reached MISC of 7 in 6 minutes) in EYES-OFF-ROAD trial and the right figure shows that of a non-sensitive participant (maximal MISC was 2 in the 30-minutes trial) also in EYES-OFF-ROAD trial. It is found that the non-sensitive participant even had larger body sway especially in horizontal plane, so that the relative 'postural instability' was not found among the participants who had severe motion sickness symptoms.

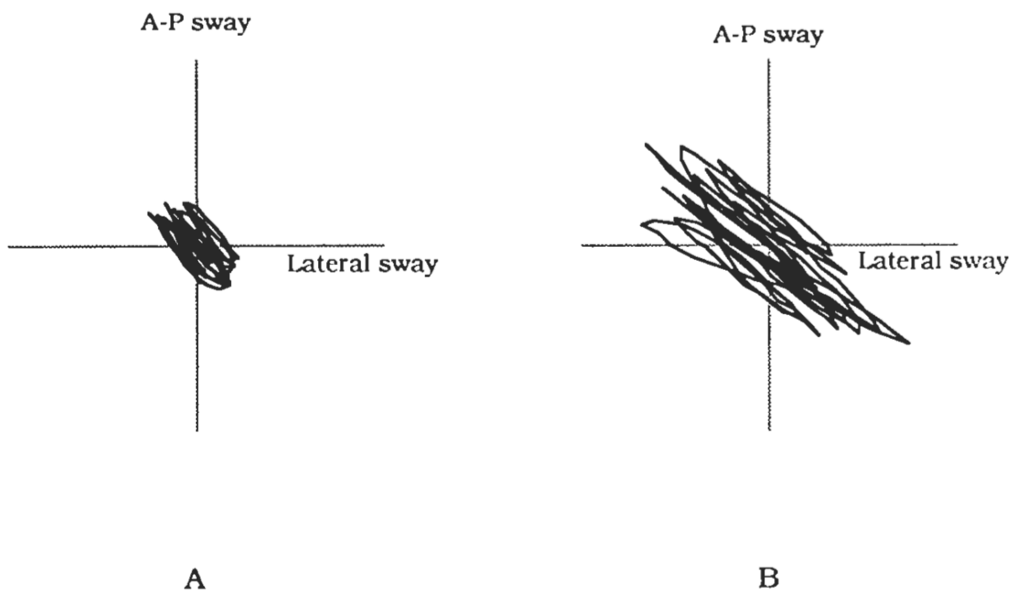

Fig.4.3 Hypothetical body sway in horizontal plane with stable (A) and unstable (B) posture (Riccio & Stoffregen, 1991)

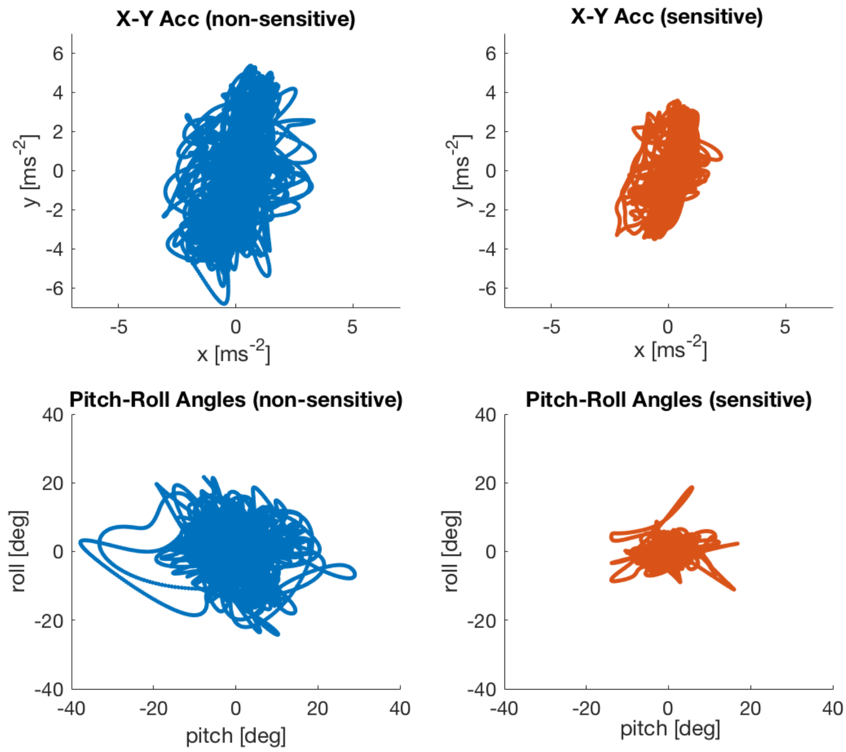

Fig.4.4 An example of head sway in lateral (lateral acceleration) and roll (roll angles) direction (after a bandwidth filter of 0.05-1 Hz) for a sensitive (blue, reached MISC of 7 in 6 minutes) and a non-sensitive (red, maximal MISC of 2 in 30 minutes) participant in EYES-OFF-ROAD trial. (for other participants see Appendix C)

2. Riccio and Stoffregen assumed that postural instability would reduce the coherence in lower frequencies between the environmental disturbances and body movements (Fig.4.5). However, in our experiment, the coherence between body segments (head, sternum and pelvis) and the car seat in both lateral and roll directions appeared to be higher in sensitive group instead of non-sensitive group (Table 3.4). Fig.4.6 shows the seat-to-head coherence averaged for sensitive (reached a MISC of 7, 12 of 22 trials) and non-sensitive group (not reached a MISC of 7), furthermore indicating that sensitive participants tended to have a higher seat-to-head coherence in lower frequencies around 0.2 Hz.

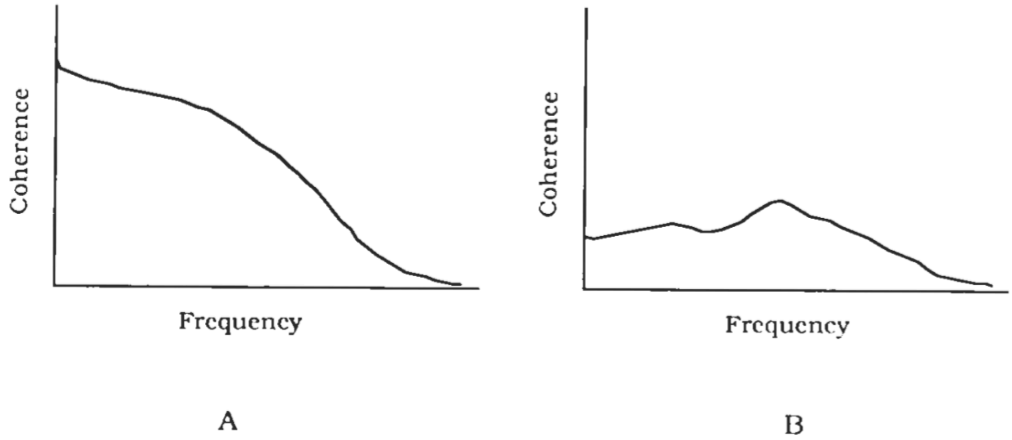

Fig.4.5 Hypothetical coherence between the external disturbances and self-body movements with stable (A) and unstable (B) posture (Riccio & Stoffregen, 1991)

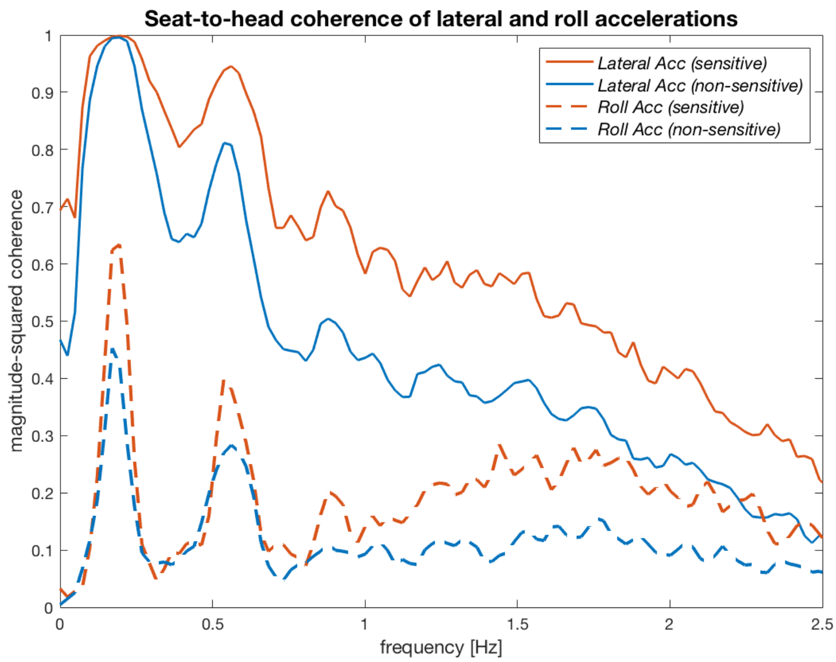

Fig.4.6 Averaged seat-to-head coherence in lateral and roll accelerations for sensitive (reached MISC of 7) and non-sensitive group

Inconsistency between the results of our experiment and Riccio and Stoffregen's 'instability' hypothesis indicates that the 'postural instability' was not observed different either between our participants with different susceptibility to motion sickness, or between EYES-ON-ROAD and eye-off-road condition, so that the 'postural instability' could not explain the motion sickness difference between visual conditions in this experiment. Nonetheless, the car motion was only stimulated at 0.2 Hz in our experiment that could influence the body sway and coherence in lower frequencies. And the sample size in our experiment is relatively small (11 with motion data). It affects the power of statistical tests especially when the data was not normally distributed.

Whether or not the participants' motion sickness level will be influenced by their body motion must be further investigated by stimulating multi-frequency disturbances.

4.4 Future Studies

Several orientations for future studies are suggested according to the results of this experiment.

- The body sway of sitting car passengers could be studied in a stable environment ahead of being studied in a moving vehicle. According to the ecological theory, the passengers' postural sway could predict their susceptibility. Stoffregen et al. (2010) found such effects on standing sway which could be also investigated in seated postures. Such postural control strategies could be reflected in their body motion in a stable rather than moving environment. The latter contains passive movements that could affect the analysis.
- To further examine the ecological theory, relatively stabilized posture could be created for car passengers as a control group. For example, motion sickness in passengers with fixed head or body position with respect to the car could be compared with that in passengers with free body motion.
- The reason of external vision superiority could be further examined by controlling the visual cues or anticipatory information. For example, sitting backwards could maintain the visual cues but remove anticipation; and providing artificial anticipatory information could remove the effect of visual cues and see the effect of anticipation per se.
- Since motion sickness has been found varying significantly between external vision and internal vision, internal visual tasks could be added to further mimic natural life. Some internal visual tasks could further increase motion sickness (visual search tasks), and the others could reduce motion sickness instead (mental tasks).

5. Conclusion

This thesis investigated the relations between vision, body motion and motion sickness in car passengers, when the car was performing a slalom manual driving for at most 30 minutes. The car lateral acceleration was successfully realized with a frequency of 0.17 Hz and a maximal magnitude of 0.4g. Car passengers' head and body motion has been successfully collected during the driving, providing valuable data for motion sickness modelling.

Based on the sensory conflict theory and ecological theory, 4 hypotheses were examined in our carsickness experiment:

1) The benefit of external vision was validated, in line with previous studies. Car passengers rated a significantly higher average MISC, gastrointestinal symptom score, central symptom score as well as peripheral symptom score when external vision was blocked. The motion sickness ratings in EYES-OFF-ROAD condition increased more rapidly in time especially at the first 10 minutes.

2) No significant difference was found in car passengers' head and body motion between the visual conditions. The effect of vision was not seen on either absolute head or body motion or head in torso relative motion. Passengers' postural control strategies were found being maintained the same during this experiment in the two visual conditions.

3) Car passengers' postural stability reflected from their head and body motion was not found related to their motion sickness susceptibility. The motion was examined in both time and frequency domain, in terms of body sway and seat-to-body or torso-to-head coherence. No significant difference was found in either means or standard deviations of absolute as well as relative head and body motion between sensitive and non-sensitive passengers.

4) No evidence indicates that the car passengers' postural stability reflected from their head and body motion was changing in time. The absolute and relative motions were examined in 3 windows respectively at the beginning, middle and end of the trials. No significant difference was found between the 3 windows.

The results of this experiment proved the importance of external vision in carsickness, in accordance with the sensory conflict theory. According to the sensory conflict theory, the visual and vestibular senses were continuously integrated in a vehicle, and lacking consistency between the two senses would increase motion sickness.

However, this experiment did not find postural motion evidence for the ecological theory. The ecological theory suggests the postural instability would predict the motion susceptibility in a vehicle. While the participants' postural instability reflected from their body sway as well as seat-to-body coherence did not vary between sensitive or non-sensitive group or visual conditions.

The stationary head and body motion in time does not support the hypothesis that accumulated motion or sickness symptoms would increase body instability.

Apart from the 4 hypotheses, there were also some other findings from the experiment:

5) In both visual conditions, the participants' MISC ratings correlated with the car MSDV, but the correlation varies hugely between individuals due to individual susceptibility.

6) The participants MISCs were also found correlated with their gastrointestinal and central symptom scores reported through the MSAQ. It indicates that the 11-point MISC we used in the experiment was mainly based on the rating of gastrointestinal and central symptoms rather than other symptoms like peripheral or sopite-related ones. And the peripheral or sopite-related symptoms could also be induced by environment and self-conditions rather than motion sickness.

7) The participants MISCs correlated with their susceptibility reported by MSSQ only in EYES-ON-ROAD condition. For EYES-OFF-ROAD condition, the MSSQ did not correlate significantly with MSI. The failure of current MSSQ in predicting motion sickness for EYES-OFF-ROAD conditions indicates that some new susceptibility investigation methods need to be developed.

8) The transmissibility peaks at around 1.5 Hz for lateral acceleration and 2 Hz for roll acceleration, which are consistent with previous studies. But the transmission gain below 1 Hz was always around 1 for both conditions in this study. It is might because that the motion with only one frequency was dominantly stimulated, and the transmission becomes less indicative in frequency domain. Multi-frequency motion needs to be involved in future studies to investigate the seat-to-head motion transmission in vehicles.

References

Angelaki, D. E., Gu, Y., & DeAngelis, G. C. (2011). Visual and vestibular cue integration for heading perception in extrastriate visual cortex. *The Journal of physiology*, *589*(4), 825-833.

Bertolini, G., & Straumann, D. (2016). Moving in a moving world: a review on vestibular motion sickness. *Frontiers in neurology*, *7*.

Bos, J. E., & Bles, W. (1998). Modelling motion sickness and subjective vertical mismatch detailed for vertical motions. *Brain Research Bulletin*, *47*(5), 537-542.

Bos, J. E., MacKinnon, S. N., & Patterson, A. (2005). Motion sickness symptoms in a ship motion simulator: effects of inside, outside, and no view. *Aviation, space, and environmental medicine, 76*(12), 1111-1118.

Butler, C. A., & Griffin, M. J. (2006). Motion sickness during fore-and-aft oscillation: Effect of the visual scene. *Aviation, space, and environmental medicine*, *77*(12), 1236-1243.

Coolican, H. (2009). Research Methods and Statistics in Psychology Hodder Education. *London, UK.*

Damgrave, R. G. J., & Lutters, D. (2009). The drift of the xsens moven motion capturing suit during common movements in a working environment. In *Proceedings of the 19th CIRP Design Conference–Competitive Design*. Cranfield University Press.

Donohew, B. E., & Griffin, M. J. (2004). Motion sickness: effect of the frequency of lateral oscillation. *Aviation, Space, and Environmental Medicine*, *75*(8), 649-656.

Faber, G. S., Chang, C. C., Kingma, I., Dennerlein, J. T., & van Dieën, J. H. (2016). Estimating 3D L5/S1 moments and ground reaction forces during trunk bending using a full-body ambulatory inertial motion capture system. *Journal of biomechanics, 49*(6), 904-912.

Feenstra, P. J., Bos, J. E., & van Gent, R. N. (2011). A visual display enhancing comfort by counteracting airsickness. *Displays*, *32*(4), 194-200.

Fetsch, C. R., Turner, A. H., DeAngelis, G. C., & Angelaki, D. E. (2009). Dynamic reweighting of visual and vestibular cues during self-motion perception. *Journal of Neuroscience, 29*(49), 15601-15612.

Fritz, C. O., Morris, P. E., & Richler, J. J. (2012). Effect size estimates: current use, calculations, and interpretation. *Journal of experimental psychology: General, 141*(1), 2.

Gallet, C., & Julien, C. (2011). The significance threshold for coherence when using the Welch's periodogram method: effect of overlapping segments. Biomedical *Signal Processing and Control, 6*(4), 405-409.

Gianaros, P. J., Muth, E. R., Mordkoff, J. T., Levine, M. E., & Stern, R. M. (2001). A questionnaire for the assessment of the multiple dimensions of motion sickness. *Aviation, space, and environmental medicine, 72*(2), 115.

Golding, J. F., Markey, H. M., & Stott, J. R. R. (1995). The effects of motion direction, body axis, and posture on motion sickness induced by low frequency linear oscillation. *Aviation, space, and environmental medicine*.

Golding, J. F. (1998). Motion sickness susceptibility questionnaire revised and its relationship to other forms of sickness. *Brain research bulletin, 47*(5), 507-516.

Golding, J. F. (2006). Predicting individual differences in motion sickness susceptibility by questionnaire. *Personality and Individual Differences*, *41*(2), 237-248.

Griffin, M. J., & Howarth, H. V. C. (2000). Motion sickness history questionnaire.

Griffin, M. J., & Mills, K. L. (2002). Effect of frequency and direction of horizontal oscillation on motion sickness. *Aviation, space, and environmental medicine*, *73*(6), 537-543.

Griffin, M. J., & Newman, M. M. (2004). Visual field effects on motion sickness in cars. *Aviation, space, and environmental medicine*, *75*(9), 739-748.

Happee, R., de Bruijn, E., Forbes, P. A., & van der Helm, F. C. (2017). Dynamic head-neck stabilization and modulation with perturbation bandwidth investigated using a multisegment neuromuscular model. *Journal of Biomechanics, 58*, 203-211.

Howard, K. I., Kopta, S. M., Krause, M. S., & Orlinsky, D. E. (1986). The dose–effect relationship in psychotherapy. *American psychologist*, *41*(2), 159.

Irwin, J. A. (1881). THE PATHOLOGY OF SEA-SICKNESS. *The Lancet*, *118*(3039), 907-909.

International Organization for Standardization. (1997). *Mechanical vibration and shock-Evaluation of human exposure to whole-body vibration-Part 1: General requirements.* The Organization.

Keshner, E. A., Cromwell, R. L., & Peterson, B. W. (1995). Mechanisms controlling human head stabilization. II. Head-neck characteristics during random rotations in the vertical plane. *Journal of neurophysiology*, *73*(6), 2302-2312.

Lackner, J. R. (2014). Motion sickness: more than nausea and vomiting. *Experimental brain research*, *232*(8), 2493-2510.

Lawther, A., & Griffin, M. J. (1986). The motion of a ship at sea and the consequent motion sickness amongst passengers. *Ergonomics*, *29*(4), 535-552.

Lawther, A., & Griffin, M. J. (1987). Prediction of the incidence of motion sickness from the magnitude, frequency, and duration of vertical oscillation. *The Journal of the Acoustical Society of America*, *82*(3), 957-966.

McCauley, M. E., Royal, J. W., Wylie, C. D., O'Hanlon, J. F., & Mackie, R. R. (1976). *MSI: Exploratory studies of habituation, pitch and roll, and the refinement of a mathematical model* (No. 1733-2). Canyon Research Group Inc Goleta Ca Human Factors Research Div.

O'Hanlon, J. F., & McCauley, M. E. (1973). *MSI as a function of the frequency and acceleration of vertical sinusoidal motion* (No. 1733-1). CANYON RESEARCH GROUP INC GOLETA CA HUMAN FACTORS RESEARCH DIV.

Oman, C. M. (1982). A heuristic mathematical model for the dynamics of sensory conflict and motion sickness hearing in classical musicians. *Acta Oto-Laryngologica*, *94*(sup392), 4-44.

Oosterveld, W. J. (1995). Motion sickness. *Journal of travel medicine*, *2*(3), 182-185.

Owen, N., Leadbetter, A. G., & Yardley, L. (1998). Relationship between postural control and motion sickness in healthy subjects. *Brain research bulletin*, *47*(5), 471-474.

Paddan, G. S., & Griffin, M. J. (1988). The transmission of translational seat vibration to the head—II. Horizontal seat vibration. *Journal of biomechanics, 21*(3), 199-206.

Reason, J. T. (1978). Motion sickness adaptation: a neural mismatch model. *Journal of the Royal Society of Medicine*, *71*(11), 819.

Riccio, G. E., & Stoffregen, T. A. (1991). An ecological theory of motion sickness and postural instability. *Ecological psychology*, 3(3), 195-240.

Roetenberg, D., Luinge, H., & Slycke, P. (2013). Xsens MVN: full 6DOF human motion tracking using miniature inertial sensors (Version April 3, 2013).

Rolnick, A., & Lubow, R. E. (1991). Why is the driver rarely motion sick? The role of controllability in motion sickness. *Ergonomics*, *34*(7), 867-879.

Smart, L. J., Pagulayan, R. J., & Stoffregen, T. A. (1998). Self-induced motion sickness in unperturbed stance. *Brain research bulletin*, 47(5), 449-457.

Stoffregen, T. A., Chen, Y. C., & Koslucher, F. C. (2014). Motion control, motion sickness, and the postural dynamics of mobile devices. *Experimental brain research*, 232(4), 1389-1397.

Stoffregen, T. A., Yoshida, K., Villard, S., Scibora, L., & Bardy, B. G. (2010). Stance width influences postural stability and motion sickness. *Ecological Psychology*, *22*(3), 169-191.

Stott, J. R. R. (1986). Mechanisms and treatment of motion illness. In *Nausea and vomiting: Mechanisms and treatment*(pp. 110-129). Springer, Berlin, Heidelberg.

Thompson, R. O. (1979). Coherence significance levels. *J. atmos. Sci.*, *36*, 2020-2021.

Treisman, M. (1977). Motion sickness: an evolutionary hypothesis. *Science, 197*(4302), 493-495.

Turner, M. (1999). Motion sickness in public road transport: passenger behaviour and susceptibility. *Ergonomics, 42*(3), 444-461.

Turner, M., & Griffin, M. J. (1999a). Motion sickness in public road transport: the relative importance of motion, vision and individual differences. *British Journal of Psychology*, *90*(4), 519-530.

Turner, M., & Griffin, M. J. (1999b). Motion sickness in public road transport: the effect of driver, route and vehicle. *Ergonomics*, *42*(12), 1646-1664.

Vogel, H., Kohlhaas, R., & von Baumgarten, R. J. (1982). Dependence of motion sickness in automobiles on the direction of linear acceleration. *European journal of applied physiology and occupational physiology*, *48*(3), 399-405.

Wada, T., & Yoshida, K. (2016). Effect of passengers' active head tilt and opening/closure of eyes on motion sickness in lateral acceleration environment of cars. *Ergonomics*, *59*(8), 1050-1059.

Webb, N. A. (2000). Visual acuity, eye movements, the illusion of motion and motion sickness with optokinetic stimuli. *PhD Thesis, University of Southampton*.

Wedmark, J., & Janson, M. (2018). Investigation of methods for quantifying sitting postures in cars.

Weisstein, E. W. (2004). Bonferroni correction.

Zheng, G., Qiu, Y., & Griffin, M. J. (2012). Vertical and dual-axis vibration of the seated human body: nonlinearity, cross-axis coupling, and associations between resonances in transmissibility and apparent mass. *Journal of Sound and Vibration*, *331*(26), 5880-5894.

Appendices

A Motion Sickness Susceptibility Questionnaire (MSSQ)

MOTION SICKNESS SUSCEPTIBILITY QUESTIONNAIRE

(Griffin & Howarth, 2000)

INSTRUCTIONS

This questionnaire is primarily concerned with: (i) your susceptibility to motion sickness, and (ii) what types of motion are most effective in causing this sickness.

Please read the questions carefully and answer them ALL by either TICKING or FILLING IN the boxes which most closely correspond to you as an individual.

All the information you give is CONFIDENTIAL and will be used for research purposed only.

Thank you very much for your co-operation.

NAME ___________________________________ AGE ___________

SEX __________________________________ CURRENT OCCUPATION ___________

APPROXIMATE BODY WEIGHT ___________ HEIGHT _____________

EMAIL ____________________________________

1. In the past YEAR, how many times have you travelled AS A PASSENGER in the following types of transport?

	NEVER	1	2-3	4-15	16-63	64-255	256+
CARS							
BUSES							
COACHES							
SMALL BOATS							
SHIPS							
AEROPLANES							
TRAINS							

2. In the past YEAR, how many times have you felt ill, whilst travelling AS A PASSENGER in the following types of transport?

	NEVER	1	2	3	4-7	8-15	16+
CARS							
BUSES							
COACHES							
SMALL BOATS							
SHIPS							
AEROPLANES							
TRAINS							

3. In the past YEAR, how many times have you VOMITTED whilst travelling AS A PASSENGER in the following types of transport?

	NEVER	1	2	3	4-7	8-15	16+
CARS							
BUSES							
COACHES							
SMALL BOATS							
SHIPS							
AEROPLANES							
TRAINS							

4. Do you EVER feel HOT or SWEAT whilst travelling AS A PASSENGER in the following types of transport?

	NEVER	OCCASIONALLY	OFTEN	ALWAYS
CARS				
BUSES				
COACHES				
SMALL BOATS				
SHIPS				
AEROPLANES				
TRAINS				

5. Do you EVER suffer from HEADACHES whilst travelling AS A PASSENGER in the following types of transport?

	NEVER	OCCASIONALLY	OFTEN	ALWAYS
CARS				
BUSES				
COACHES				
SMALL BOATS				
SHIPS				
AEROPLANES				

TRAINS				

6. Do you EVER suffer from LOSS/CHANGE OF SKIN COLOUR (go pale) whilst travelling AS A PASSENGER in the following types of transport?

	NEVER	OCCASIONALLY	OFTEN	ALWAYS
CARS				
BUSES				
COACHES				
SMALL BOATS				
SHIPS				
AEROPLANES				
TRAINS				

7. Do you EVER suffer from MOUTH WATERING whilst travelling AS A PASSENGER in the following types of transport?

	NEVER	OCCASIONALLY	OFTEN	ALWAYS
CARS				
BUSES				
COACHES				
SMALL BOATS				
SHIPS				
AEROPLANES				
TRAINS				

8. Do you EVER feel DROWSY whilst travelling AS A PASSENGER in the following types of transport?

	NEVER	OCCASIONALLY	OFTEN	ALWAYS
CARS				
BUSES				
COACHES				
SMALL BOATS				
SHIPS				

AEROPLANES				
TRAINS				

9. Do you <u>EVER feel DIZZY</u> whilst travelling AS A PASSENGER in the following types of transport?

	NEVER	OCCASIONALLY	OFTEN	ALWAYS
CARS				
BUSES				
COACHES				
SMALL BOATS				
SHIPS				
AEROPLANES				
TRAINS				

10. Do you <u>EVER suffer from NAUSEA (stomach discomfort, feeling sick)</u> whilst travelling AS A PASSENGER in the following types of transport?

	NEVER	OCCASIONALLY	OFTEN	ALWAYS
CARS				
BUSES				
COACHES				
SMALL BOATS				
SHIPS				
AEROPLANES				
TRAINS				

11. Have you EVER VOMITTED whilst travelling AS A PASSENGER in the following types of transport?

	NO	YES
CARS		
BUSES		
COACHES		
SMALL BOATS		
SHIPS		

AEROPLANES		
TRAINS		

12. Would you avoid any of the following types of transport because of motion sickness?

	NEVER	OCCASIONALLY	OFTEN	ALWAYS
CARS				
BUSES				
COACHES				
SMALL BOATS				
SHIPS				
AEROPLANES				
TRAINS				

13. Which of the following best describes your SUSCEPTIBILITY to motion sickness?

MUCH LESS THAN AVERAGE	
LESS THAN AVERAGE	
AVERAGE	
MORE THAN AVERAGE	
MUCH MORE THAN AVERAGE	

14. Have you ever suffered from any serious illness or injury?

NO ☐ YES ☐

15. Are you under medical treatment or suffering a disability affecting daily life?

NO ☐ YES ☐

B Normality Test

Before doing statistical tests, the normality of tested datasets was examined by Shapiro-Wilk normality test in SPSS. An example is shown below by testing body absolute acceleration and roll for sensitive group. The results of Shapiro-Wilk test are shown in Table B.1. It is found only the sternum acceleration and head roll were not normally distributed (the null hypothesis of normal distribution was rejected with $\alpha = 0.05$). However, since the sample size is too small (12 this case), the data normality could not be confirmed based on the result of Shapiro-Wilk test. So the histogram and QQ-plot were also examined (Fig.B.1-B.3).

Fig.B.1 shows the histogram and QQ-plot of pelvis acceleration in Table B.1, where the significance tested by Shapiro-Wilk is 0.938 (the null hypothesis is highly accepted). The histogram and QQ-plot also show a symmetric distribution implying normal distribution. So the pelvis acceleration for sensitive group was assumed normally distributed.

Fig.B.2 and Fig.B.3 show the histogram and QQ-plot of head roll and acceleration in Table B.1. The head roll is rejected as normal distribution by Shapiro-Wilk test and shows a non-normal distribution in histogram and QQ-plot as well. However, the head acceleration is accepted as normal distribution by Shapiro-Wilk test, but an apparently large skewness is observed in QQ-plot. So, both head roll and acceleration was rejected the normal distribution in this case.

Table B.1 Shapiro-Wilk normality test for body absolute acceleration and roll in EYES-ON-ROAD condition

Test of Normality			
	Shapiro-Wilk		
	Statistic	df	Sig.
HeadAcc	.925	12	.334
SternumAcc	.801	12	.010
PelvisAcc	.973	12	.938
HeadRoll	.825	12	.018
SternumRoll	.963	12	.821
PelvisRoll	.960	12	.777

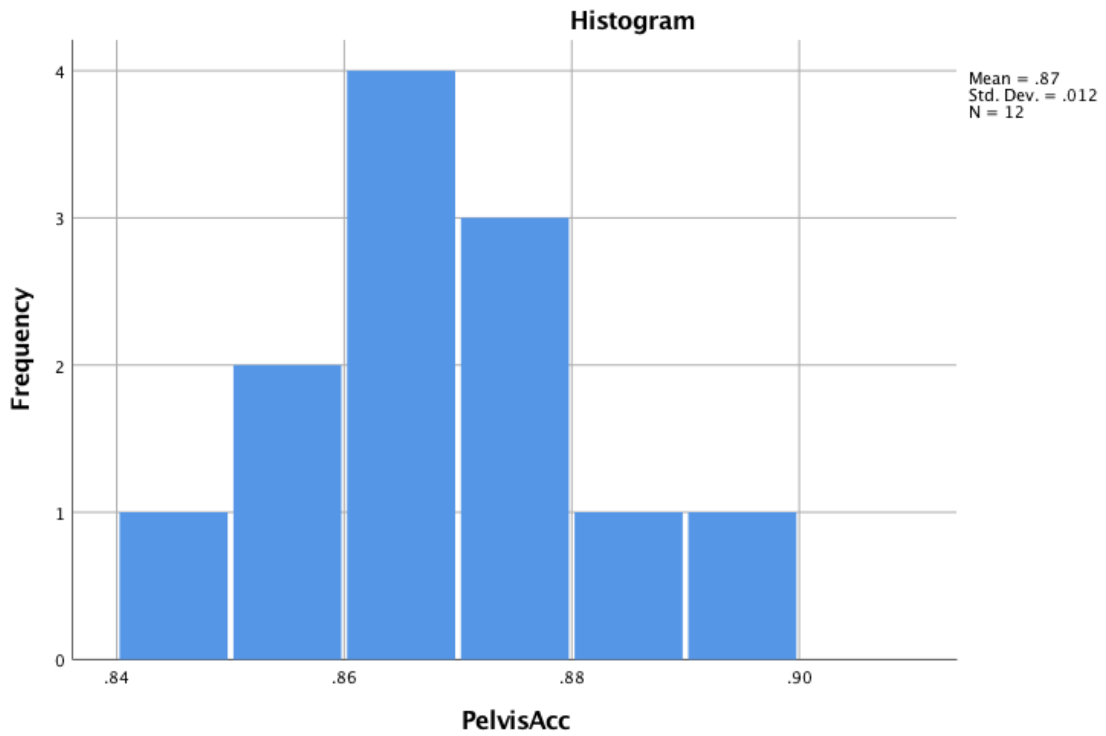

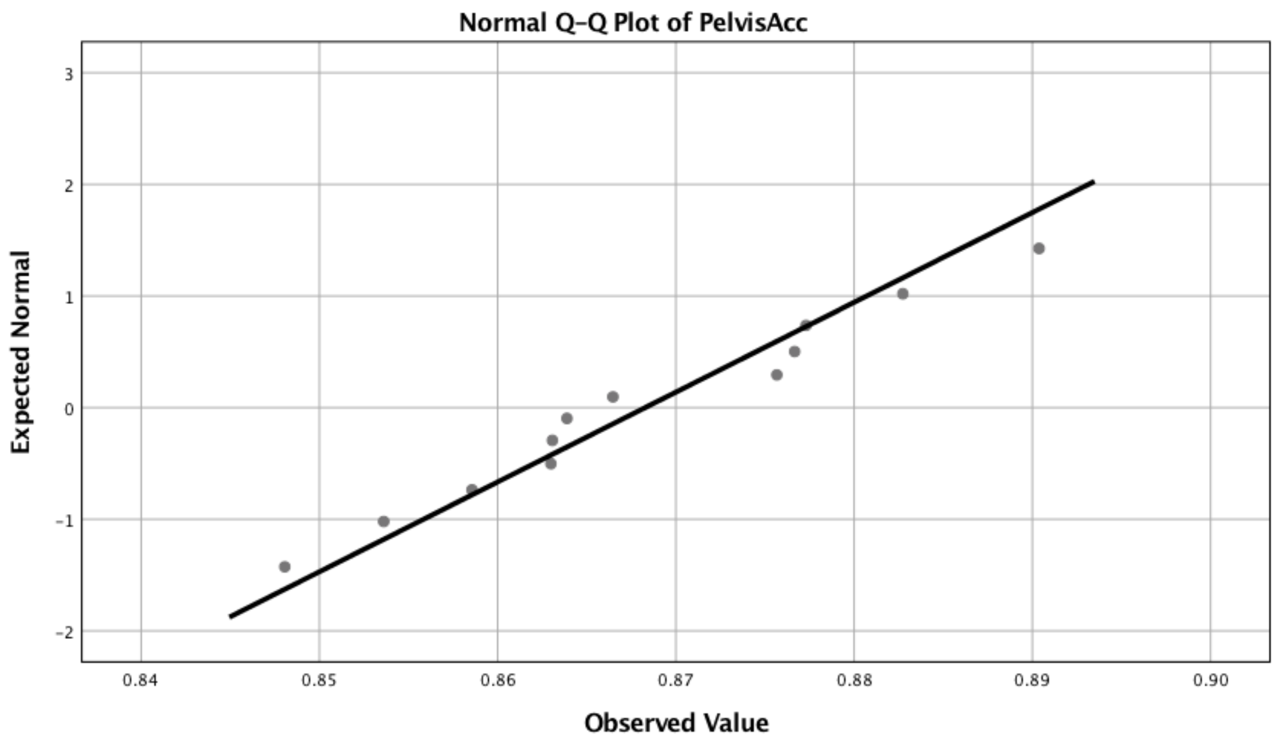

Fig.B.1 Histogram and QQ-plot of absolute pelvis acceleration for sensitive group (12 trials)

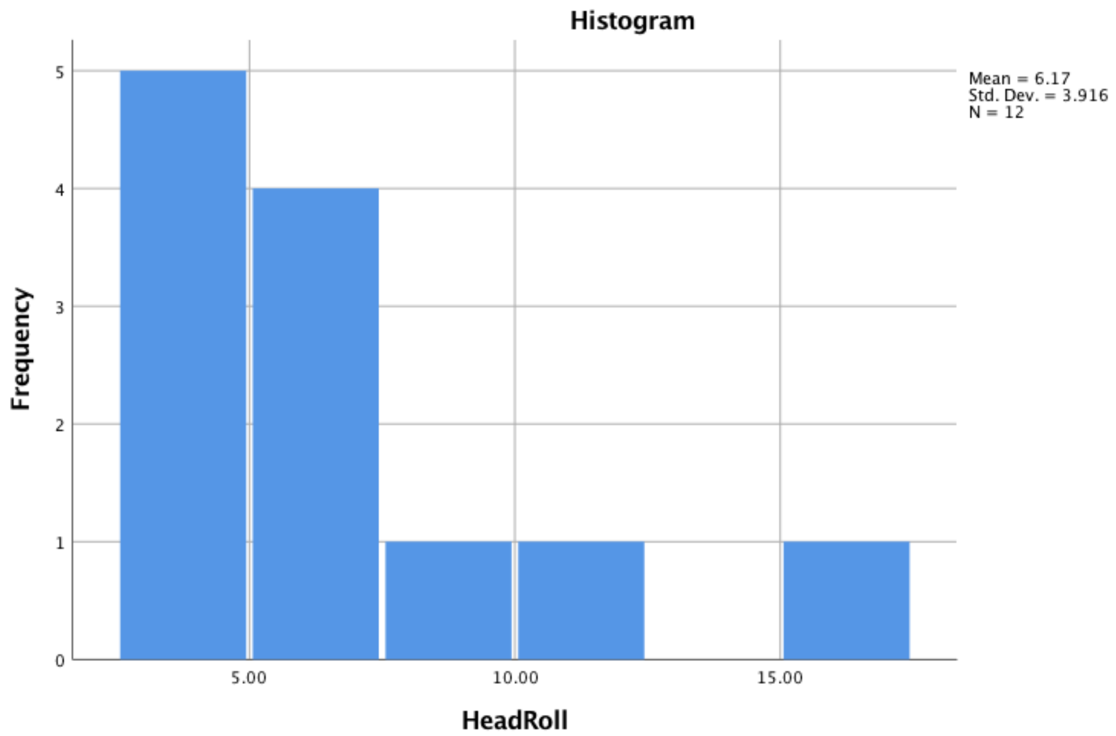

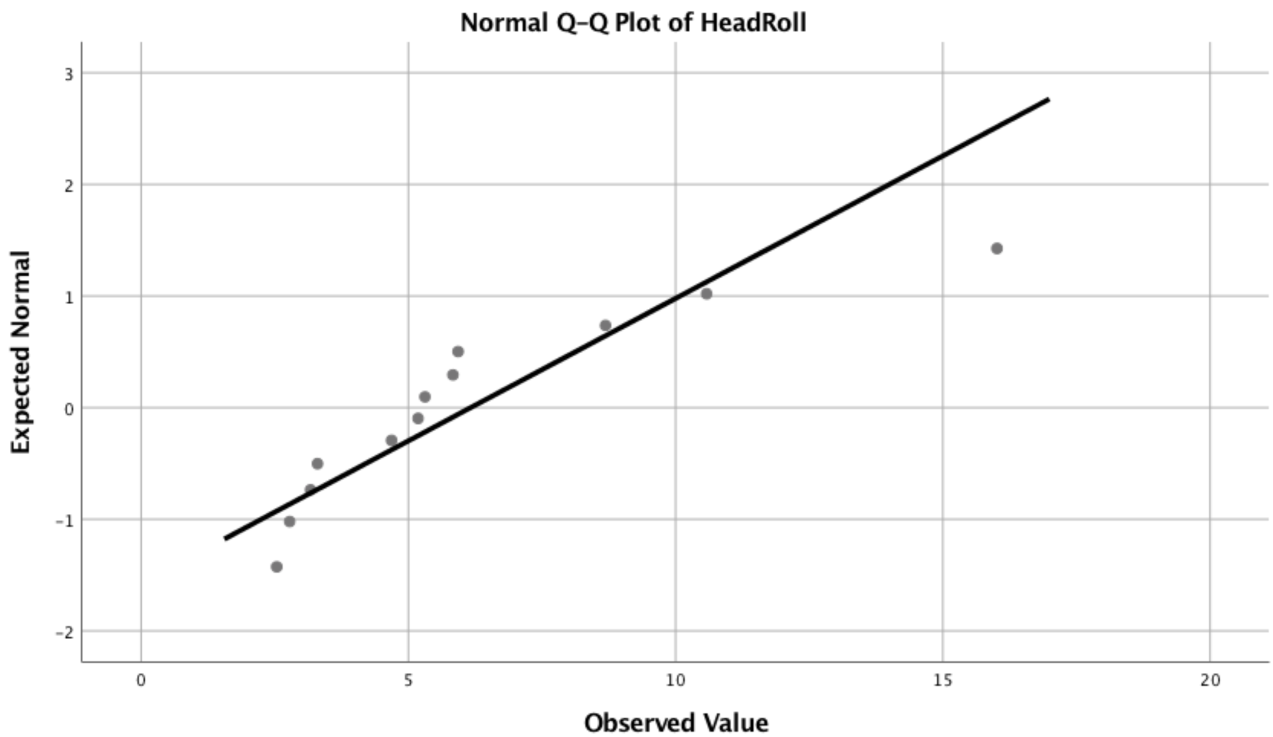

Fig.B.2 Histogram and QQ-plot of absolute head roll for sensitive group (12 trials)

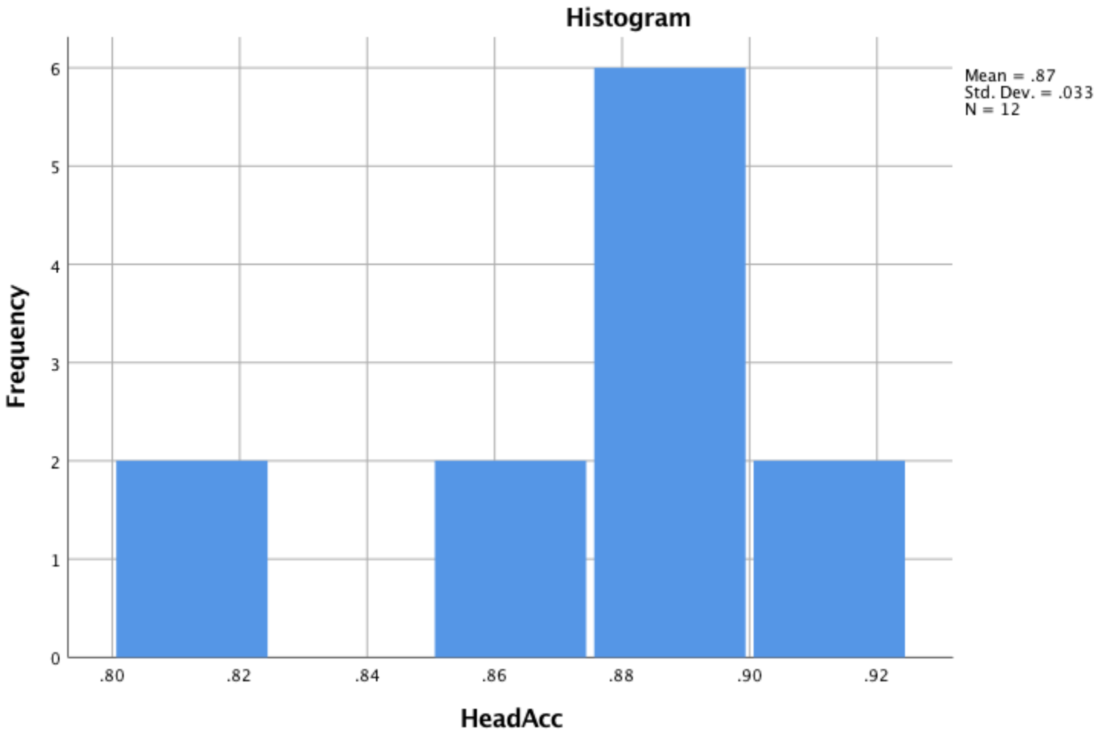

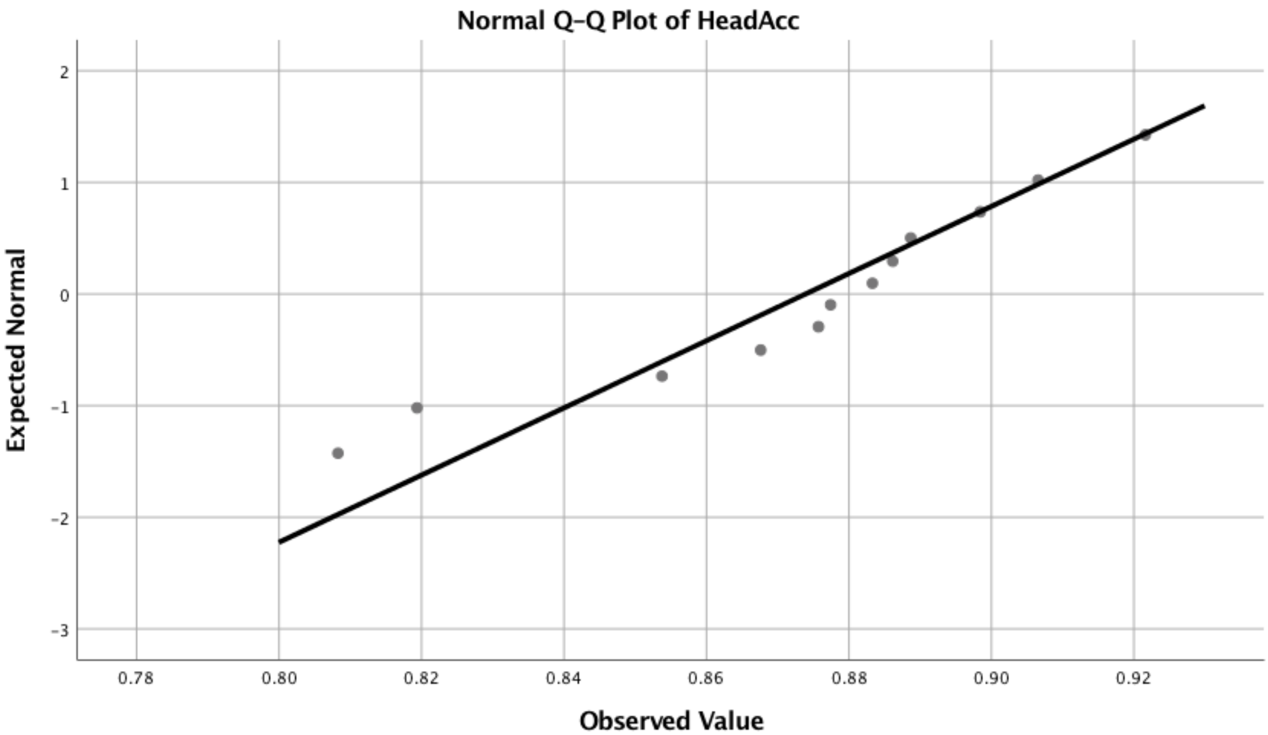

Fig.B.1 Histogram and QQ-plot of absolute sternum acceleration for sensitive group (12 trials)

C Body Sway for All Participants

The 11 participants x-y accelerations and pitch-roll angles for two visual conditions are plotted below. No apparent difference is seen between sensitive (red, MISC reached 7) and non-sensitive (blue) participants.

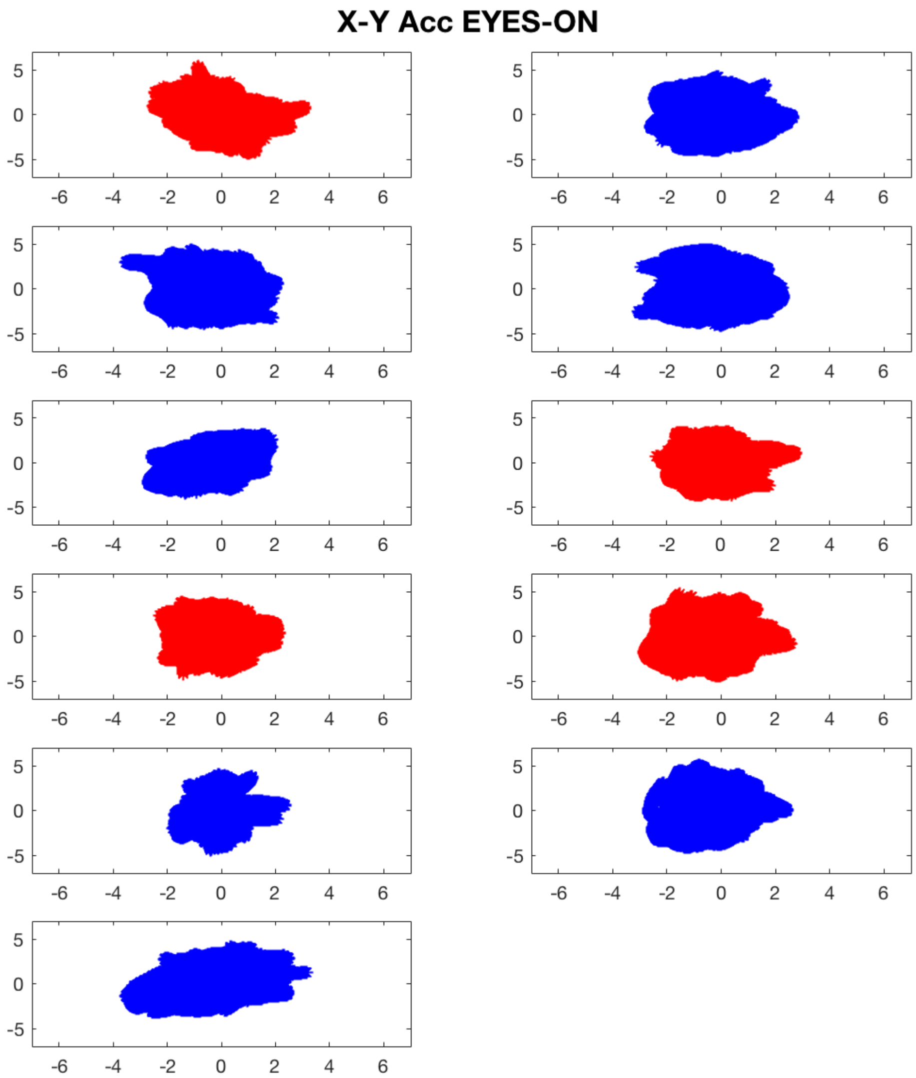

X-Y Acc EYES-OFF

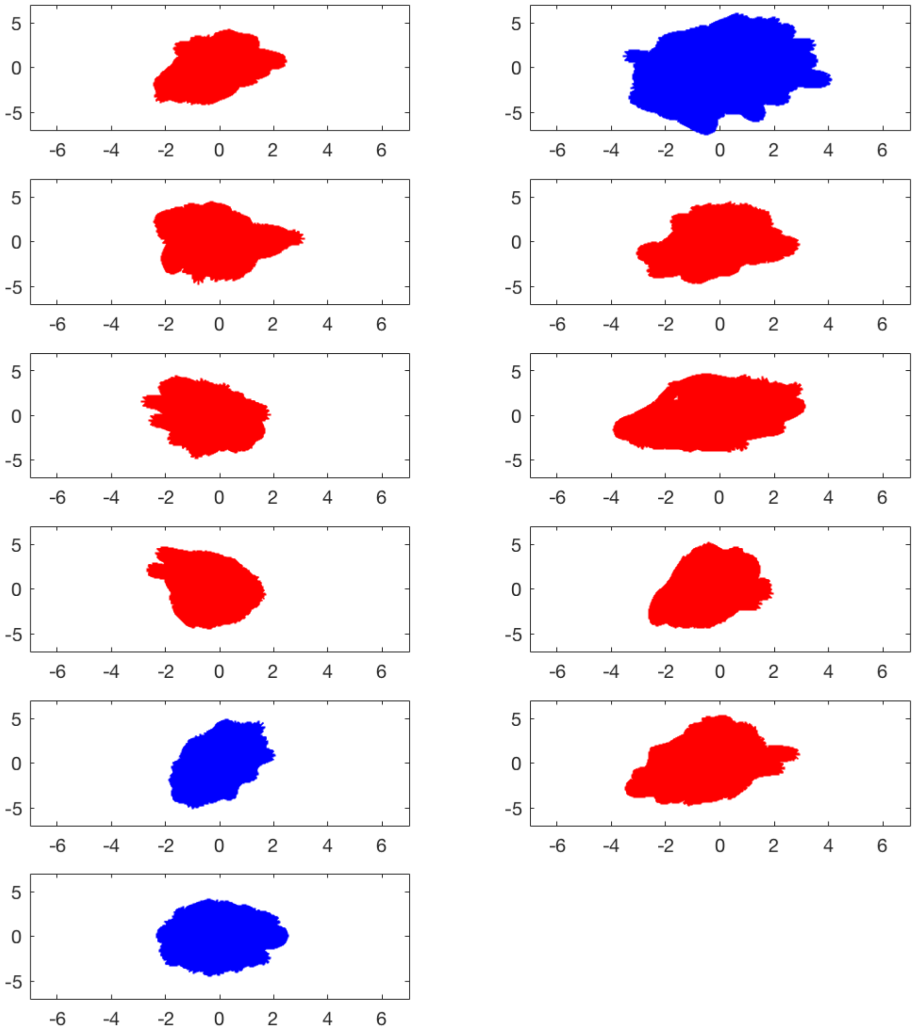

Pitch-Roll EYES-ON

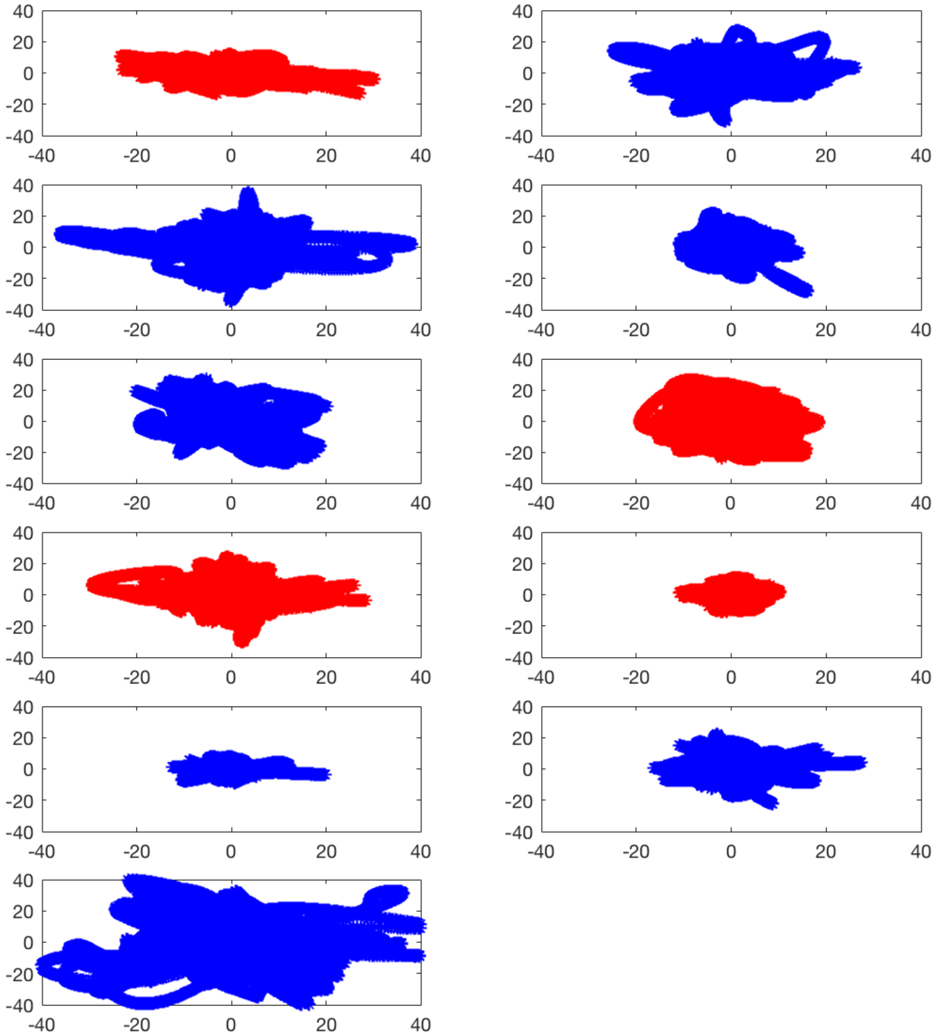

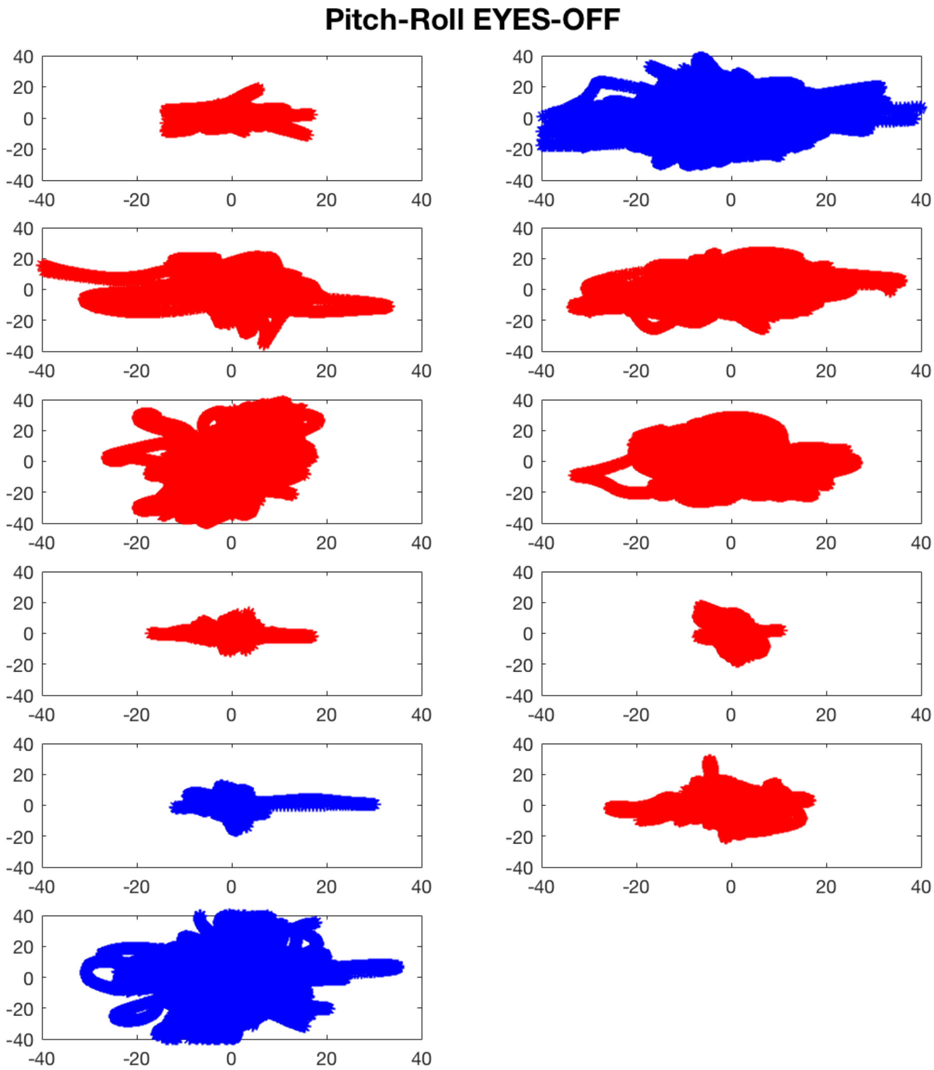

Fig.C.1 x-y acceleration and pitch-roll sway for 11 participants in EYES-ON-ROAD and EYES-OFF-ROAD condition (red – sensitive participants, MISC reached 7; blue – non-sensitive participants, MISC less than 7 for 30 minutes)